10

Factorization and subtractions

In Sec. 9.13 we saw how factorization theorems give a lot of predictive power to QCD. They are essential in the analysis of data at high-energy colliders, not just for understanding the QCD aspects but also in searches for new physics, for example.

So far we have seen a genuine proof (Sec. 8.9) only for inclusive DIS, and only in a model theory without gauge fields. In this chapter we will formulate the principles that apply very generally, to other reactions, and when dealing with the full complications of a gauge theory.

The general class of problem concerns the extraction of the asymptotic behavior of amplitudes and cross sections as some external parameter, like a momentum, gets large. In general discussions, we denote the large parameter by Q. As well as factorization theorems in their broadest sense, such asymptotic problems also encompass simpler situations like renormalization, the operator product expansion (OPE), and the IR divergence issue[1] in QED.

There is a common and general mathematical structure in these different problems that could undoubtedly use further codification. Perhaps methods based on Hopf algebras, or some generalization, would provide an appropriate mathematical structure. So far these methods have been applied to renormalization (e.g., Connes and Kreimer, 2000, 2002).

In this chapter, I interleave a general formal treatment with its application to the Sudakov form factor, including explicit calculations at one-loop order. The general treatment will underlie all further work in this book. The Sudakov form factor illustrates the issues that are characteristic of asymptotic problems in Minkowski space, especially in a gauge theory. Factorization for the Sudakov form factor is a prototype for many important applications.

First I will give an overview of the method, which is a general subtractive procedure generalizing Bogoliubov's procedure for renormalization. The Libby-Sterman analysis is used to determine the leading regions R for a graph Γ for the process under consideration. For each region R of a graph Γ there is defined an approximator T_R. From T_R, with the aid of subtractions to cancel double counting between regions, is constructed the contribution $C_R \Gamma$ associated with the region.

Then I will define an implementation of these ideas for the Sudakov form factor, complete with a specific calculation for a one-loop graph. After that will be a proof that the general

---

[1] Which concerns a small photon mass instead of a large scale Q.

313

subtraction method works. This will require that the region approximators T_R obey certain conditions, that will be especially critical in QCD. The one-loop example will help to explain the rationale for these conditions and to show how to satisfy them in general.

Then I will derive factorization and evolution equations for the Sudakov form factor.

Many elements of the proofs given here can be found in the literature. However, the presentation as a whole represents a new treatment, which is intended to be a substantial improvement on previous work.

Although the methods presented here apply to perturbation theory, it should be evident, just as in Sec. 8.9, that much structure is seen that has a reality beyond perturbation theory. But exactly how to capture this structure in a strict deductive framework is not so clear, and there are some important open problems.

10.1 Subtraction method

To understand the rationale for a subtraction procedure, recall the successive approximation method outlined in Sec. 8.8. This starts from the smallest region for a graph for some process, for which we find a useful approximation. The approximation typically corresponds to a product or convolution of a lowest-order partonic subgraph and a matrix element of some operator. The operator in the matrix element determines the definition of, for example, a parton density.

We then sequentially construct approximations suitable for successively larger regions. When constructing the contribution C_R associated with some region R, subtractions must be applied to compensate double counting of the contributions $C_{R'}$ from smaller regions R', contributions that have already been constructed. Finally, we sum over the regions for each graph Γ, and over graphs. This results in factorization, by an argument with the pattern given in Sec. 8.2.

A simple example was given by the derivation of leading-twist factorization for DIS in a non-gauge theory in Sec. 8.9. It is a useful exercise to show how the formulae in that section, like (8.70) and (8.74), give particular cases of the more general formulae in the present chapter.

In a gauge theory like QCD, the basic argument will need to be supplemented, notably by an application of Ward identities to extract gluons of scalar polarization from the hard scattering, to convert them to attachments to Wilson lines. Further issues concern the exact nature of the leading regions and the accuracy of the approximators T_R. These are much harder than for relatively simple Euclidean asymptotic problems like the OPE.

10.1.1 Overall view

We let Q denote the large scale for the process under consideration. Each graph Γ has a set of leading regions, and up to power-suppressed terms, we aim to write Γ as a sum over terms for its leading regions:

$$\Gamma = \sum_{R \text{ of } \Gamma} C_R \Gamma + \text{power-suppressed}. \tag{10.1}$$

For the processes of interest, the regions and the associated powers of Q are determined by the Libby-Sterman analysis (Ch. 5). Normally we treat only the leading power. As explained in Ch. 5, each region is specified by a skeleton in loop-momentum space, i.e., the position of the associated pinch-singular surface (PSS) in a massless theory. Each region also corresponds to a decomposition of the whole graph Γ into subgraphs (e.g., Fig. 5.17) where each subgraph has momenta of a particular kind: hard, collinear in some direction, or soft. There can be finer decompositions needed under some circumstances, but that does not affect the principles.

The general definition of the contribution $C_R\Gamma$ associated with a region R of a graph Γ will be made in (10.4) in terms of an "approximator" T_R, together with subtractions to eliminate double counting between regions. A key element in applying (10.1) and in enabling factorization to be derived is the construction of suitable approximators T_R.

10.1.2 Regions: terminology

We review some terminology and definitions from Ch. 5.

- A region R of a graph Γ is specified by a PSS in the massless theory, as determined by the Libby-Sterman method.
- A region is called leading if Libby-Sterman power-counting gives it a leading power, usually defined by dimensional analysis, e.g., Q^0 for a DIS structure function.
- Some regions occur with a super-leading power in individual graphs, when all the gluons exchanged between hard and collinear subgraphs are of scalar polarization. Since such super-leading contributions cancel very generally after a sum over graphs, we choose the definition of the leading power accordingly.
- Our factorization arguments will be applied to regions which give at least a certain chosen power of Q. The term "power-suppressed" in (10.1) means with respect to the chosen power of Q.

   Typically, this is the power of Q we call leading. But extensions of our methods to non-leading powers are possible. Since T_R is essentially a truncation of a Taylor series expansion about a PSS, keeping more terms in the Taylor series corresponds to keeping more non-leading powers of Q.

   When we use dimensional regularization, with $4 - 2\epsilon$ dimensions, some exponents in power laws have ϵ dependence. In categorizing powers as leading or non-leading, we generally work close to $\epsilon = 0$ and ignore changes in exponents that are of order ϵ.
- At each PSS R we choose a set of intrinsic coordinates labeling points within the PSS, and there is a set of normal coordinates labeling deviations off the surface (Sec. 5.7).
- We can convert the normal coordinates for a region R into a radial coordinate λ_R and a set of angle-like coordinates specifying direction. We saw a number of examples in Ch. 5. Power-counting is conveniently done using the one-dimensional integral over λ_R. We require λ_R to have the dimensions of mass.
- Ordering between the regions is defined by set-theoretic inclusion on the skeletons defined technically in Sec. 5.4.1, and reviewed in the next section, 10.1.3.

10.1.3 Regions: properties

Relations between regions

In simple cases, all the leading regions for a graph are nested. A typical example is DIS in a non-gauge theory (Sec. 8.9). For that case, the leading regions are where some number of rungs at the top of a ladder graph, Fig. 8.12, form the hard subgraph, and the rest of the graph is target-collinear. The hard subgraph corresponds to a graphical factor AK^j in Fig. 8.12. If we use R_j to denote the corresponding region, then the ordering of leading regions can be represented along a line:

$$R_0 < R_1 < R_2 < \cdots < R_N. \tag{10.2}$$

This situation is called a total ordering, i.e., any two leading regions, R_1 and R_2, obey exactly one of $R_1 < R_2$, $R_2 < R_1$ or $R_1 = R_2$.

But in general, the ordering is only a partial ordering. That is, between any two regions R_1 and R_2, exactly one of the following holds:

- $R_1 < R_2$: R_1 is smaller than R_2.
- $R_1 > R_2$: R_1 is bigger than R_2.
- $R_1 = R_2$: they are the same region.
- They overlap. That is, the intersection of their skeletons is non-empty, $R_1 \cap R_2 \neq \emptyset$, but none of the preceding three cases hold.[2] Thus $R_1 \cap R_2$ is non-empty and strictly smaller than both of R_1 and R_2. An example is given by R_A and R_B in (5.21). We denote this situation by R_1 ovrlp R_2.
- R_1 and R_2 do not intersect at all: $R_1 \cap R_2 = \emptyset$. An example is given by $R_{A'}$ and $R_{B'}$ in (5.21).

Separation of non-intersecting regions

Suppose two regions R_1 and R_2 do not intersect. Then there is a non-zero separation between them, because the (empty) intersection is of their skeletons, which are *closed* sets. Thus if λ_1 and λ_2 are radial variables for the two regions, then there is a non-zero range $0 \leq \lambda_j \leq L_j$ for which points around each PSS do not intersect the other. Since the PSS are defined from the massless theory, each of these ranges in λ_j is of order Q.

Minimal region(s)

We define a region R_0 to be minimal if it has no smaller regions, i.e., if there is no R' for which $R' < R_0$. One example is for a handbag diagram for DIS. Its minimal region gives the parton model. A non-trivial example is for the one-loop vertex graph treated in Sec. 5.4. It has three minimal regions $R_{A'}$, $R_{B'}$ and R_S. (But only R_S is leading.)

Note that a minimal region R_0 cannot overlap with any region. For every other region, either R_0 is contained in it or does not intersect it.

---

[2] $\emptyset$ denotes the empty set.

Hierarchy

Ordering between the different regions of a graph allows them to be organized in a hierarchy which can be diagrammed as in (5.21).

10.1.4 Definition of region term $C_R \Gamma$

C_R for minimal region

For a minimal region R_0, its contribution is simply defined to be the action of its approximator on the unapproximated graph:

$$C_{R_0}\Gamma \overset{\text{def}}{=} T_{R_0}\Gamma. \tag{10.3}$$

In DIS in a non-gauge theory in Ch. 8, a suitable approximator for a minimal leading region was given in (8.68).

As that equation illustrates, a natural definition of the approximator can lead to extra UV divergences, which are to be removed by renormalization of parton densities (and of similar objects, in the general case). Therefore we define the approximator to include such renormalization.

Alternatively, the approximator can be defined to include a suitable cutoff. The comparative advantages and disadvantages of the renormalization and cutoff approaches were discussed in Sec. 8.3.1.

C_R for larger regions

In the contributions from larger regions, we use subtractions to avoid double counting of the contributions from smaller regions. So we define

$$C_R\Gamma \overset{\text{def}}{=} T_R\left(\Gamma - \sum_{R' < R} C_{R'}\Gamma\right). \tag{10.4}$$

For a minimal region, (10.4) reduces to (10.3). Thus (10.4) gives a valid recursive definition of $C_R\Gamma$, starting from the minimal region(s).

The factor in parentheses is the original graph minus subtractions for regions smaller than R. For the case treated in Ch. 8, this factor was found in (8.74); it is $A\,[1 - (1 - \overleftarrow{T}\,|V)K]^{-1}$ on the last line of that equation.[3] In that situation, it was evident that the factor is power-suppressed in regions smaller than R. Thus the smallest region where $C_R\Gamma$ is leading is actually R.

But in more general cases, like the Sudakov form factor, such statements will need some modifications.

It is also possible to start from an approximation for a maximal region, and then work to smaller regions, as in Tkachov (1994). But starting from the smaller regions, as we have done, gives a more direct relation to the parton model and makes clearer the relation to a non-perturbative definition of the parton densities.

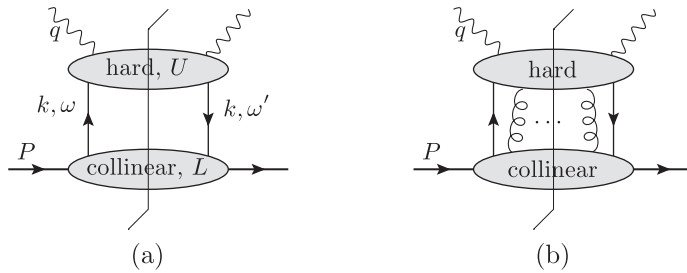[3] That formula does not explicitly include the needed parton-density renormalization.

Fig. 10.1. Leading regions for DIS: (a) in a theory without gauge fields, (b) in a gauge theory.

10.1.5 Remainder

We define the remainder of a graph to be

$$r(\Gamma) \overset{\text{def}}{=} \Gamma - \sum_{R \text{ of } \Gamma} C_R \Gamma. \tag{10.5}$$

It is essential to prove that this is actually power-suppressed, given a particular implementation of the region approximators $T_R \Gamma$.

10.1.6 Relation to factorization

The above formalism focuses on an additive structure for a particular graph. To get a factorized form, we sum over graphs. As observed in Sec. 8.2, the sum over regions and graphs corresponds to independent sums over subgraphs associated with the regions, e.g., independent sums over the hard and collinear subgraphs for DIS in Fig. 10.1.

In the simplest cases, exemplified by Fig. 10.1(a), we have a fixed number of lines joining the subgraphs, and the graphical structure directly corresponds to a factorization formula. Then to prove factorization we need to prove that (1) the approximators T_R respect the factorized structure, (2) UV renormalization needed on the parton densities respects the factorized structure, and (3) the subtractions in (10.4) actually have their intended effect of removing double counting between the terms for different regions.

But as illustrated in Fig. 10.1(b), the situation is more complicated in a gauge theory, because arbitrarily many gauge-field lines can connect the collinear and hard subgraphs,[4] without any power-suppression.

Therefore the graphical representation of the regions does not directly correspond to factorization.

An example of the necessary argument was given in Sec. 7.7 for a gauge-theory version of the parton model. We applied Ward identities to convert the extra gluons into attachments to the Wilson line in the definition of a gauge-invariant quark density. To do this requires an appropriate choice of the approximators T_R, together with a demonstration that the Wilson

---

[4] And also soft and collinear subgraphs in a general case

lines are actually obtained. Only after this work do we find that

$$\sum_{R,\Gamma} C_R \Gamma = \text{factorized form.} \tag{10.6}$$

We could conceive that Fig. 10.1(b) itself represents a generalized factorization structure. But the structure would involve an infinite collection of parton-density-like objects, each with a different number of gluon lines, and each with a different hard-scattering factor. Without further information, such a factorization would not be useful for phenomenology.

10.1.7 Which formulation for calculations?

Often in realistic QCD calculations, there are many graphs to consider. The decomposition (10.1) produces multiple terms for each graph, resulting in an apparently even more elaborate structure. Is it actually necessary to use it?

An alternative calculational approach was described in Sec. 9.6, and corresponds to many practical calculations. The aim is to compute the hard-scattering coefficient in a factorization formula, and the method uses the observation that the hard scattering does not depend on the type of particle used for the target. One first makes a direct computation of Feynman graphs for the process under consideration, but with a partonic target. Then one computes the densities of partons in partons to the relevant order, and then applies factorization on a partonic target to deduce the hard-scattering coefficients. Because factorization has taken account of simplifications due to the use of Ward identities, there are generally fewer terms to calculate than by a direct use of (10.1), which requires a listing of all the leading regions for every graph computed.

This would appear to relegate the subtraction formalism to a key tool in a careful derivation of factorization.

However, direct calculation of partonic Feynman graphs involves the cancellation of various kinds of collinear and soft divergences between different graphs; it thereby entails the use of a regulator. This is satisfactory if calculations are done analytically rather than numerically. But if numerical calculations are used, the cancellation of divergences between graphs is tricky to implement; it is a classic situation where rounding errors can dominate a numerical calculation. To set up a numerical integral for the hard scattering one can apply subtractions directly to the integrand of a hard-scattering subgraph. All necessary cancellations of divergences are then in the integrand, and the integral can be evaluated directly in four dimensions, without a regulator. We saw a very simple example in Sec. 9.7.5.

There is much recent work in implementing subtractions numerically, e.g., Binoth *et al.* (2008); Dittmaier, Kabelschacht, and Kasprzik (2008); Frederix, Gehrmann, and Greiner (2008); Hasegawa, Moch, and Uwer (2008); Seymour and Tevlin (2008).

Since there are many regions involved in high-order graphs, practical application of a subtraction procedure must be automated. If the subtractions are not formulated correctly, there can remain divergences, which manifest themselves in badly behaved numerical integrals over a high-dimensional space.
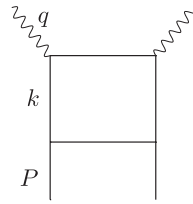
Fig. 10.2. One-loop graph for DIS on elementary target.

10.2 Simple example of subtraction method

With suitable definitions of the region approximators T_R, we will derive factorization for many processes of interest from the structure of the sum over regions and graphs, $\sum_{\Gamma,R} C_R \Gamma$. So to prove factorization is accurate up to a power-law error, we need to prove that for each individual graph the sum over regions, $\sum_R C_R \Gamma$, itself approximates Γ, up to a power-law error, i.e., that the remainder $r(\Gamma)$ is power-suppressed.

Now the approximator T_R is always designed so that $T_R \Gamma$ gives an accurate approximation when the momentum configuration is both close to the PSS defining the region R, and away from the intersections with the PSSs for regions that are smaller than or overlap with R. The complications in making a satisfactory proof that $r(\Gamma)$ is power-suppressed arise from the combination of multiple regions, with the possibility of double counting, and from the fact that there are intermediate configurations of momenta where the individual approximations degrade in accuracy.

The simplest proof is when all the relevant regions are nested, as in Sec. 8.9. Our aim in this chapter is to construct better methods that also work when there are more complicated relations between regions, e.g., (5.21).

But first I illustrate the general notation with a simple mathematical example motivated by a one-loop graph for DIS in a model theory, Fig. 10.2. There are two leading regions: R_0, where the top rung is hard and the bottom rung collinear, and R_1, where the whole loop is hard. They obey $R_0 < R_1$. The simple example is obtained by replacing the full Feynman graph by the following one-dimensional integral

$$I(Q, P, m) = \int_0^\infty dk\, \Gamma(k, Q, P, m) = \int_0^\infty dk\, \frac{Q}{Q + k + m} \frac{1}{k + P + m}. \qquad (10.7)$$

The factor of Q in the numerator makes the integral dimensionless, and gives an overall leading power of Q^0.

If our general subtraction method works, then the leading-power asymptote for the graph is

$$C_{R_0} \Gamma + C_{R_1} \Gamma = T_{R_0} \Gamma + T_{R_1}(1 - T_{R_0})\Gamma. \qquad (10.8)$$

We define the approximators T_R to be applied to the integrand, Γ, rather than to the integral as a whole. Each T_R sets to zero the (lower) external momentum and the internal mass of

the hard scattering. Thus

$$C_{R_0}\Gamma = T_{R_0}\Gamma = \frac{Q}{Q}\frac{1}{k+P+m} = \frac{1}{k+P+m}, \tag{10.9a}$$

$$(1 - T_{R_0})\Gamma = \left(\frac{Q}{Q+k+m} - 1\right)\frac{1}{k+P+m}, \tag{10.9b}$$

$$T_{R_1}\Gamma = \frac{Q}{Q+k}\frac{1}{k}, \tag{10.9c}$$

$$C_{R_1}\Gamma = T_{R_1}(1 - T_{R_0})\Gamma = \left(\frac{Q}{Q+k} - 1\right)\frac{1}{k}, \tag{10.9d}$$

so that the remainder is

$$r(\Gamma) = \Gamma - C_{R_0}\Gamma - C_{R_1}\Gamma = (1 - T_{R_1})(1 - T_{R_0})\Gamma$$

$$= \left(\frac{Q}{Q+k+m} - 1\right)\frac{1}{k+P+m} - \left(\frac{Q}{Q+k} - 1\right)\frac{1}{k}. \tag{10.10}$$

Applying $1 - T_{R_0}$ gives a suppression by k/Q or m/Q, whichever is larger, in the factors in parentheses on the last line of (10.10). This has a minimum of m/Q, which is the desired overall error, but the error degrades as k increases towards Q.

Applying $1 - T_{R_1}$ gives a suppression by m/Q or m/k. (We assume P is of order m.) The intrinsic variable of the large region R_1 is k, and T_{R_1} is designed to give an accurate approximation when $k \sim Q$. But as k approaches R_0 the accuracy of an approximation of Γ by $T_{R_1}\Gamma$ degrades to m/k. But multiplying this error by the previously determined factor of k/Q compensates this, to leave an overall relative error of m/Q.

Notice that the error in $(1 - T_{R_1})\Gamma$ gets even worse if $k \ll m$, because T_{R_1} makes a massless approximation, replacing $1/(k + P + m)$ by $1/k$. By itself, this would give an actual divergence in the integral at $k = 0$. But the $1 - T_{R_0}$ factor applied in this same massless approximation gives a k/Q factor to kill the divergence.

10.3 Sudakov form factor

The fundamental object in our method is the approximator $T_R\Gamma$ for a region R of a graph Γ. We let λ_R be the radial variable, we let $\overline{k}_R$ be the angular variables surrounding R, and we let z_R be the intrinsic variables for R (Secs. 5.5 and 5.7). The approximator must give a good approximation to Γ in the core of the region R, i.e., where λ_R is small and the $\overline{k}_R$ variables are not close to larger regions.

In simple examples, as in Sec. 10.2, the accuracy of T_R only degrades when the intrinsic variable(s) of R approach the PSS of a smaller region. However, when we treat soft gluons, the accuracy of T_R also degrades when the angular variables $\overline{k}_R$ approach *larger* PSSs than R. This issue is responsible for complications in many QCD processes, when they are compared with simple Euclidean problems, like the OPE.

A simple case to illustrate these issues is the Sudakov form factor, i.e., the electromagnetic form factor of an elementary particle at high Q. We defined the Sudakov form
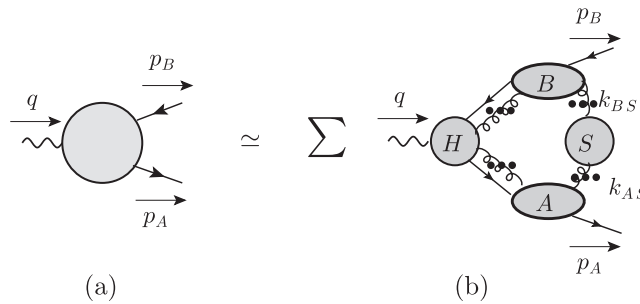
Fig. 10.3. (a) Sudakov form factor. (b) Its leading regions with loop momenta connecting the subgraphs. The dots indicate arbitrarily many gluons exchanged between the neighboring subgraphs. Note that the soft subgraph *S may be empty or may have more than one connected component*. The complete amplitude is approximated by a sum over regions and graphs when the contribution of each region is interpreted as $C_R \Gamma$.

factor and its kinematics in Sec. 5.1.1. Our aims now are to make suitable definitions of the approximators T_R, and to derive factorization. The form factor and its leading regions are shown in Fig. 10.3.

10.3.1 Factorization

We will obtain a factorization property in which the form factor F is the product of a hard factor H, collinear factors A and B for each external quark, and a soft factor S:

$$F = HABS + \text{power-suppressed}, \tag{10.11}$$

each with dependence on only some parameters of F. Later we will redefine the factors so that a square root of S is absorbed into each collinear factor. (We will accompany this by some further redefinitions of A and B.) Then S will not appear in the final factorization formula.

10.3.2 Overall motivation for factorization approach

At this point, I review the rationale for using the factorization approach in QCD. This will indicate the kinds of theorem we need to formulate.

Typically, multiple regions contribute to an amplitude or cross section when there are large momenta. In perturbative calculations, this gives rise to large logarithms which prevent a straightforward use of perturbation theory in QCD. The two logarithms per loop present in many cases like the Sudakov form factor are particularly bothersome.

Moreover, in almost all interesting cases in QCD, some momenta in leading regions have low virtualities, where the effective coupling is large, so that low-order perturbative calculations are inapplicable.

In a factorized formula like (10.11), the different factors are each concerned with a particular kind of 4-momentum. Besides dependence on external kinematic variables, each
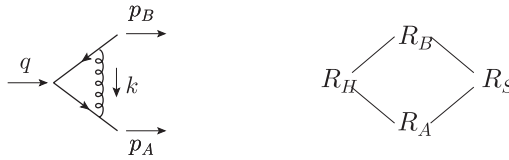
Fig. 10.4. One-loop graph for Sudakov form factor, and the hierarchy of its leading regions. In each case, the name of the region, e.g., "R_S", refers to the category of the gluon's momentum. A line connecting two regions denotes that they are ordered, with the bigger region on the left. Thus the diagram component $R_2 - R_1$ means that $R_2 > R_1$ in the sense defined in Sec. 10.1.2.

factor has dependence on one or more auxiliary parameters (like a renormalization scale). The auxiliary parameters can be roughly characterized as setting the boundaries between kinematic regions. The logarithms can be tamed by deriving evolution equations for the dependence on the auxiliary parameters. The kernels of the evolution equations are free of logarithms in the parameter whose dependence is governed by the evolution equation, and thus the kernels are susceptible to perturbative calculations (and hence *prediction* from first principles).

After the application of evolution equations, we need the individual factors, each at appropriate reference values of the auxiliary parameters. Some factors depend on low momentum scales, and are therefore genuinely non-perturbative in QCD. Others depend only on a single large scale, and therefore are perturbatively calculable in QCD. The non-perturbative quantities in QCD are typified by parton densities. They will be proved to be universal, i.e., the same parton densities appear in many different reactions. As explained in Sec. 9.13, universality underlies much of the predictive power of QCD: The non-perturbative quantities can be measured from a limited set of data, and then predictions are made for a wide variety of other experiments, with the aid of perturbative calculations for hard-scattering coefficients and evolution kernels.

10.3.3 Sudakov: regions for one- and two-loop graphs

As explained in Secs. 5.4.1 and 10.1.3, the regions for a graph can be organized as a hierarchy. To illustrate this, Figs. 10.4 and 10.5 show some important one- and two-loop graphs for the Sudakov form factor together with a representation of the hierarchies of their leading regions. A useful exercise is to check the hierarchies.

10.4 Region approximator T_R for Sudakov form factor

The definition in this section of the region approximator T_R uses the methods of Collins, Rogers, and Staśto (2008).

10.4.1 Decomposition of graph for one region

Consider a particular graph Γ for the Sudakov form factor. A leading region R corresponds to a graphical decomposition of the form of Fig. 10.3(b), with subgraphs which we label H,
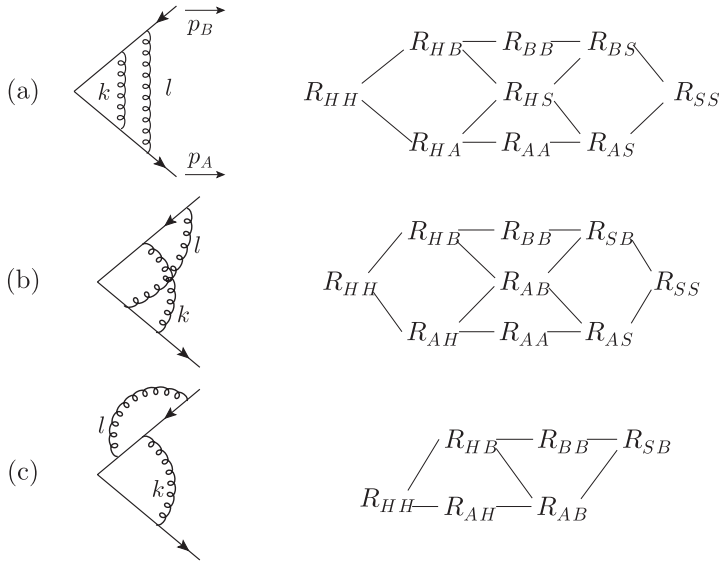
Fig. 10.5. Some two-loop graphs for the Sudakov form factor, and their leading-region hierarchies. The two-lettered code for a region, e.g., in "R_{HS}", refers to the categories of gluon k and gluon l.

A, B, and S.[5] We choose loop momenta coupling the subgraphs as follows. Momenta on external lines of the soft subgraph circulate into one collinear subgraph, round through the hard subgraph and back by the other collinear subgraph. Remaining loops involve momenta from each collinear subgraph entering the hard subgraph and circulating back to the same collinear subgraph. Thus we write the integral for the graph as

$$I = \int dk_{AS} \, dk_{BS} \, dk_{HA} \, dk_{HB} \; H(q, k_{HA} + k_{HAS}, k_{HB} + k_{HBS}, m)$$

$$\times \, A(p_A, k_{HA}, k_{AS}) \, B(p_B, k_{HB}, k_{BS}) \, S(k_{BS}, k_{AS}). \tag{10.12}$$

Here k_{AS} denotes the array of momenta flowing from the A subgraph into the S subgraph, and similarly for k_{BS}. These momenta flow through the hard subgraph, with k_{HAS} and k_{HBS} denoting how the circulating soft momenta are apportioned among lines entering H. The remaining momenta circulating between the H and A subgraphs are k_{HA}, and similarly for k_{HB}. Thus to denote the full set of momenta entering the hard subgraph from each collinear subgraph we use $k_{HA} + k_{HAS}$ and $k_{HB} + k_{HBS}$.

The soft factor is defined to include a momentum-conservation factor for each of its connected components. All loops contained entirely within the separate subgraphs do not need to be indicated explicitly. Although the integrals in (10.12) are commonly of high

---

[5] Note that the use of these symbols is different than in Figs. 10.4 and 10.5, where the symbols refer to particular categories of gluon momentum instead of subgraphs with momenta in a category.

dimension, it is possible that some or all are absent, for example when the soft subgraph is empty, or when only a single line connects a collinear graph to the hard subgraph.

Although to construct the definition of T_R we will examine properties of the graph when the values of momenta correspond to the region under consideration, we do not intend the loop momenta in (10.12) *to be restricted to the region. In that sense,* (10.12) *is an exact expression for the whole Feynman graph. The purpose of this decomposition is simply to provide a convenient notation for use in a general definition of T_R.*

When the momenta are near the PSS of R, some propagator denominators are particularly small. In general, we can make a suitable approximant by expanding in powers of small variables compared with large variables. Since we are concerned here only with the leading power of Q, the first term in the series suffices, i.e., we simply neglect the small variables compared with the large variables.

One complication now arises. As follows from the discussion in Sec. 5.10.2, there are two clashing characterizations of a collinear momentum. One is that it has energy of order Q and low virtuality. The other is that it has high center-of-mass rapidity. The distinction is particularly important when we deal with graphs with a massless gluon, as in QCD, and it is the second, more general, characterization that is more appropriate.

The use of this second definition strongly influences our construction of the region approximator T_R, since it affects the characterization of large and small variables. There can be leading contributions when some gluons are simultaneously soft and collinear, in the sense that all their momentum components are much less than Q and that their rapidities are large.

10.4.2 Definition of T_R

We consider the region R of a graph Γ associated with the decomposition (10.12). We also label momenta of particular lines by their category (soft, collinear-to-A, etc.) at the PSS for the region. The power-counting for the momentum components was given in Sec. 5.7.4.

The basic method to construct the region approximator T_R is to expand to leading power in the radial variable λ_R for the region. This will tend to introduce divergences. Some of the divergences are endpoint divergences, associated with regions R' that are smaller than R; these we will find to be canceled by the subtractions in the definition (10.4) of the region's contribution $C_R\Gamma$. Other divergences arise when we extend loop-momentum integration beyond the immediate neighborhood of R. These are essentially UV divergences removed by conventional renormalization that we include in the definition of T_R.

For simple Euclidean asymptotic problems like the OPE, there are no further divergences. But characteristic of asymptotic problems in Minkowski space with soft gluons are further divergences, which we term rapidity divergences; see the discussion around (10.35) below. We will modify the definition of T_R to cut off rapidity divergences. The evolution equations with respect to the cutoffs are essential to using the factorization theorem, and we will see important applications in Ch. 13. The only place where a modification is needed is in the approximation of soft momenta entering the collinear subgraphs. Later, in Sec. 10.11,

we will reorganize the factorization formula into a form where the cutoffs on rapidity divergences can be removed.

The approximator's definition is made in three stages. The first is to extract the leading power of λ_R in the numerators and denominators of the subgraphs, with modifications to cut off rapidity divergences, and to improve properties of the hard scattering. It is implemented by defining linear projectors on loop momenta: P_{AS}, P_{BS} for soft loop momenta in the A and B subgraphs, and P_{HA}, P_{HB} for collinear and soft loop momenta in the H subgraph. Then certain adjustments of the momenta in H are implemented by non-linear functions R_{HA} and R_{HB}, so that the following replacement is made:

$$
I \mapsto \int \mathrm{d}k_{AS}\,\mathrm{d}k_{BS}\,\mathrm{d}k_{HA}\,\mathrm{d}k_{HB}\ H\left(q, \hat{k}_{HA}, \hat{k}_{HB}, 0\right)
$$

$$
\times\, A\left(p_A, k_{HA}, \hat{k}_{AS}\right) B\left(p_B, k_{HB}, \hat{k}_{BS}\right) S\left(k_{BS}, k_{AS}\right), \tag{10.13}
$$

where

$$
\hat{k}_{AS} = P_{AS}(k_{AS}), \tag{10.14a}
$$

$$
\hat{k}_{BS} = P_{BS}(k_{BS}), \tag{10.14b}
$$

$$
\hat{k}_{HA} = R_{HA} P_{HA}\left(k_{HA} + P_{AS}(k_{HAS})\right) = R_{HA} P_{HA}(k_{HA}), \tag{10.14c}
$$

$$
\hat{k}_{HB} = R_{HB} P_{HB}\left(k_{HB} + P_{BS}(k_{HBS})\right) = R_{HB} P_{HB}(k_{HB}). \tag{10.14d}
$$

It will be a considerable convenience that soft momenta are approximated by exactly zero in the hard subgraph H, which is enforced by defining projectors so that $P_{HA} P_{AS} = P_{HB} P_{BS} = 0$.

The second stage of the definition of T_R is to apply corresponding approximations to the numerator factors in the lines connecting the subgraphs. The final stage is renormalization of UV divergences.

The approximator makes use of some auxiliary vectors to define particular directions in the (t, z) plane:

$$
w_1 = (1, 0, \mathbf{0}_{\mathrm{T}}), \quad w_2 = (0, 1, \mathbf{0}_{\mathrm{T}}), \tag{10.15a}
$$

$$
n_1 = \left(1, -e^{-2y_1}, \mathbf{0}_{\mathrm{T}}\right), \quad n_2 = \left(-e^{2y_2}, 1, \mathbf{0}_{\mathrm{T}}\right). \tag{10.15b}
$$

Thus w_1 and w_2 are light-like vectors corresponding to the external momenta p_A and p_B, while n_1 and n_2 are similar vectors that are slightly space-like. The rapidity parameters y_1 and y_2 are among the auxiliary parameters referred to earlier, for which evolution equations will be derived; initially they are chosen to be comparable to the rapidities y_{p_A} and y_{p_B} of the external on-shell lines. The vectors in (10.15) specify directions, and all their uses will be unchanged if any of the vectors is scaled by a positive non-zero number.

I now present the detailed definitions that make up T_R, leaving some details of the justification to Sec. 10.6.

1. *Soft to collinear-A:* Consider a momentum k_{AS} flowing from A into S. The denominator for a line in A has the form $(k_A + k_{AS}^2) - m^2 = k_A^2 - m^2 + 2k_A \cdot k_{AS} + k_{AS}^2$, where k_A

is a momentum classified as collinear-to-A. From Sec. 5.7.4, the leading power of λ_R is λ_R^2, for the terms k_A^2 and $2k_A^+ k_{AS}^-$. So the basic leading-power approximation for subgraph A is to neglect all but the minus component of k_{AS}, i.e., to make the replacement $k_{AS} \mapsto (0, k_{AS}^-, \mathbf{0}_T)$. To cut off rapidity divergences we then modify the minus component slightly, and define T_R to use the following projector:

$$k_{AS} \mapsto \hat{k}_{AS} = P_{AS}(k_{AS}) = (0, 1, \mathbf{0}_T) \left(k_{AS}^- - e^{-2y_1} k_{AS}^+ \right). \tag{10.16}$$

In covariant form this is

$$\hat{k}_{AS} = P_{AS}(k_{AS}) = \frac{w_2^\mu \, k_{AS} \cdot n_1}{w_2 \cdot n_1}, \tag{10.17}$$

where n_1 and w_2 are defined in (10.15), with y_1 in the definition of n_1 being a large positive rapidity appropriate to the p_A particle. But the precise value of y_1 is not critical; the effect of changes in y_1 will cancel in the complete factorization formula.

The use of k_{AS} in (10.12) treats k_{AS} as the array of loop momenta flowing from A into S. So the above definition is to be applied separately to each of the momenta in the array.

The justification of the exact form of the above projector will be given in Sec. 10.6, including the choice that n_1 is space-like.

2. *Soft to collinear-B:* A similar replacement is applied to soft momenta in the B subgraph, with the roles of plus and minus components exchanged:

$$k_{BS} \mapsto \hat{k}_{BS} = P_{BS}(k_{BS}) = \frac{w_1^\mu \, k_{BS} \cdot n_2}{w_1 \cdot n_2}. \tag{10.18}$$

Naturally y_2 in the definition of n_2 should be a large negative rapidity appropriate to p_B.

3. *Collinear-A and collinear-B to H:* In the hard subgraph H, the basic approximation is to replace momenta $k_{HA} + k_{HAS}$ from the A subgraph by their plus components and momenta $k_{HB} + k_{HBS}$ from the B subgraph by their minus components:

$$P_{HA}(k_{HA}) = \frac{w_1 \, (k_{HA} + \hat{k}_{HAS}) \cdot w_2}{w_1 \cdot w_2} = (k_{HA}^+, 0, \mathbf{0}_T), \tag{10.19a}$$

$$P_{HB}(k_{HB}) = \frac{w_2 \, (k_{HB} + \hat{k}_{HBS}) \cdot w_1}{w_2 \cdot w_1} = (0, k_{HB}^-, \mathbf{0}_T). \tag{10.19b}$$

Hence soft momenta are replaced by zero in the hard subgraph.

4. *Masses in H:* We also normally replace masses by zero in H. Under some circumstances, it is appropriate to retain masses. In that case it is normally appropriate to put on-shell the external massive quark lines of the hard subgraph by modifying P_{HA} and P_{HB}.

5. *Alternative for H:* In applications, like QCD, where the gluon is massless, there can be important contributions from gluons that are soft in the sense of having very low energy, but collinear in the sense of having rapidity comparable to that of p_A or p_B. Such gluons we call "*soft-collinear*". From the point of view of regions and approximations, we will treat them as collinear. They can be external lines of the hard scattering.

To treat them adequately, we modify the definition of the approximator for a hard subgraph: masses are left unapproximated, and the external quark lines of the hard scattering are put on-shell, but now massive. The projectors for Dirac matrix connections between collinear and hard subgraphs are modified to project onto massive wave functions.

After use of Ward identities to extract the extra collinear gluons from the hard subgraph, the modified H subgraph can be replaced by the standard one.

6. *Numerators connecting subgraphs:* We project on the leading-power part of the numerators for Dirac lines and for gluons connecting the H, A, B and S subgraphs as follows:

   (a) For the attachment of a gluon from S to A, insert the following matrix to implement a Grammer-Yennie approximation (modified from (5.51)):

   $$\frac{\hat{k}_{AS}^{\mu} n_1^{\nu}}{k_{AS} \cdot n_1 + i0}. \tag{10.20}$$

   Note that $k_{AS} \cdot n_1 = \hat{k}_{AS} \cdot n_1$. The $i0$ prescription is correct when k_{AS} is defined to flow *out* of the collinear subgraph. The μ index is contracted with the A subgraph and ν with S. We will see that because the *approximated* A subgraph is contracted with the *approximated* momentum $\hat{k}_{AS}$, exact Ward identities can be applied to convert the S-to-A couplings to a Wilson line in direction n_1.

   Thus the following replacement is made on the product of the A and S subgraphs:

   $$A(p_A, k_{AS,1}, \ldots, k_{AS,N})^{\mu_1 \ldots \mu_N} S(k_{AS,1}, \ldots, k_{AS,N})_{\mu_1 \ldots \mu_N}$$

   $$\mapsto A(p_A, \hat{k}_{AS,1}, \ldots, \hat{k}_{AS,N})^{\mu_1 \ldots \mu_N}$$

   $$\times \prod_{j=1}^{N} \frac{\hat{k}_{AS,j,\mu_j} n_{1,\nu_j}}{k_{AS,j} \cdot n_1 + i0} S(k_{AS,1}, \ldots, k_{AS,N})^{\nu_1 \ldots \nu_N}, \tag{10.21}$$

   where the individual momenta of the array k_{AS} are denoted by $k_{AS,j}$. It can be verified that the approximation is accurate to leading power when the k_{AS} momenta are in the soft region: i.e., all components are much less than Q, their rapidities are much lower than those of the collinear-to-A lines, and they are not in the Glauber region.

   (b) Similarly, for the attachment of a gluon from S to B, insert

   $$\frac{\hat{k}_{BS}^{\mu} n_2^{\nu}}{k_{BS} \cdot n_2 + i0}, \tag{10.22}$$

   where the momentum is flowing out of B.

   (c) For a gluon of momentum $k_{HA} + k_{HAS}$ out of H into the A subgraph, make the insertion

   $$\frac{P_{HA}(k_{HA})^{\mu} w_2^{\nu}}{k_{HA} \cdot w_2 + i0}. \tag{10.23}$$

(d) For a gluon of momentum $k_{HB} + k_{HBS}$ out of H into the B subgraph, make the insertion

$$\frac{P_{HA}(k_{HB})^{\mu} w_1^{\nu}}{k_{HB} \cdot w_1 + i0}. \tag{10.24}$$

(e) For a Dirac line *entering* H from B, and for a Dirac line *leaving* H to A, insert the projector $\mathcal{P}_B = \frac{1}{2}\gamma^+\gamma^-$. This and the next item are cases of the Dirac spinor projector derived for the parton model in Sec. 6.1.2.

(f) But for a quark line in the reverse direction, use $\mathcal{P}_A = \frac{1}{2}\gamma^-\gamma^+$.

(g) If a version of the approximator is used in which approximated quark momenta are massive (and on-shell), then the projectors need to be modified, but in such a way that their massless limits exist. See problem 10.8 for possible definitions.

7. *Slightly scaled H:* The approximated hard scattering will generally not obey momentum conservation:

$$\sum_j (k_{HA,\,j}^+, 0, \mathbf{0}_{\mathrm{T}}) + \sum_j (0, k_{HB,\,j}^-, \mathbf{0}_{\mathrm{T}}) \neq q. \qquad \text{(Pre-rescaling)} \tag{10.25}$$

Here j labels the lines carrying the relevant momenta. To correct momentum conservation, we apply overall scaling factors separately to the plus and minus components:

$$k_{HA,\,j}^+ \mapsto \tilde{k}_{HA,\,j}^+ = k_{HA,\,j}^+ \frac{q^+}{\sum_{j'} k_{HA,\,j'}^+}, \tag{10.26a}$$

$$k_{HB,\,j}^- \mapsto \tilde{k}_{HB,\,j}^- = k_{HB,\,j}^- \frac{q^-}{\sum_{j'} k_{HB,\,j'}^-}, \tag{10.26b}$$

a replacement to be made in H alone. Since we defined q to have $\mathbf{q}_{\mathrm{T}} = 0$, no correction of approximated transverse momenta is needed. After the rescaling, we have exact momentum conservation:

$$\sum_j (\tilde{k}_{HA,\,j}^+, 0, \mathbf{0}_{\mathrm{T}}) + \sum_j (0, \tilde{k}_{HB,\,j}^-, \mathbf{0}_{\mathrm{T}}) = q. \qquad \text{(Post-rescaling)} \tag{10.27}$$

The correction factors in (10.26) differ from unity by order m^2/Q^2. This is because the sums of the unapproximated collinear momenta are the external momenta: $\sum_j k_{HA,\,j} = p_A$, $\sum_j k_{HB,\,j} = p_B$, while p_A^-/p_A^+ and p_B^+/p_B^- are of order m^2/Q^2.

8. *Renormalization of extra UV divergences:* As in our treatment of DIS in a non-gauge theory, the approximator short-circuits certain loop-momentum components, thereby inducing UV divergences beyond those renormalized in the Lagrangian. These are removed by UV counterterms defined, for example, in the $\overline{\mathrm{MS}}$ scheme with the use of dimensional regularization. After we obtain factorization, renormalization will behave much like that for the local operators used in the OPE (e.g., Collins, 1984), but now applied to the operators defining the soft and collinear factors. We will generally leave this renormalization implicit until we do actual calculations.
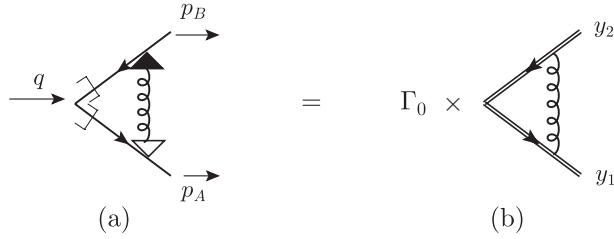
Fig. 10.6. Representation of soft term (10.29) for vertex graph, (a) before and (b) after use of Ward identities.

10.5 One-loop Sudakov form factor

We now illustrate the general definitions given in Sec. 10.4 by applying them to the one-loop graph, Fig. 10.4. The external fermions are on-shell, and the gluon has a non-zero mass m_g. But some issues will be illustrated by taking m_g to zero and/or taking the fermions off-shell.

The graph is

$$\Gamma_1 = \frac{ig^2}{(2\pi)^n} \int d^n k \, \frac{-g_{\kappa\lambda}}{(k^2 - m_g^2 + i0)} \frac{\bar{u}_A \gamma^\kappa (\slashed{p}_A - \slashed{k} + m) \gamma^\mu (-\slashed{p}_B - \slashed{k} + m) \gamma^\lambda v_B}{[(p_A - k)^2 - m^2 + i0] \, [(p_B + k)^2 - m^2 + i0]}, \tag{10.28}$$

where u_A and v_B are the Dirac wave functions for the outgoing quark and antiquark. Its leading regions are R_S, R_A, R_B and R_H, where the subscripts indicate the type of gluon momentum. For a compact notation, the region approximators and the region contributions are written $T_S \stackrel{\text{def}}{=} T_{R_S}$, $C_S \stackrel{\text{def}}{=} C_{R_S}$, etc.

10.5.1 Soft-gluon term C_S

The soft region R_S is a minimal region, so its term is obtained by applying the region's approximator, as defined in the list starting on p. 326:

$$
\begin{aligned}
C_S \Gamma_1 = T_S \Gamma_1 &= \frac{ig^2}{(2\pi)^n} \int d^n k \, \frac{-g_{\kappa\lambda}}{(k^2 - m_g^2 + i0)} \frac{n_1^\kappa}{-n_1 \cdot k + i0} \frac{n_2^\lambda}{n_2 \cdot k + i0} \\
&\quad \times \frac{\bar{u}_A (-\slashed{k}_1)(\slashed{p}_A - \slashed{k}_1 + m) \mathcal{P}_B \gamma^\mu \mathcal{P}_B (-\slashed{p}_B - \slashed{k}_2 + m) \slashed{k}_2 v_B}{[(p_A - k_1)^2 - m^2 + i0] \, [(p_B + k_2)^2 - m^2 + i0]} \\
&= \frac{ig^2}{(2\pi)^n} \int d^n k \, \frac{n_1 \cdot n_2 \, \bar{u}_A \mathcal{P}_B \gamma^\mu \mathcal{P}_B v_B}{(k^2 - m_g^2 + i0)(-n_1 \cdot k + i0)(n_2 \cdot k + i0)}, \tag{10.29}
\end{aligned}
$$

which we write diagrammatically in Fig. 10.6. The hard scattering is just the factor γ^μ; it is surrounded by factors of $\mathcal{P}_B = \frac{1}{2}\gamma^+ \gamma^-$, to project onto the appropriate on-shell massless Dirac wave functions. This is indicated by the hooks in Fig. 10.6(a), just as for the parton model in Fig. 6.4.

From (10.17) and (10.18), the projected gluon momenta in the collinear subgraphs are

$$k_1 = (0, k^- - e^{-2y_1} k^+, \mathbf{0}_{\mathrm{T}}) \quad \text{and} \quad k_2 = (k^+ - e^{2y_2} k^-, 0, \mathbf{0}_{\mathrm{T}}). \tag{10.30}$$

At the ends of the gluon line are applied the Grammer-Yennie approximants (10.20) and (10.22). The result is notated by the arrows at the ends of the gluon in Fig. 10.6(a).

To get the last line of (10.29), we applied the identities $\not{k}_2 = (\not{p}_B + \not{k}_2 + m) - (\not{p}_B + m)$ and $\not{k}_1 = (\not{p}_A - m) - (\not{p}_A - \not{k}_1 - m)$. For each of these, one term gives zero on a Dirac wave function and the other cancels the neighboring quark propagator. The result is represented in Fig. 10.6(b). On the left is a lowest-order vertex

$$\Gamma_0 = \bar{u}_A \mathcal{P}_B \gamma^\mu \mathcal{P}_B v_B. \tag{10.31}$$

On the right, the two double lines represent the $gn_1/(-n_1 \cdot k + i0)$ and $-gn_2/(n_2 \cdot k + i0)$ factors in (10.29). With two changes, these factors are just as the first-order application of the Feynman rules, Figs. 7.10 and 7.11, for Wilson lines, as in the gauge-invariant definition of a parton density, (7.40). One change is that we have two Wilson-line segments in different directions. The other is that the Wilson line in direction n_2 has a reversed sign of the coupling; physically this is because it approximates an outgoing antiquark, with the opposite charge to a quark.

We therefore identify $C_S \Gamma_1$ as Γ_0 times the one-loop value of the vacuum matrix element of two Wilson lines of opposite charge, joined at the origin:

$$\text{soft factor}_{\text{ver. 1}} = \langle 0 | \, W(\infty, 0, n_2)^\dagger \, W(\infty, 0, n_1) \, | 0 \rangle, \tag{10.32}$$

where W is defined by

$$W(\infty, 0; n) = P \left\{ e^{-i g_0 \int_0^\infty \mathrm{d}\lambda \; n \cdot A_{(0)\alpha}(\lambda n) \, t_\alpha} \right\}. \tag{10.33}$$

Notice that this definition uses the bare coupling and field, as needed to get the correct gauge-transformation properties. A factor of a representation matrix t_α of the gauge group appears in the exponent to give a formula that is also appropriate for a non-abelian theory. In the simpler case of an abelian gauge theory, one omits the t_α factor, and one can replace the coupling and field by their renormalized counterparts, since $g_0 A_{(0)} = g \mu^\epsilon A$ in an abelian theory. The opposite charge of the Wilson line for direction n_2 is implemented by a hermitian conjugation in (10.32).

After we formulate a factorization theorem, we will see that the formula for the one-loop soft factor, $C_S \Gamma_1$, is sufficient to determine almost completely the Wilson-line definition. However, we will modify some details of the definition. Hence we include a version subscript on the left-hand side of (10.32). The matrix element in (10.33) is a primary ingredient in the later redefinitions.

The approximations used to give $C_S \Gamma_1$ are valid in the soft region, provided we deform the integration contour out of the Glauber region. As we will show in Sec. 10.6.4, the choice of space-like vectors (10.15b) for n_1 and n_2, and of the $i0$ prescriptions in (10.29) is needed to be compatible with the contour deformation.
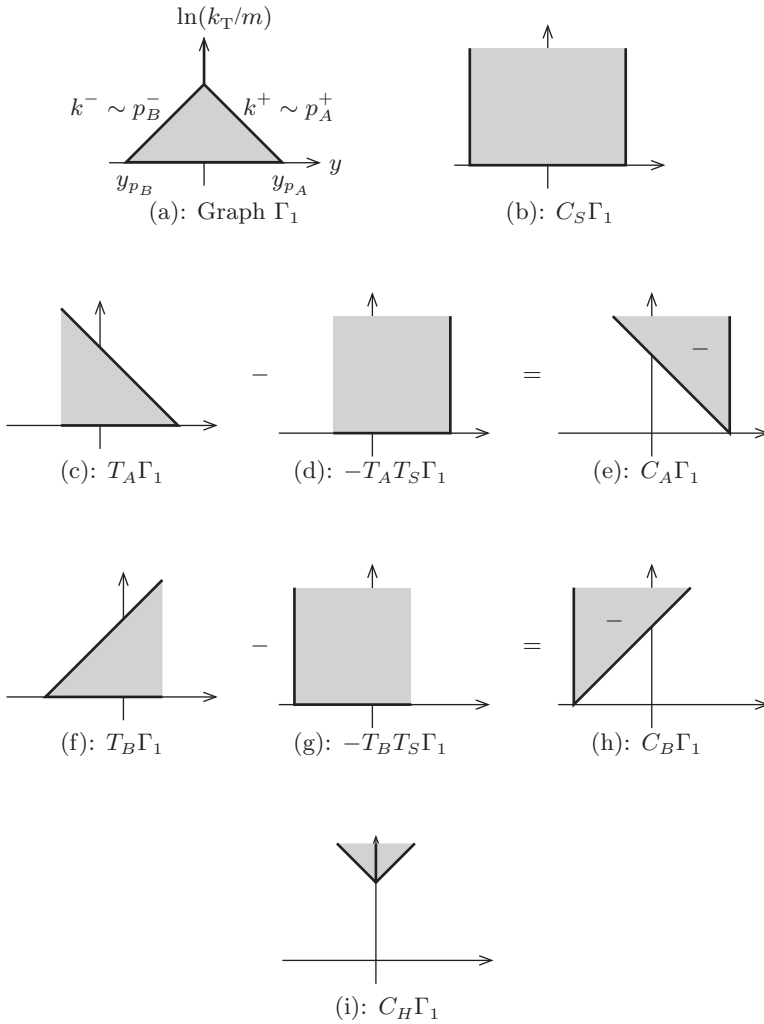
Fig. 10.7. Main regions in y and k_T for one-loop Sudakov form factor. The shaded areas indicate where there are leading-power contributions, and the thick lines show where there is a cutoff. A lack of a thick edge to a shaded area indicates that the area goes to infinity. These diagrams are for the original graph and for various terms in the decomposition of the graph by regions, with subtractions. The $-$ signs on a shaded region indicate a negative contribution. The top of the triangle in graph (a) is at $\ln(k_T/m) = \ln(Q/m)$.

10.5.2 (Double) leading-logarithm approximation

To understand the nature of the approximation, we make plots in the space of $\ln k_T$ and y, where y is the gluon rapidity $y = \frac{1}{2}\ln|k^+/k^-|$, and examine where the main contributions arise, both for the original graph and for terms contributing to each $C_R\Gamma_1$. These are shown in Fig. 10.7.

The variables are logarithmic in ordinary momentum components. With respect to these variables, we will find that the original integral Γ_1 has a uniform integrand in the interior of the triangle in Fig. 10.7(a). This uniform value is in fact that of the soft approximation $C_S\Gamma_1$. Outside of the triangle, the integrand falls off, so that a first approximation to the original graph is the uniform integrand times the area of the triangle, which is a coefficient times $\ln^2 Q$. This gives the double leading-logarithm approximation (LLA) to Γ_1. The edges and corners of the triangle give non-leading logarithms, and remaining contributions are in fact power-suppressed.

We will see that the soft term, $C_S\Gamma_1$, also has important contributions from outside the triangle. But we will find that these other contributions cancel corresponding parts of the terms $C_R\Gamma_1$ for other regions R; see Fig. 10.7(b–i). The total reproduces Γ_1 up to a power-suppressed remainder.

In the core of the soft region the original graph Γ_1 is correctly approximated by the soft term $C_S\Gamma_1$, and the approximation remains correct when n_1 and n_2 are replaced by light-like vectors, to give

$$\frac{ig^2}{(2\pi)^4} \int_{\text{core of soft region}} \mathrm{d}^4k \, \frac{\bar{u}_A \mathcal{P}_B \gamma^\mu \mathcal{P}_B v_B}{(k^2 - m_g^2 + i0)(-k^- + i0)(k^+ + i0)}, \tag{10.34}$$

where we now work in four-dimensional space-time. We apply contour integration to the k^- integral,[6] which gives a non-zero result only for $k^+ > 0$. By closing the contour on the gluon pole and changing variables from k^+ to $y = \frac{1}{2}\ln|k^+/k^-|$ and from $\boldsymbol{k}_\mathrm{T}$ to $\ln k_\mathrm{T}$, we obtain:

$$\frac{-g^2}{4\pi^2} \int_{\text{core of soft region}} \mathrm{d}\ln k_\mathrm{T}\, \mathrm{d}y\; \bar{u}_A \mathcal{P}_B \gamma^\mu \mathcal{P}_B v_B\; \frac{k_\mathrm{T}^2}{k_\mathrm{T}^2 + m_g^2}$$

$$\simeq \frac{-g^2}{4\pi^2} \int_{\text{core of soft region}} \mathrm{d}\ln k_\mathrm{T}\, \mathrm{d}y\; \bar{u}_A \mathcal{P}_B \gamma^\mu \mathcal{P}_B v_B. \tag{10.35}$$

The right-hand form is obtained by restricting attention, for reasons that will soon be apparent, to large enough k_T that we can neglect the gluon mass.

Original graph

The result has a uniform integrand, and so we estimate the size of the original unapproximated graph by the area of the relevant part of the plane of $\ln k_\mathrm{T}$ and y. We will find that the integrand falls off relative to (10.35) near the edges of the triangle in Fig. 10.7(a), so the area is that of the triangle. We examine the limits provided by each propagator denominator in turn.

In the gluon propagator, the gluon mass effectively cuts off the k_T integral at m_g, and this gives the lower boundary of the triangle, at $\ln(k_\mathrm{T}/m_g) \simeq 0$. This is a fuzzy cutoff, not a sharp cutoff. Given that the dimensions of the triangle are of order $\ln(Q/m)$, the width of the fuzzy edge relative to the triangle is small, of order $1/\ln(Q/m)$.

---

[6] Strictly speaking, this application of contour integration includes values of k^- all the way to infinity, i.e., outside the soft region. To see that this is not a problem, observe that the contribution we use in later equations is from the gluon pole. The errors, i.e., the non-pole terms, are from a non-soft region which does not concern us here.

The A-quark denominator (after setting k on the gluon mass-shell from the contour integration and after setting $p_A^2 = m^2$) is

$$(p_A - k)^2 - m^2 = -2p_A^+ k^- - 2p_A^- k^+ + m_g^2. \tag{10.36}$$

We write $2p_A^+ k^-$ in terms of rapidities as $m\sqrt{k_T^2 + m_g^2}\, e^{y_{p_A} - y}$, where y_{p_A} is the rapidity of the A quark, also taken as the rapidity of the n_1 vector. The simplest soft approximation replaces the denominator by $-2p_A^+ k^-$. The second term in the denominator becomes equally important when the rapidity of the gluon is comparable to that of p_A, thereby providing a cutoff requiring $y \lesssim y_{p_A}$. Next, in the unapproximated graph, the k^- poles are all in the lower half plane if $k^+ > p_A^+$; this limits k^+ to be less than p_A^+. The m_g^2 term in (10.36) provides no stronger constraint.

Similar limits are associated with the B quark.

If the gluon mass is comparable to the quark mass, as we will assume for the moment, then the limits $k_T \gtrsim m$, $k^+ \lesssim p_A^+$, and $k^- \lesssim p_B^-$ dominate, giving the triangle in Fig. 10.7(a). The two diagonal lines give $y_{p_B} + \ln(k_T/m) \lesssim y \lesssim y_{p_A} - \ln(k_T/m)$, which intersect at $k_T \sim Q$.

But when the gluon mass is made small or zero (as in QCD perturbation theory), the range of k_T extends down, and other limits become important.

Finally, the graph has a renormalized UV divergence for $k_T \gg Q$. We assign this to the line going vertically up from the top vertex of the triangle.

The area of the triangle is $\frac{1}{2}(y_{p_A} - y_{p_B})\ln(Q^2/m^2) = \frac{1}{2}\ln^2(Q^2/m^2)$, which gives the leading-logarithm approximation

$$\text{LLA of } \Gamma_1 = \frac{-g^2 \ln^2(Q^2/m^2)}{16\pi^2}\, \bar{u}_A \mathcal{P}_B \gamma^\mu \mathcal{P}_B v_B. \tag{10.37}$$

This has two logarithms for a one-loop graph, unlike the case for ordinary renormalization-group (RG) logarithms, which are one per loop. At high energy the approximated vertex $\bar{u}_A \mathcal{P}_B \gamma^\mu \mathcal{P}_B v_B$ equals the unapproximated vertex $\bar{u}_A \gamma^\mu v_B$, up to a power-suppressed correction.

The effects of the cutoffs are important only in a finite range of y and $\ln k_T$ near the edges of the triangle. Thus they do not affect the double logarithm. At large Q^2, the sides of the triangle contribute single logarithms, while the vertices contribute constants. The vertical line above the triangle gives an RG single logarithm. Further contributions are suppressed by a power of Q.

All-orders sum of LLA

This line of argumentation can be extended to higher loops, to give the leading logarithms (Sudakov, 1956; Jackiw, 1968) for every order of perturbation theory. These form an exponential series. If the assumption is made that it is sufficient to retain the leading logarithm in each order, then one obtains the LLA for the form factor:

$$F \simeq e^{-g^2 \ln^2(Q^2/m^2)/(16\pi^2)}\, \bar{u}_A \mathcal{P}_B \gamma^\mu \mathcal{P}_B v_B. \tag{10.38}$$

We will derive this from our general factorization approach in Sec. 10.11.5. The result given above is for the case of a massive gluon with on-shell external quarks, and was first found
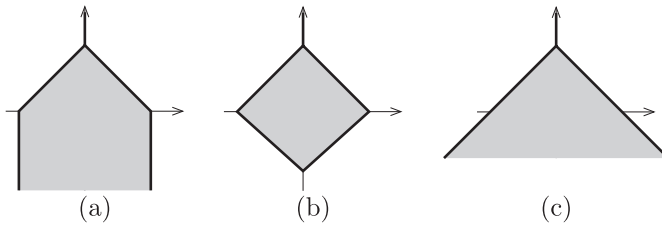
Fig. 10.8. Modifications to Fig. 10.7(a) when: (a) the gluon mass is zero; (b) the gluon mass is zero but the external quarks are off-shell; (c) the quark and the gluon masses are both zero, and the external quarks are on-shell.

by Jackiw (1968). As we will see below, the case of a massless gluon with off-shell external quarks has double the coefficient of the double logarithm, and this was what Sudakov (1956) actually calculated.

At large Q the LLA form factor drops faster than any power of Q. This obviously indicates that power-law corrections might dominate, for sufficiently large Q. However, without further information, there is no guarantee that non-leading logarithms have to fall into the same pattern of summing to a strongly decreasing function of Q. For example, as a hypothetical example, if the non-leading logarithms consisted of a single term g^2, this would be non-vanishing at large Q, and would dominate the LLA. In some analogous problems in QCD (Ch. 13) such a phenomenon does occur, a standard example being the Drell-Yan cross section at small transverse momentum; the LLA does not even get correct the qualitative behavior of the cross section. The factorization approach provides a much more systematic and powerful approach to dealing with these issues.

10.5.3 Massless gluon; off-shell external quarks

The above estimates assumed that the gluon and quark masses are comparable, and that the external quarks are on-shell. But in QCD the gluon is massless. Although a massive gluon might be considered more representative of the real physics of a theory with quark and gluon confinement, perturbative calculations definitely need a massless gluon. Moreover applications to QED require a massless photon instead. We will also need to consider vertex graphs embedded in bigger graphs, so it is also useful to understand the effect of taking the external quarks off-shell.

Figure 10.8(a) shows the effect of setting $m_g = 0$, which is to remove the lower cutoff on k_T. Thus a leading contribution occurs all the way to $k_T = 0$, or minus infinity on a logarithmic scale. As for the rapidity range at low k, the dominant restriction is caused by the rapidities of the external quarks, which give the lower vertical lines. The integral has a divergence, which is a conventional IR divergence, as in QED, with a coefficient that grows with energy like $y_{p_A} - y_{p_B}$.

The IR divergence arises from the $1/(k^- k^+)$ factor in the soft approximation. If we now set the external quarks off-shell, there is an extra term in the quark denominators. This cuts off the k_T integral at the lower end. If the external quark virtuality is of the order of

the quark mass, i.e., m^2, the result is shown in Fig. 10.8(b). There are effective cutoffs at k^- and k^+ of order m^2/Q. The leading-logarithm result comes from the diamond-shaped region, which has twice the area of the triangle in the massive gluon case, thereby doubling the coefficient of the double logarithm.

The general factorization theory we will establish requires the use of Ward identities. In a real physical quantity, we must combine the off-shell form factor with the contributions from other graphs, so the off-shell form factor does not represent the final result for a physical quantity.

Finally there is the case of the on-shell form factor with all particles massless. In that case, there is no longer a cutoff caused by the rapidities of the external lines, so we have the region shown in Fig. 10.8(c), where we effectively have a doubly logarithmic divergence composed of both IR and collinear divergences.

10.5.4 Region for $C_S \Gamma_1$

In contrast to the actual denominators of the quark propagators, the approximated eikonal denominators $(n_2 \cdot k + i0)(-n_1 \cdot k + i0)$ in the soft term C_S provide cutoffs only at the rapidities of the Wilson line. As illustrated in Fig. 10.7(b), the limits on gluon rapidity, $y_2 \lesssim y \lesssim y_1$, are the same at all k_T. We choose the rapidities of n_1 and n_2 to be approximately the same as the rapidities of the external quark lines p_A and p_B. The soft term forms a good approximation at small y and k_T. It is most accurate at the center of the bottom line in Fig. 10.7(a) and (b), and in fact is equally good for even smaller k_T. The approximation degrades as one approaches the upper lines of the triangle; one can characterize these lines as where the error in the soft term is around 100%.

The soft term obviously contributes in a region where the original graph does not. This is above the triangle, and therefore where at least one of the following holds: the energy of the gluon is large, its rapidity is large, and/or its transverse momentum is large. These all concern other regions than the soft region. Compensation for the extra area for the soft term will be obtained from subtraction terms in the terms for regions bigger than the soft region.

We can apply the same area argument as we used for the LLA for the original graph. There is evidently an infinity (multiplied by $y_1 - y_2$) for the infinite range of k_T. This can be regulated dimensionally and renormalized, although we will not exhibit the calculation yet.

Our general proof will require us to understand the errors in the soft approximation more systematically. To do this we return to ordinary non-logarithmic momentum space. The PSSs forming the skeletons of the leading regions are shown in Fig. 10.9(a). The relative error in approximating the integrand is

$$\frac{|C_S I_1 - I_1|}{\|C_S I_1\|} = O\left(\frac{|k^+|}{p_A^+}, \frac{|k^-|}{p_B^-}, e^{-2(y_{p_A} - y)}, e^{-2(y - y_{p_B})}\right). \tag{10.39}$$

Here I_1 denotes the integrand. One might expect the denominator to be just the absolute value $|C_S I_1|$. But we use the double bars, $\|C_S I_1\|$, to indicate that in a more general situation
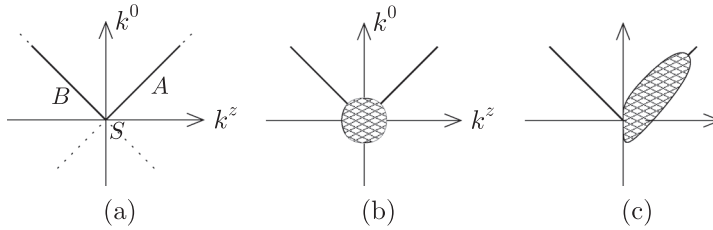
Fig. 10.9. (a) Leading PSSs for one-loop Sudakov form factor. (b) Neighborhood of S for evaluating errors in soft approximation. (c) Neighborhood of A for evaluating errors in collinear-to-A approximation. The squashing on the left indicates that we restrict attention to positive rapidity.

a modification is needed. The problem is that there may be what we can term accidental cancellations; for example, a numerator might have a variable sign, with necessarily a zero at some place in the integration. We wish to use the general order of magnitude of the integrand, for which we use the power-counting estimate of $C_S I_1$, obtained by the methods of Sec. 5.8, with avoidance of any accidental cancellations. The result is denoted $\|C_S I_1\|$. We also use the approximated integrand $C_S I_1$ in $\|C_S I_1\|$, rather than the original integrand I_1.

The right-hand side of (10.39) simply comes from listing the sources of error in the soft approximation, i.e., from examining the terms in the quark denominators and numerators that were neglected in making the soft approximation. The first two terms simply measure distance from the center of the soft region, viewed in the center-of-mass frame; these sources of error are roughly constant on surfaces such as those in Fig. 10.9(b) surrounding S. In a purely Euclidean asymptotic problem, this would be the whole story.

But in a Minkowski-space problem, such as ours, the errors worsen as the rapidity of the gluon gets large, and approaches the A and B lines. The errors are given quantitatively by the last two terms in (10.39). These are of order m^2/Q^2 when the gluon rapidity y is small. But when the gluon rapidity is comparable to that of one of the external quarks, the errors become of order unity.

10.5.5 Why integrate $C_S \Gamma_1$, etc., over all k?

Given that $C_S \Gamma_1$ has important contributions from a much broader range of loop momentum than has Γ_1, it is natural to want to restrict the integration to, for example, the triangular range in Fig. 10.7(a). Nevertheless we define $C_S \Gamma_1$ (and all other C_R) to have an integral over *all* loop momenta. The combination of $C_S \Gamma_1$ with terms for other leading regions will not only cancel the large excess regions, but will correct the inaccuracies in the soft approximation at the edges of the triangle. Then the sum over $C_R \Gamma_1$ will give a complete and useful representation of the leading-power part of Γ_1.

The reasons for not using cutoffs (beyond those given by the finite rapidities of the Wilson lines) are as follows. To get a systematic treatment, we need to have operator definitions for the factors in the factorization theorem. An example definition is (10.32),

whose main one-loop graph gives $C_S\Gamma_1$. A cutoff on the loop momentum k would require an unpleasantly complicated operator. It is not known how to do this and combine it with the Ward identities that we use later. Proving Ward identities needs shifts in loop momenta and uses gauge-invariance properties of the operators; these are difficult to make consistent with a cutoff. Instead, without cutoffs we are led directly to simple Wilson-line operators whose gauge-invariance properties are obvious.

10.5.6 Collinear-A term C_A

We now construct $C_A\Gamma$, corresponding to the gluon being collinear to p_A. First we just apply the approximator for region R_A. Using the definitions in the list starting on p. 326 we get

$$
\begin{aligned}
T_A\Gamma_1 &= \frac{ig^2}{(2\pi)^n}\int d^n k \,\frac{-g_{\kappa\lambda}}{(k^2-m_g^2+i0)}\,\frac{w_2^\lambda}{w_2\cdot k+i0} \\
&\quad \times \frac{\bar u_A\gamma^\kappa\,(\slashed p_A-\slashed k+m)\,\mathcal P_B\gamma^\mu\,(-p_B^-\gamma^+-\gamma^-k^+)\,\gamma^- k^+\mathcal P_B v_B}{[(p_A-k)^2-m^2+i0]\,[2p_B^-k^++i0]} \\
&= \frac{ig^2}{(2\pi)^n}\int d^n k\,\frac{-g_{\kappa\lambda}}{(k^2-m_g^2+i0)}\,\frac{\bar u_A\gamma^\kappa\,(\slashed p_A-\slashed k+m)\,\mathcal P_B\gamma^\mu\mathcal P_B(-w_2^\lambda)v_B}{[(p_A-k)^2-m^2+i0]\,(w_2\cdot k+i0)}. \quad (10.40)
\end{aligned}
$$

The collinear approximant changes the quark denominator $(p_B+k)^2-m^2$ to $2p_B^-k^+$, because in the hard subgraph it replaces p_B and k by massless vectors in the minus and plus directions, and sets masses to zero. Examining the neglected terms $2p_B^+k^-$ and k^2, with the knowledge that $2k^+k^-$ and k_T^2 are comparable shows that the relative errors in this approximation are of order $e^{-2(y-y_{p_B})}$ and $e^{-(y-y_{p_B})}k_T/m$. Thus the approximant is accurate when the gluon rapidity is much larger than the rapidity of the B line. There is also a degradation for large $k_T\gg m$, but that concerns the hard-gluon region, to be treated later.

The region of (y,k_T) space for $T_A\Gamma_1$ is shown in Fig. 10.7(c). Since the eikonal denominator $w_2\cdot k$ is k^+, without an additional k^- term, the integral has a rapidity divergence, where the rapidity of the gluon goes to negative infinity.

Our aim is to construct a term for the collinear-to-A region such that $C_A\Gamma_1+C_S\Gamma_1$ is accurate over the whole of the soft and collinear-to-A regions. Observe both of the soft term and the collinear approximation contribute in each other's regions. So we compensate the double counting by subtracting

$$
T_A T_S\Gamma_1 = \frac{ig^2}{(2\pi)^n}\int d^n k\,\frac{-g_{\kappa\lambda}}{(k^2-m_g^2+i0)}\,\frac{n_1^\kappa(-w_2^\lambda)\,\bar u_A\mathcal P_B\gamma^\mu\mathcal P_B v_B}{(-n_1\cdot k+i0)\,(w_2\cdot k+i0)}. \quad (10.41)
$$

The $n_2/(n_2\cdot k+i0)$ factor of $T_S\Gamma_1$ is in the hard subgraph with respect to the collinear-to-A approximator T_A. Hence applying T_A, defined by (10.19a) and (10.23), changes n_2 to the light-like vector w_2.

We therefore define the term for the A region by

$$C_A \Gamma_1 = T_A (1 - T_S) \Gamma_1$$

$$= \frac{ig^2}{(2\pi)^n} \int d^n k \, \frac{-g_{\kappa\lambda}}{(k^2 - m_g^2 + i0)} \left[\frac{\bar{u}_A \gamma^\kappa (\not{p}_A - \not{k} + m)}{(p_A - k)^2 - m^2 + i0} - \frac{\bar{u}_A n_1^\kappa}{-n_1 \cdot k + i0} \right]$$

$$\times \frac{(-w_2^\lambda)}{(w_2 \cdot k + i0)} \, \mathcal{P}_B \gamma^\mu \mathcal{P}_B v_B. \tag{10.42}$$

This results in the cancellation of the rapidity divergence, justifying our use of a light-like vector in the collinear approximant. The cancellation is because the soft approximant on the A side is accurate when the gluon has large negative rapidity relative to p_A. Thus we get a cancellation in the square-bracket term in (10.42) with the result going to zero as the gluon's rapidity goes to minus infinity.

The placement of the Dirac projectors $\mathcal{P}_B$ is also critical to making the formalism work correctly.

The result is that the $C_A \Gamma_1$ term is power-suppressed in the soft region; Fig. 10.7(e). The combination of the terms constructed so far, $C_S \Gamma_1 + C_A \Gamma_1$, gives a good approximation to Γ_1 over the whole of the soft and the collinear-A regions, with a restriction to the positive rapidity side.

We can see this by observing that the remainder is $\Gamma_1 - C_S \Gamma_1 - C_A \Gamma_1 = (1 - T_A)(1 - T_S) \Gamma_1$. The $1 - T_S$ factor gives a suppression basically by a power of $|k|/Q$ but with a degradation to $e^{-(y_{p_A} - y)}$ as we go around the soft PSS and approach the PSS A, given that y_1 is close to y_{p_A}. At this point we restrict to positive gluon rapidity, leaving negative rapidity to our treatment of $C_B \Gamma_1$. The $1 - T_A$ factor gives a suppression e^{-y}, when $k_T \lesssim m$. At the soft end of the A region, this compensates the worsening of $1 - T_S$ factor. It also gives a power-suppression over the rest of the A region, a power of k_T/Q. Thus we get surfaces of constant error for $C_S \Gamma_1 + C_A \Gamma_1$ as symbolized in Fig. 10.9(c).

The collinear-to-A term itself is suppressed in the soft region, because of the $1 - T_S$ factor, as illustrated in Fig. 10.7(e). Thus for central rapidity only the C_S term is needed to get a good approximation to Γ_1, which it was constructed to do.

Furthermore, the soft subtraction has ensured that the C_A term is also suppressed in the whole of the opposite collinear region. This is an example of a general result critical to our general treatment of overlapping regions: C_A is suppressed both in regions smaller than A, i.e., S, and in regions that overlap with it, in this case the B region.

A generally applicable argument is that in applying T_A we made the first term in the expansion of the B propagator in powers of k^- and k_T. In $T_A (1 - T_S) \Gamma_1$, the $1 - T_S$ factor gives a suppression for small k^+ and k_T from its application to the A side. Going to the B region involves extrapolating the common B-side factor to large k^-. The suppression at small k^+ and k_T continues to apply.

Effectively, once the approximator for the A region, T_A, is applied, the power-counting in the B region corresponds to that for the intersection of the two overlapping regions, i.e., $A \cap B = S$.

In contrast to these cancellations, there is a contribution in the upper region in Fig. 10.7(e), where the gluon rapidity is positive, but its k^+ is much larger than p_A^+. Such a contribution is not present in the original graph, but is an artifact of the soft subtraction, in the term $-T_A T_S \Gamma_1$, as is the divergence when $k_T \to \infty$. Strange though this contribution might appear, it will allow us to derive convenient evolution equations by differentiating with respect to the rapidity cutoffs associated with the vertical lines in Fig. 10.7(b), (e), and (h). When we add C_S, C_A, and C_B, there is a cancellation of these extra contributions for the case that $k_T \lesssim Q$. This leaves only the region $k_T \gtrsim Q$, which is the province of the hard region H, which we have yet to treat, and whose double-counting subtractions will compensate for the incorrect value of $C_S + C_A + C_B$ in the hard region. There is also an actual divergence as $k_T \to \infty$, which we remove by UV renormalization, which will correspond to conventional UV renormalization defining the operators used to construct the soft and collinear factors in the factorization property.

Note that when the transverse momentum is large, $k_T \gg Q$, there is also an important region of *negative* gluon rapidity. This is surprising given that $C_A \Gamma_1$ is intended to deal with gluons that are collinear to p_A, i.e., of positive rapidity. But the problematic region is of hard momenta, and so its full treatment will also bring in the term $C_H \Gamma_1$, whose subtraction terms will correct the apparently problematic regions.

10.5.7 Collinear-B term C_B

The collinear-to-B term is constructed exactly similarly to the collinear-to-A term:

$$
\begin{aligned}
C_B \Gamma_1 &= T_B (1 - T_S) \Gamma_1 \\[6pt]
&= \frac{i g^2}{(2\pi)^n} \int \mathrm{d}^n k \, \frac{-g_{\kappa\lambda}}{(k^2 - m_g^2 + i0)} \frac{\bar{u}_A \mathcal{P}_B \gamma^\mu \mathcal{P}_B w_1^\kappa}{-w_1 \cdot k + i0} \\[6pt]
&\quad \times \left[\frac{(-\not{p}_B - \not{k} + m)\gamma^\lambda v_B}{(p_B + k)^2 - m^2 + i0} - \frac{-n_2^\lambda v_B}{n_2 \cdot k + i0} \right].
\end{aligned}
\tag{10.43}
$$

The contributing regions for this term and its components, shown in Fig. 10.7(f)–(h), are, naturally, a mirror image of those for the A region.

Just as before, the sum of the soft and collinear-to-B terms, i.e., $C_S \Gamma_1 + C_B \Gamma_1$, gives a good approximation in the combination of the S and B regions. We next observe that each of $C_A \Gamma_1$ and $C_B \Gamma_1$ is suppressed in both the central soft region and the opposite collinear region. Thus we can add all three terms to get $C_S \Gamma_1 + C_A \Gamma_1 + C_B \Gamma_1$ and the result provides a good approximation to Γ_1 over all three regions, including both positive and negative rapidity.

10.5.8 Hard term C_H

The only degradation in $C_S \Gamma_1 + C_A \Gamma_1 + C_B \Gamma_1$ as an approximation to Γ_1 occurs as we move away from the combined $S \cup A \cup B$ regions, i.e., as we go into the hard region H of large transverse momenta and of virtualities of order Q^2. We define the approximator T_H

for this region to make a massless approximation. As before, we avoid double counting in the C_H term specific to this region by applying the approximator to Γ_1 only after subtracting the contributions from smaller regions, i.e.,

$$C_H\Gamma_1 = T_H(\Gamma_1 - C_S\Gamma_1 - C_A\Gamma_1 - C_B\Gamma_1)$$

$$= T_H(1 - T_A - T_B)(1 - T_S)\Gamma_1. \tag{10.44}$$

We have seen that $C_S\Gamma_1 + C_A\Gamma_1 + C_B\Gamma_1$ gives a good approximation to Γ_1 near the combined S, A, and B regions, so that $\Gamma_1 - C_S\Gamma_1 - C_A\Gamma_1 - C_B\Gamma_1$ is power-suppressed in the distance to any of these regions. Thus the remaining contribution is when the momenta are hard, i.e., for k_T of order Q or larger, i.e., in the H region. So we define the approximator T_H for this region to set masses to zero, and to make p_A and p_B massless. It also replaces the n_1 and n_2 vectors (in the definition of T_S) by light-like versions: $n_1 \mapsto w_1 = (1, 0, \mathbf{0}_T)$, and $n_2 \mapsto w_2 = (0, 1, \mathbf{0}_T)$. The soft term $T_S\Gamma_1$ and the soft subtractions in $C_A\Gamma_1$ and $C_B\Gamma_1$ now have the same light-like vectors, so they combine to a single added term, and we get

$$C_H\Gamma_1 = \frac{ig^2}{(2\pi)^n} \int d^n k \frac{-1}{(k^2 + i0)} \bar{u}_A \mathcal{P}_B \left\{ \frac{\gamma^\kappa (p_A^+ \gamma^- - \slashed{k})\gamma^\mu(-p_B^-\gamma^+ - \slashed{k})\gamma_\kappa}{[-2p_A^+k^- + k^2 + i0][2p_B^-k^+ + k^2 + i0]} \right.$$

$$- \frac{\gamma^+(p_A^+\gamma^- - \slashed{k})}{-2p_A^+k^- + k^2 + i0}\gamma^\mu \frac{-1}{k^+ + i0} - \frac{1}{-k^- + i0}\gamma^\mu \frac{(-p_B^-\gamma^+ - \slashed{k})\gamma^-}{2p_B^-k^+ + k^2 + i0}$$

$$\left. + \frac{1}{-k^- + i0}\gamma^\mu \frac{-1}{k^+ + i0} \right\} \mathcal{P}_B v_B. \tag{10.45}$$

10.5.9 UV divergences

The original graph Γ_1 has a UV divergence. This is canceled in a complete calculation of the one-loop vertex when the correct definition is used for the current at the photon vertex. The current is a Noether current for a conserved charge, with unit coefficient when the current is expressed in terms of bare fields: $j^\mu = \bar{\psi}_0\gamma^\mu\psi_0$. In terms of renormalized fields, it has a factor Z_2: $j^\mu = Z_2\bar{\psi}\gamma^\mu\psi$, and this factor of Z_2 cancels the divergences in the loop calculations. This is a well-known standard result in renormalization theory.[7] This results in a non-zero anomalous dimension associated with the one-loop graph. In the full form factor calculation, we must also allow for the LSZ residue factors for the external on-shell quarks. These are also associated with Z_2, but inversely, so that the complete form factor is RG invariant.

However, the hard, collinear and soft factors in (10.11) all have their own UV renormalization and need renormalization that is different from that in the current itself. This is illustrated by the one-loop quantities computed above, $C_S\Gamma_1$, $C_A\Gamma_1$, $C_B\Gamma_1$, and $C_H\Gamma_1$. Their UV divergences are associated with new vertices: where a Wilson line attaches to an ordinary field (in $C_A\Gamma_1$ and $C_B\Gamma_1$) and where two Wilson lines attach to each other (in

---

[7] However, there are some complications beyond the ones seen in most textbooks. See Collins, Manohar, and Wise (2006) for a correct treatment.

$C_S\Gamma_1$ and the subtractions in $C_A\Gamma_1$ and $C_B\Gamma_1$). As we will see, all these divergences are logarithmic. Our ultimate definitions of the region contributions include renormalization counterterms to remove the UV divergences.

Finally, $C_H\Gamma_1$ is formed from the original graph together with subtractions for the smaller regions, all taken in the massless limit. Therefore, in the sum over all regions, i.e., $C_S\Gamma_1 + C_A\Gamma_1 + C_B\Gamma_1 + C_H\Gamma_1$, the extra UV divergences cancel to leave just the same UV divergence as in Γ_1. This is necessary if this sum is to give a correct large-Q asymptote for Γ_1.

We will treat the extra UV divergences and their renormalization in more detail later.

But for now we just examine one simple case, the UV divergence for $C_S\Gamma_1$, and indicate some interesting properties, notably that it depends on the directions of the Wilson lines, and more specifically on the hyperbolic angle between them.

In the formula (10.29) for $C_S\Gamma_1$, the integrals over the longitudinal momenta are readily performed, e.g., by contour integration over k^- followed by an elementary integral over k^+. Without the UV counterterm

$$\frac{C_S\Gamma_1}{\Gamma_0} \overset{\text{no c.t.}}{=} \frac{-g^2(2\pi\mu)^{2\epsilon}}{8\pi^2}(y_1 - y_2)\coth(y_1 - y_2)\int \mathrm{d}^{2-2\epsilon}\boldsymbol{k}_{\mathrm{T}}\,\frac{1}{k_{\mathrm{T}}^2 + m_g^2}$$

$$= \frac{-g^2}{8\pi^2}(y_1 - y_2)\coth(y_1 - y_2)\Gamma(\epsilon)\left(\frac{4\pi\mu^2}{m_g^2}\right)^\epsilon, \tag{10.46}$$

where Γ_0 is given by (10.31). The UV counterterm in the $\overline{\mathrm{MS}}$ scheme is

$$\frac{g^2 S_\epsilon}{8\pi^2\epsilon}(y_1 - y_2)\coth(y_1 - y_2), \tag{10.47}$$

so that the renormalized $C_S\Gamma_1$ is

$$\frac{C_S\Gamma_1}{\Gamma_0} \overset{\text{renorm.}}{=} \frac{-g^2}{8\pi^2}(y_1 - y_2)\coth(y_1 - y_2)\ln\frac{\mu^2}{m_g^2}. \tag{10.48}$$

Observe the dependence on the difference in rapidities between the lines. (Lorentz invariance requires that the dependence is on the rapidity difference, not on the rapidities separately, since we can always transform to a frame in which one rapidity, y_2 say, is zero, in which case the other line's rapidity is changed to $y_1 - y_2$.)

Since $e^{-(y_1-y_2)} \sim m^2/Q^2$ at large Q, a correct leading-power approximation is to replace $\coth(y_1 - y_2)$ by unity. This leaves the remaining factor of $y_1 - y_2$. Therefore, there is a further divergence if we take the Wilson lines light-like, an explicit example of a rapidity divergence.

We call $y_1 - y_2$ the hyperbolic angle between the two vectors. The name is appropriate because if we continue y_1 and y_2 to imaginary values, with $y_1 - y_2 = i\theta$, then n_1 and n_2 are vectors in Euclidean space, and θ is the ordinary angle between them. (Actually θ is the angle between n_1 and $-n_2$.)

We have seen that $C_S\Gamma_1$ is a one-loop term in the vacuum expectation value (10.32) of a Wilson line composed of two straight line segments in directions n_1 and n_2, joined at a
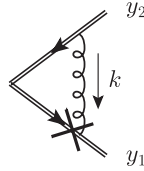
Fig. 10.10. Notation for derivative of $C_S\Gamma_1$ with respect to y_1. The crossed vertex is defined as a rapidity derivative of the Wilson line, in (10.49).

cusp. Our calculation has shown that there is a UV divergence associated with the cusp and that both the divergence and the associated anomalous dimension depend on the hyperbolic angle between the two lines.

10.5.10 Evolution with respect to Wilson-line rapidity

To illustrate evolution of the soft factor with respect to the direction of a Wilson line, consider the derivative of the one-loop soft term $C_S\Gamma_1$ with respect to y_1. This is obtained by differentiating the n_1-dependent factor:

$$\frac{\partial}{\partial y_1}\left(\frac{n_1}{-n_1\cdot k + i0}\right) = \frac{\partial}{\partial y_1}\left(\frac{(1, -e^{-2y_1}, \mathbf{0}_{\mathrm{T}})}{-k^- + e^{-2y_1}k^+ + i0}\right)$$

$$= \frac{-n_1^2\tilde{k}}{(-n_1\cdot k + i0)^2}, \tag{10.49}$$

where $\tilde{k} \stackrel{\text{def}}{=} (k^+, -k^-, \mathbf{0}_{\mathrm{T}})$. Let us represent this object by a vertex with a cross, as in Fig. 10.10. Then the derivative of $C_S\Gamma_1$ is

$$\frac{\partial\, C_S\Gamma_1}{\partial y_1} = \frac{ig^2}{(2\pi)^n}\int d^n k\, \frac{1}{(k^2 - m_g^2 + i0)}\, \frac{-n_1^2\tilde{k}\cdot n_2\,\Gamma_0}{(-n_1\cdot k + i0)^2\,(n_2\cdot k + i0)} + \text{UV c.t.} \tag{10.50}$$

The key to further simplifications in the full evolution equation is that the derivative with respect to y_1 restricts the integral over k to rapidities near y_1, to leading power, so that we can take the limit $y_2 \to -\infty$ without a rapidity divergence. To see this, we observe that in the integrand of (10.50), when the rapidity y of the gluon is much less than y_1, the factor $1/(-n_1\cdot k)^2$ becomes $1/(k^-)^2 \propto e^{2y}$, which gives a suppression. So (10.50) concerns gluons of rapidity close to y_1.

Therefore in (10.50) we replace n_2 by a light-like vector w_2 in the minus direction. The numerator and denominator factors $n_2\cdot\tilde{k}$ and $n_2\cdot k$ both become $w_2^-k^+$, and therefore cancel, so that

$$\frac{\partial\, C_S\Gamma_1}{\partial y_1} = \frac{ig^2}{(2\pi)^n}\int d^n k\, \frac{1}{(k^2 - m_g^2 + i0)}\, \frac{2\Gamma_0}{(-e^{y_1}k^- + e^{-y_1}k^+ + i0)^2}$$

$$+ \text{UV c.t.} + O\!\left(e^{-2(y_1 - y_2)}\right). \tag{10.51}$$

The unsuppressed first term is independent of y_1. The k^- and k^+ integrals are easy to evaluate, giving

$$\frac{\partial \, C_S \Gamma_1}{\partial y_1} = \frac{-g^2}{(2\pi)^{n-1}} \int \frac{\mathrm{d}^{n-2} \boldsymbol{k}_{\mathrm{T}}}{k_{\mathrm{T}}^2 + m_g^2} \, \Gamma_0 \; + \; \text{UV c.t.} + O\!\left(e^{-2(y_1 - y_2)}\right), \qquad (10.52)$$

consistent with (10.46) and (10.48).

We will see that the evolution equation for the soft factor S in the factorization property (10.11) has the form

$$\frac{\partial \ln S}{\partial y_1} = \frac{1}{2} K(m_g, m, \mu, g(\mu)) + O\!\left(e^{-2(y_1 - y_2)}\right), \qquad (10.53)$$

with the kernel K being independent of y_1 and y_2. The right-hand side of (10.52) is in fact the first term in the perturbation expansion of $\frac{1}{2} K$. In accordance with the convention in Collins (1989); Collins and Soper (1981); Collins, Soper, and Sterman (1985b), a factor $\frac{1}{2}$ is defined to accompany K. The lowest-order value of K, from (10.52), is

$$K = \frac{-g^2}{4\pi^2} \ln \frac{\mu^2}{m_g^2} + O(g^4). \qquad (10.54)$$

It follows from (10.53) that S depends exponentially on $y_1 - y_2$:

$$S(y_1 - y_2) = S_0 e^{\frac{1}{2}(y_1 - y_2) K} \left[1 + O\!\left(e^{-2(y_1 - y_2)}\right) \right], \qquad (10.55)$$

with S_0 independent of $y_1 - y_2$.

The quantity K also plays a key role in the evolution of the other factors in (10.11), and analogous results hold for factorization theorems for other processes, like Drell-Yan with measured transverse momentum for the lepton pair. In using the factorization theorems, it will be necessary to use different values of the renormalization scale μ in different factors, e.g., $\mu \sim Q$ in the hard factor H, but $\mu \sim$ mass in the soft and collinear factors. Thus the RG equation for K is also important. This has the form

$$\frac{\mathrm{d} K}{\mathrm{d} \ln \mu} = -\gamma_K(g). \qquad (10.56)$$

From (10.52), we read off the one-loop term in the anomalous dimension:

$$\gamma_K = \frac{g^2}{2\pi^2} + O(g^4), \qquad (10.57)$$

which plays a central role in applications.

This anomalous dimension has two roles, of the kernel of the RGE for K, and as controlling the rapidity dependence of the anomalous dimension γ_S of the soft factor S:

$$\gamma_K = -\frac{\mathrm{d} K}{\mathrm{d} \ln \mu} = -2 \frac{\mathrm{d}}{\mathrm{d} \ln \mu} \frac{\partial \ln S}{\partial y_1} = -2 \frac{\partial}{\partial y_1} \frac{\mathrm{d} \ln S}{\mathrm{d} \ln \mu} = -2 \frac{\partial \gamma_S}{\partial y_1}, \qquad (10.58)$$

where we have dropped power-suppressed terms of order $e^{-2(y_1 - y_2)}$.

10.6 Rationale for definition of T_R

The definition of the region approximator T_R in Sec. 10.4.2 is obtained from the first term in an expansion in powers of small variables. However, the actual soft-to-collinear approximators were modified, to use space-like auxiliary vectors in (10.17) and (10.18), and to have specific $i0$ prescriptions in (10.20)–(10.24). We now justify these modifications. The modifications are unique, given some mild assumptions which are used to ensure the proofs are relatively simple.

Some of the justifications are more readily understood by referring to the one-loop example in Sec. 10.5.

The Grammer and Yennie (1973) paper gives a general approach to obtaining a leading approximation for soft gluons (and for related situations). But their approximator (in their K term) differs significantly in form from what we wrote in Sec. 10.4.2. This indicates that a variety of alternative approximators are conceivable, and we should justify a particular choice of approximator.

The Grammer-Yennie method was constructed to deal with IR divergences in QED; it concerns regions where photon momenta go to zero. In that situation IR photons do not interact with each other, even via loops of lines for electrons and any other matter fields. The Ward identities are particularly simple in an abelian theory. Not only do the IR divergences factorize from the rest of the cross section, but it was shown that the complete IR factor is the exponential of its one-loop value. The correctly computed divergence includes contributions from IR photons with rapidities comparable to that of an external charged line.

In the asymptotic problems treated in this book, what we mean by soft momenta is much broader; we include momenta whose absolute size may be large, but still much less than Q. Thus interactions of soft lines are important: the S factor in Fig. 10.3(b) is an arbitrary multigluon graph. However, we do not require the soft factor to correctly treat low-energy gluons of high rapidity; these belong in the collinear factors with other high-rapidity phenomena. The soft factor becomes a matrix element of Wilson lines, as do the collinear-to-hard gluon couplings. Furthermore the non-abelian Ward identities used in QCD are more complicated than the Ward identities in QED.

Consider our soft-to-A approximant, (10.21). In comparison, the original Grammer-Yennie approach would use no approximation of k_{AS} on the A subgraph, and would have a more complicated non-linear function in place of our denominator $k_{AS, j} \cdot n_1$. We will also need to justify the particular $i0$ prescriptions used in the denominators in (10.20)–(10.24).

10.6.1 Structure of soft and collinear approximants

The structure of all our generalized Grammer-Yennie approximants is

$$A(k)^\mu S(k)_\mu \mapsto A(\hat{k})^\mu \frac{u_\mu v^\nu}{u \cdot v} S(k)_\nu = A(\hat{k})^\mu \frac{\hat{k}_\mu v^\nu}{k \cdot v} S(k)_\nu, \tag{10.59}$$

where

$$\hat{k}^{\mu} = \frac{u^{\mu}\, k \cdot v}{u \cdot v}. \tag{10.60}$$

Here u and v are fixed vectors chosen so as to extract the leading behavior of $A \cdot S$ in the design region of the approximant. (That means, for example, that a soft-to-collinear-A approximant should give an approximation that is accurate to leading power when the momenta in S are soft and the momenta in A are collinear-to-A.) The names of the vectors in (10.59) are changed from our original formula, to indicate that we address general structural issues, allowing possible modifications of the formalism.

In general, multiple applications of (10.59) are used, one for each gluon joining A and S, as in (10.21). All the considerations in this section apply equally if the pair AS is replaced by BS, HA, or HB, merely needing a choice of appropriate auxiliary vectors u and v.

10.6.2 Requirements on soft and collinear approximants

To show that this form is required, and to determine further restrictions on the auxiliary vectors w_1, n_1, etc., we apply the requirements on region approximators T_R.

1. T_R should give an approximation correct to leading power at its design region R.
2. It should be compatible as necessary with contour deformations applied to the original graph.

   We have already dealt with the consequences of this requirement.
3. The conversion of the sum over graphs and regions to a Wilson-line form should be exact. Compare the derivation of the gauge-invariant parton model in Sec. 7.7.

   That is, in applying the Ward identities to Grammer-Yennie approximants, there should be no remainder terms. Typically such remainder terms are power-suppressed and hence innocuous in the design region of T_R, but can be unsuppressed elsewhere. These terms are not in principle undesirable, but they make it hard to construct complete proofs of factorization.
4. The approximant should be exact when applied to the Wilson lines derived from it.

   Ward identities applied to the approximated Wilson line give back exactly the Wilson line, as required by item 3. So the remainders between the graph and approximant must sum to zero. It avoids a probably hard subsidiary proof if the remainders are not zero term-by-term.
5. Summing the gluon attachments should actually give a Wilson line with a straight path, rather than some more general object, at least if this is possible consistently.[8]

   One can imagine more general ways of constructing gauge-invariant operators, e.g., by having Wilson lines with non-rectilinear paths, or by having an integral or sum over Wilson lines with different paths and given endpoints. All such cases are even more complicated than what we are already dealing with, so we should avoid them if possible.

[8] In the applications treated in Ch. 13, the definition of gauge-invariant transverse-momentum-dependent parton densities will require a minor modification to this assumption, with an extra segment of a Wilson line at infinity. The effects of the modification will cancel in the ultimate results.
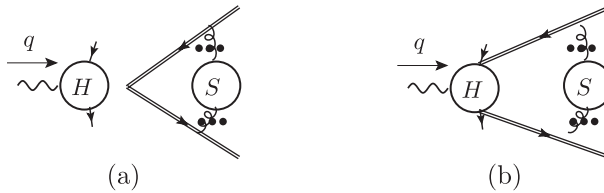
Fig. 10.11. Hard factor times (a) normal local soft factor, (b) conceivable non-local soft factor.

6. After applying T_R, the hard subgraph should not depend on soft momenta.

   Close to the design region of T_R, the hard subgraph obviously has a power-suppressed dependence on soft momenta. But if the dependence is not removed exactly in the definition of T_R, there will be significant dependence of H on soft momenta, and this will introduce a complicated non-locality in the operator defining the soft factor. From the sum over Fig. 10.3(b), we will derive a factorization with soft factors defined by the vacuum matrix element of two Wilson lines joined at a point, so that the hard factor times soft factor is as in Fig. 10.11(a). But if the hard subgraph H had dependence on momenta circulating from the soft factor, the hard subgraph would give non-locality between the otherwise-joined ends of the Wilson lines, as in Fig. 10.11(b). We could avoid this by a subsidiary expansion of H *after* the use of Ward identities, but at the expense of hard-to-control remainders in diagrammatic treatments: the subtraction formalism would not correspond exactly to factorization. There would also be issues with gauge invariance of H. It is simpler if we avoid the extra step, as we will be able to.

7. An approximated momentum $\hat{k}$ is a linear function of the unapproximated momentum $\hat{k} = P(k)$. Applying the approximator a second time reproduces $\hat{k}$, i.e., $P(P(k)) = P(k)$.

One can find other requirements, but these are the ones that impinge most directly on the issues we wish to discuss. Evidently some of the requirements are not absolute, but are to prevent us from going outside known general ideas on gauge-invariant parton densities, etc. unless we are absolutely forced to.

10.6.3 General form of Grammer-Yennie-type approximation

The different cases of a Grammer-Yennie-type approximant are very similar. So to obtain its general form from the above requirements, it is sufficient to treat the case of a gluon of momentum k connecting the S to the A subgraph. The relevant approximant is the approximated A subgraph multiplied by a special factor and the unapproximated S subgraph, as in (10.59). We regard this as the approximated A subgraph (which is 1PI in the gluon) times the matrix element with a gluonic operator that defines S. To connect this to the Wilson-line formulation, the result is to be expressed by a Fourier transformation in terms of an integral over the coordinate-space gluon field.

The Wilson-line requirement implies that the coordinate-space integral is along a straight line, of some direction v, which we will identify with the same vector in (10.59) and (10.60).

That is, in coordinate space the product of S and the approximated A subgraph has the form

$$\int \mathrm{d}\lambda \ F_A(\lambda) \, X(\lambda v), \tag{10.61}$$

for some function F_A, with $X(x)$ being the Fourier transform of $S(k)$,

$$X(x) = \int \frac{\mathrm{d}^4 k}{(2\pi)^4} \, e^{ik\cdot x} \, S(k). \tag{10.62}$$

In momentum space the product of S and approximated A is

$$\int \frac{\mathrm{d}^4 k}{(2\pi)^4} \, f_A(k \cdot v) S(k), \tag{10.63}$$

where

$$f_A(k \cdot v) = \int \mathrm{d}\lambda \, e^{ik\cdot v\lambda} F_A(\lambda). \tag{10.64}$$

Hence the approximated A is a function of $v \cdot k$. Since $\hat{k}$ is a linear function of k, it is a fixed vector times $v \cdot k$. Reapplication of the approximator reproduces $\hat{k}$, so $\hat{k}$ must be of the form (10.60).

The exactness of the Ward identities in a non-abelian theory requires the vectors u to be the same at all gluons connecting S to A.

At each gluon between S and A, the approximant therefore has the form

$$A(k)^\mu S(k)_\mu \mapsto A(\hat{k})^\mu M(\hat{k})_\mu{}^\nu S(k)_\nu, \tag{10.65}$$

where M is some matrix to be determined. The approximant is exact if A^μ is obtained from a Wilson line in direction v; in that case A is some function of $k \cdot v$ times the vector v. The function is unchanged by the approximant, since $\hat{k} \cdot v = k \cdot v$. So the requirement of exactness of approximating a Wilson line gives

$$v^\mu M(\hat{k})_\mu{}^\nu = v^\nu, \tag{10.66}$$

from which we find that $M_\mu{}^\nu$ is of the form $a_\mu v^\nu/(a \cdot v)$ for some vector a. For the Ward identities to work exactly, we need $a^\mu \propto \hat{k}^\mu$. The structure in (10.59) follows.

10.6.4 Auxiliary vectors in soft approximation

In setting up the soft-to-collinear approximators, (10.21) etc., the natural expansion in small variables would make the vectors n_1 and n_2 light-like, in the plus and minus directions. But to cut off rapidity divergences, we made them non-light-like with rapidities y_1 and y_2.

We now derive the $i0$ prescription in (10.20) and (10.22), and determine that n_1 and n_2 are space-like. Examination of one-loop examples is sufficient for this. As we saw in Sec. 5.5.10, the soft approximation fails in the Glauber region, i.e., when $|k^+k^-| \ll k_{\mathrm{T}}^2$. We avoid the Glauber region by deforming the k^+ and k^- integrals away from the poles on the quark propagators. The approximators are applied on the deformed contours, so

the denominators in (10.20) and (10.22) must use $i0$ prescriptions compatible with the deformed contours.

In (10.28), the simplest deformation is symmetric. Where the real parts of k^+ and k^- are in the Glauber region, we deform k^+ into the upper half plane away from the $p_B + k$ pole, and we deform k^- into the lower half plane away from the $p_A - k$ pole:

$$k^+ \mapsto k^+ + i\Delta, \qquad k^- \mapsto k^- - i\Delta, \tag{10.67}$$

where Δ is positive and of order k_T. The signs reflect that both the quark and antiquark are in the final state relative to the hard interaction, and the reversed sign between k^+ and k^- is because k flows into the A subgraph but out of the B subgraph. In (10.29), the Grammer-Yennie denominators are

$$\frac{1}{(-n_1 \cdot k + i0)(n_2 \cdot k + i0)} = \frac{1}{(-k^- + e^{-2y_1}k^+ + i0)(k^+ - e^{2y_2}k^- + i0)}. \tag{10.68}$$

Not obstructing the contour deformation determines the $k^+ + i0$ and $-k^- + i0$ parts to be as written, since e^{2y_2} and e^{-2y_1} are much less than one.

Fourier transformation of the Feynman rules for the Wilson lines shows that in coordinate space they are future-pointing, corresponding to the fact that the external quark and antiquark are in the final state.

We will also use factorization for other processes, and it is important that, if possible, we have universality of the collinear and soft factors between processes. Now, as explained by Collins and Metz (2004), other processes require an asymmetric contour deformation. As we will see in Sec. 12.14.3, in DIS we would use a contour deformation in k^+ only:

$$k^+ \mapsto k^+ + iO(Q), \qquad k^- \mapsto k^-. \tag{10.69}$$

The large k^+ deformation is away from final-state singularities, but k^- is generally trapped at small values by a combination of initial- and final-state singularities associated with the hadron target in DIS. This asymmetric deformation takes k from a Glauber configuration to a collinear-to-A configuration, and hence out of the soft region. But the soft approximant is to be integrated over all momenta, and it is used in a subtraction in collinear terms, so auxiliary denominators must not obstruct the contour deformation.

To get maximum universality of the soft and collinear factors, we should avoid changing the Wilson lines when we change processes, if possible. This requires (Collins and Metz, 2004) that our soft approximant for the Sudakov form factor also be compatible with the asymmetric deformation (10.69). This is achieved if the relative signs between the $i0$s and the k^+ terms in (10.68) all be the same, and therefore as written. A similar argument applies to the k^- terms. This determines all the signs in (10.68), from which we deduce that n_1 and n_2 are space-like, in agreement with our definitions.

An important advantage is that, since gluon fields commute at space-like separation, the use of space-like Wilson lines ensures automatic compatibility between the path ordering defining the Wilson lines and the time ordering used to define Green functions.

A disadvantage arises when one extends the use of the approximations to cases with emission of real gluons. Then singularities at $k \cdot n = 0$ with n space-like occur in the region of physical gluon emission. But with a time-like vector, the singularity is restricted to $k = 0$, because of the positive energy condition on a physical state. (In the rest frame of n, $k \cdot n = k^0$, which is positive for a physical state.)

If one gave up the argument about universality, one could use time-like auxiliary vectors. In the Sudakov form factor (and generally in reactions in $e^+e^- \to$ hadrons) one could use time-like future-pointing vectors. In DIS one would still need a future-pointing vector on the struck quark side, but a *past*-pointing vector on the target side. The issues of universality in this context need further investigation.

10.6.5 Auxiliary vectors in the collinear approximants

As for the collinear-to-hard approximants, subtractions for soft regions cancel the possible rapidity divergences; we will see this as general result. Therefore it is sufficient to use light-like vectors in the collinear approximants, as given in (10.19), (10.23), and (10.24).

The $i0$ prescriptions in (10.23) and (10.24) are determined in the same way as in the soft approximants. The signs are in fact the same, and correspond to future-pointing Wilson lines. Although the Glauber region appears to have nothing to do with a collinear region, the approximators are applied to the graph as a whole with a deformed momentum contour. The momentum denominators in the collinear approximant must therefore be compatible with the contour deformation out of the Glauber region.

10.6.6 Alternative definition of the collinear-to-hard approximants

In our definitions in Sec. 10.4.2, we chose all the approximated momenta to be light-like. Thus in (10.59), the vector u is light-like. Although this is generally the most convenient choice, other choices are conceivable. However, constraints arise from other requirements. In the case of the hard-scattering factor, gauge invariance is most conveniently assured, if its external lines are on-shell. This implies that these lines are light-like given that they are massless. Practical perturbative calculations are enormously much simpler when masses are zero and external lines on-shell.

We also used a light-like Wilson-line vector in the hard scattering, i.e., w_2 in (10.19a) and w_1 in (10.19b).

A constraint now arises from the requirement that the hard factor does not depend on the soft momenta, after application of an approximator. This ensures that the hard factor completely factors from the soft factor. In the notation of (10.59), let u_{AS} and v_{AS} be the vectors for the soft-to-A approximant, and let u_{HA} and v_{HA} be the vectors for the A-to-H approximant. In this general case, the approximated momentum in H is

$$\hat{k}_{HA}^\mu = u_{HA}^\mu \frac{(k_{HA} + \hat{k}_{HAS}) \cdot v_{HA}}{u_{HA} \cdot v_{HA}} \tag{10.70}$$

Since $\hat{k}_{HAS}$ is proportional to u_{AS}, we only get independence of $\hat{k}_{HA}$ from k_{AS} if

$$u_{AS} \cdot v_{HA} = 0, \tag{10.71}$$

i.e., if the approximated soft momentum is orthogonal to the Wilson-line vector for the A-to-H connections.

This is obviously satisfied for our actual choice, in (10.17) and (10.19a), that u_{AS} and v_{HA} both equal w_2, a light-like vector in the minus direction.

What other possibilities are there? We restrict to vectors in the $(+, -)$ plane, otherwise we break azimuthal rotation symmetry in our approximators, without having a transverse vector in the process's kinematics to give a preferred transverse direction.

If v_{HA} stays light-like, this requires u_{AS} to be light-like in the same direction, which is our original choice.

Given our results on $i0$ prescriptions, the other choice is a space-like vector v_{HA}. An orthogonal vector is time-like. A simple and natural case is to put v_{HA} in the z direction in the center-of-mass frame. The corresponding Wilson line restricts gluon rapidity in the A factor to be approximately positive, which is very natural; it gives a natural cutoff of the rapidity divergence in $T_A \Gamma_1$ before subtraction. Then we would need $u_{AS} \propto q^{\mu}$, a not unnatural choice.

As far as I can see, this is an legitimate alternative possibility.

However, as we will see, it is generally preferable to avoid non-light-like Wilson lines whenever possible: It makes calculations easier and avoids inhomogeneous terms in evolution equations.

10.7 General derivation of region decomposition

In this section, we prove the main result needed to apply the subtraction formalism. This is that, for a general Feynman graph for any of the many processes that we consider, the remainder, (10.5), is actually power-suppressed. That is, it is a power of Q smaller than the leading power for the process (which is, for example, Q^0 for DIS structure functions). This then demonstrates (10.1), which is the key formula for our later derivations of factorization of various kinds.

The derivation uses certain properties of the region approximators T_R, so effectively we are finding and using a set of requirements on good approximators.

A general treatment involves regions in a loop-momentum space of arbitrarily high dimension, and thus necessarily has a high degree of abstraction. As we will see, a recursive, or inductive, strategy enormously simplifies the proof by reducing it to considering relations between two generic regions. These can be visualized in a space of two dimensions, and simple examples, like those in Secs. 10.2 and especially 10.5, give the main ideas for the generic situation. It would be useful to read those sections concurrently with the present section to gain better understanding, visualization, and motivation.

Even so, it will become apparent that the rigor of the derivations is insufficient. Mathematically inclined readers are strongly urged to do better; the literature on deriving factorization leaves much to be desired.

10.7.1 Results so far

So far, we have explicitly defined the main ingredients of the method. The region contributions $C_R\Gamma$ were defined in (10.4) in terms of region approximators $T_R\Gamma$. Then the asymptotic behavior of Γ is intended to be correctly given by the sum over regions: $\Sigma_R C_R\Gamma$. Explicit definitions of the region approximators were given in Sec. 10.4 for the Sudakov form factor; these definitions apply with at most minor changes to the many other processes we will treat.

10.7.2 Overall view

It is important to keep in mind the main motivations for the subtraction formalism. First, the region approximant $T_R\Gamma$ is intended to give a good approximation to Γ near the PSS R; that is,

$$\Gamma - T_R\Gamma = \mathcal{O}\!\left(\left(\frac{\lambda_R + m}{Q}\right)^p\right)\|\Gamma\|, \tag{10.72}$$

with some qualifications that I will explain in Sec. 10.7.3. Here, λ_R is the radial variable for region R. Naturally the approximators we use are such that the soft, collinear and hard subgraphs of a region correspond to contributions to factors in a phenomenologically useful factorization property. The error specified in (10.72) improves as λ_R decreases, but only until λ_R becomes of order m. There are additional sources of error in neglecting m with respect to Q when appropriate. So all these issues are covered by adding m to λ_R in (10.72).

The approximant contributes in regions larger than R, but with an inaccurate value. To handle the consequent double counting, we defined the region contribution $C_R\Gamma$ by (10.4), where T_R is applied after subtraction of the contributions from smaller regions. This is also intended to solve the problem that the accuracy of the approximator T_R degrades close to PSSs smaller than R: the region contribution $C_R\Gamma$ is intended to be leading power at region R but suppressed in smaller regions. Including the contributions of smaller regions, $C_R\Gamma + \sum_{R'<R} C_{R'}\Gamma$, is intended to give a correct leading-power approximation near the whole of R, including smaller regions.

As we saw in Ch. 8, this setup works quite straightforwardly to give factorization, if the relevant regions are just nested inside each other, i.e., if they have a total ordering. But, in general, the regions can have more general relations involving overlaps and non-intersection, as in (5.21). This is responsible for the main complications in the proof. They are a non-trivial generalization of those involved in dealing with overlapping divergences in renormalization theory.

The most fundamental problem solved by the subtraction formalism is that the accuracy of a region approximant $T_R\Gamma$ degrades in certain places, associated with other regions. An example is at the approach to a smaller region $R_1 < R$. As we have seen in examples, the worsening of the accuracy of $T_R\Gamma$ is compensated in the subtraction formalism. In forming

$C_R\Gamma$, T_R is applied to Γ only after subtractions are used for all the smaller regions. Then it is the sum $C_R\Gamma + \sum_{R'<R} C_{R'}\Gamma$ that gives an accurate approximation to Γ over the whole of R, including smaller regions.

Another problem is the large multiplicity of regions, as in Fig. 10.5, a problem that obviously gets much worse for even higher-order graphs. Our proofs will be inductive, i.e., recursive, and a generic step of a proof will only involve a single region and its nearest neighbors in the region hierarchy. Then the most complicated relation between regions that we need to discuss explicitly is Fig. 5.32. Most of the time, the relation we treat will be essentially of the form of Fig. 5.28. So with an appropriate viewpoint, the most general situation can be reduced to many copies of what happens in one-loop graphs, or at most two-loop graphs.

Now, our aim is to derive power-law estimates of the accuracy of a factorization statement, i.e., to obtain results that are accurate to some given power of a small ratio (e.g., m/Q). But we often have logarithmic integrals interpolating between different regions, and these worsen basic power-law estimates by some number of logarithms. So it is convenient to define the following notation:

$$f(x) = \Lambda_p(x)g(x) \quad \text{as } x \to 0, \tag{10.73}$$

which means that

$$f(x) = \mathcal{O}\big(x^p |\ln x|^\alpha\big)\, g(x) \quad \text{as } x \to 0, \tag{10.74}$$

for some value of the power α of the logarithm. That is, there are constants C, α and x_0, such that

$$|f(x)| < C\, |x|^p\, |\ln x|^\alpha\, |g(x)| \quad \text{for all } |x| < x_0. \tag{10.75}$$

Normally, p is fixed for the problem we are analyzing (e.g., graphs for the Sudakov form factor to leading power), but α depends on the graph, being up to two times the number of loops.

10.7.3 Accuracy of approximator T_R

The basic form of the accuracy of a region approximator T_R was given in (10.72). We now modify it to obtain a strictly correct error estimate which will form the basis of the rest of our work.

Basic error estimate

The accuracy of the approximator for a leading region can be read off from the accuracy of its individual components, as defined in Sec. 10.4. Since we are working to leading-power accuracy, the exponent p of the power law is $p = 1$. Often such errors involve some transverse momentum relative to Q: k_{T}/Q, and these commonly vanish after an integral over angle. Then the actual error is one power better: $p = 2$. We can also imagine

improved region approximators with an expansion to more orders in small momentum components, with a correspondingly larger value of p. The precise value of p will not matter.

There are also non-leading regions, such as $R_{A'}$ defined in Sec. 5.4 for the one-loop Sudakov form factor. Since the graph is already non-leading in such a region, we can define the associated approximator to be zero, e.g., $T_{R_{A'}}\Gamma = 0$. But the use of the integrand Γ on the r.h.s. of error estimates such as (10.72) is then not appropriate; rather we need a value characteristic of the graph integrated over all regions. Thus we replace Γ on the r.h.s. of (10.72) by

$$\left\|\int_{\text{all}} \Gamma\right\|. \tag{10.76}$$

Here the double-bar notation has the same meaning as in (10.39). That is, it is a power-counting estimate of the size of the integral arranged to avoid dynamical cancellations. (Thus for DIS, we would write $\|W^{\mu\nu}\| = O(1)$, even though some specific components vanish.)

Correspondingly, we should use an integral for the l.h.s., but now over a range near the PSS R:

$$\int_{\text{local}} (\Gamma - T_R\Gamma). \tag{10.77}$$

Then λ_R on the r.h.s. of an error estimate should be interpreted as the maximum value of the radial variable in the range of integration. The integration is over some range of all variables, not just λ_R but also the angular and intrinsic coordinates for R. Naturally, the integral should be on a deformed contour if we need to avoid a Glauber region. Since there is the possibility of logarithmic enhancements in such integrals, we must replace the power-law estimate on the r.h.s. by

$$\Lambda_p\left(\frac{\lambda_R + m}{Q}\right). \tag{10.78}$$

Situations needing adjustment

We now quantify that for a given value of λ_R, the error estimates need modification for two situations, as can be obtained from the definitions in Sec. 10.4. First, they generally degrade when the intrinsic coordinates approach the positions of any particular smaller PSS $R_1 < R$, since then the conditions for neglecting a small momentum component with respect to a large component become weaker.

The second issue concerns lines with soft-collinear momenta, as in the example in Sec. 10.5.4. These lines have both a small energy and a high rapidity. The small energy allows them to be considered as soft, and the high rapidity allows them to be considered as collinear. Let R be a region in which the soft-collinear lines are part of the soft subgraph. Let R_2 be the larger region obtained from it by changing the category of the soft-collinear

lines to the appropriate collinear category. We notate this relation by

$$R_2 \overset{\text{SC}}{>} R. \tag{10.79}$$

In terms of the underlying PSSs, this relation is defined to mean that certain collinear lines at the PSS R_2 are changed to zero momentum to obtain the PSS R.

Soft-collinear lines are at an end of their collinear range in fractional momentum. But their high rapidity implies that the approximator T_{R_2} continues to be valid, removing the degradation that would otherwise occur near the smaller region R.

In the approximator T_R, the soft-collinear lines are treated as soft, but then their high rapidity implies that the approximators where they attach to the corresponding collinear subgraph degrade in accuracy. The errors become of order $e^{-\Delta y}$, where Δy is the rapidity difference between the soft and collinear lines, with the soft line always being taken as having rapidity between the two collinear groups of the whole process.

Generalizing our proof from the example in Sec. 10.5.4, we will find that these effects combine to give correctness of the subtraction method to extract the asymptotics of the graphs.

Generic degradation near smaller PSSs

The accuracy of the approximator T_R defined in Sec. 10.4 degrades when the intrinsic coordinates appropriate for PSS R approach the positions of any particular smaller PSS $R_1 < R$. For example, in a hard subgraph, we neglect a collinear transverse momentum with respect to a large momentum component of order Q. But near R_1 we may need to replace Q by the smaller value λ_{R_1}. So in our error estimate we insert a degradation factor

$$W_{R_1, R} = 1 + \Lambda_p \left(\frac{Q}{\lambda_{R_1} + m} \right), \tag{10.80}$$

with one term for each smaller region. Here, I added 1 to the basic degradation factor, so that the factor $W_{R_1, R}$ can be applied universally: close to R_1, the $\Lambda_p(\ldots)$ term dominates, but away from R_1, it decreases, leaving $W_{R_1, R}$ to relax to unity.

Soft-collinear problem

Surrounding PSS R, consider integrating around a surface of fixed λ_R, as in Fig. 5.28. Close to each larger PSS R_2 that obeys the soft-collinear relation $R_2 \overset{\text{SC}}{>} R$, we get degradation of the approximation by a factor $V_{R_2, R}$. This factor replaces $\Lambda_p(\lambda_R / Q)$ by $\Lambda_p\left(e^{-\Delta y} \right)$, where Δy is the rapidity difference between the soft-collinear lines in the soft subgraph of R and lines in the collinear subgraph of R to which they attach.

Consider next these same lines in the same momentum region in the other approximator $T_{R_2} \Gamma$. Relative to R_2, the configuration is close to the smaller region R, where there is a default degradation factor W_{R, R_2}. But the approximator applies accurately to the soft-collinear lines, so we multiply the degraded error estimate by the inverse of the large $V_{R_2, R}$ factor.

10.7.4 Overall error estimate

Putting all these components together, we have shown that the error in T_R is characterized by

$$\int_{\text{local}} (\Gamma - T_R \Gamma) = \Lambda_p \left(\frac{\lambda_R + m}{Q} \right)$$

$$\times \left[1 + \sum_{R_1 < R} W_{R_1, R} \frac{1}{1 + V_{R, R_1}} \right] \left[1 + \sum_{\substack{R_2 > R \\ \text{SC}}} V_{R_2, R} \right] \left\| \int_{\text{all}} \Gamma \right\|. \quad (10.81)$$

The $1/(1 + V_{R, R_1})$ factors only appear for subregions obeying $R_1 \overset{\text{SC}}{<} R$.

10.7.5 Theorems to be proved

I now state some theorems to be proved inductively. They generalize properties we have seen in examples. The first three theorems are properties labeled by a region.

Theorem 1_R Define $\int_{\text{local}} \bar{C}_R \Gamma \overset{\text{def}}{=} \int_{\text{local}} (\Gamma - \sum_{R' < R} C_{R'} \Gamma)$ which has subtractions for smaller regions than R. It is suppressed in all regions R_1 smaller than R, but with degradation for soft-collinear situations that concern regions R or bigger:

$$\int_{\text{local at } R_1} \bar{C}_R \Gamma = \Lambda_p \left(\frac{\lambda_{R_1} + m}{Q} \right) \left[1 + \sum_{\substack{R_2 \geq R \\ \text{SC}}} V_{R_2, R_1} \right] \left\| \int_{\text{all}} \Gamma \right\|. \quad (10.82)$$

Theorem 2_R The same property applies to $C_R \Gamma = T_R \bar{C}_R \Gamma$.

Theorem 3_R When we also subtract $C_R \Gamma$, there is a suppression at R, and the soft-collinear degradation only applies on regions strictly bigger than R:

$$\int_{\text{local at } R} \left(\Gamma - C_R \Gamma - \sum_{R' < R} C_{R'} \Gamma \right) = \int_{\text{local at } R} (1 - T_R) \bar{C}_R \Gamma$$

$$= \Lambda_p \left(\frac{\lambda_R + m}{Q} \right) \left[1 + \sum_{\substack{R_2 > R \\ \text{SC}}} V_{R_2, R} \right] \left\| \int_{\text{all}} \Gamma \right\|. \quad (10.83)$$

The suppression is uniform over the whole of R including smaller regions.

Theorem 4 The sum of $C_R \Gamma$ over all regions approximates Γ to power-law accuracy:

$$\int_{\text{all}} \left(\Gamma - \sum_R C_R \Gamma \right) = \Lambda_p \left(\frac{m}{Q} \right) \left\| \int_{\text{all}} \Gamma \right\|. \quad (10.84)$$

10.7.6 Proofs of theorems $1_{R_{\min}}$ to $3_{R_{\min}}$

We will first prove these theorems for a minimal region, and then prove them for larger regions given that they hold for all smaller regions.

Minimal regions

For a minimal region $R_{\min}$, theorems $1_{R_{\min}}$ and $2_{R_{\min}}$ are trivial because there are no smaller regions. Theorem $3_{R_{\min}}$ follows directly from the approximation property (10.81); because of the lack of smaller regions $\bar{C}_{R_{\min}}\Gamma = \Gamma$.

Theorem 1_R

For a general region R, we make the inductive hypothesis that theorems 1–3 have already been proved for regions smaller than R. Then to prove the suppression (10.82), we partition the terms in $\bar{C}_R\Gamma$ into three sets according to the relation of the relevant regions to R_1, and then consider each set separately.

First, we note the following structural properties of $\bar{C}_R\Gamma$ that follow directly from its definition.

- $\bar{C}_R\Gamma$ is a sum of terms, each of which involves a product of $-T_{R'}$ operations applied to Γ. Each product involves a sequence of strictly ordered regions, since subtractions in the definition of any particular region contribution $C_{R'}\Gamma$ only involves yet smaller regions.
- A factor $T_{R'}$ only appears in combinations that combine to form a $C_{R'}\Gamma$ factor.

The partitioning of $\bar{C}_R\Gamma$ is as follows.

- The first set consists of terms in which all the $T_{R'}$ factors are for regions that are ordered relative to R_1. The sum gives an object of the form:

$$\sum\prod_{R''}(-T_{R''})(1 - T_{R_1})\bar{C}_{R_1}\Gamma. \tag{10.85}$$

The sum is over the ways in which can appear $T_{R''}$ factors for regions R'' bigger than R_1 (and necessarily smaller than R). The two terms in the middle parentheses account for all the terms in which $-T_{R_1}$ does not or does appear.

- The second set has at least one $-T_{R'}$ overlapping with R_1, but none that fail to intersect R_1. We group these terms by the minimal such R':

$$\sum\prod_{R''}(-T_{R''})C_{R'}\Gamma, \tag{10.86}$$

where R' overlaps R_1, i.e., the intersection $R' \cap R_1$ is non-empty and strictly smaller than both R' and R_1.

- The third set is where there is at least one $-T_{R'}$ factor for a region that does not intersect at all with R_1. We group these terms by the minimal such R':

$$\sum\prod_{R''}(-T_{R''})C_{R'}\Gamma, \tag{10.87}$$

where the R'' regions are larger than R'.

For the first set, the factor $(1 - T_{R_1})\bar{C}_{R_1}\Gamma$ is suppressed by theorem 3_{R_1}, which is true by the inductive hypothesis. But this has the soft-collinear degradation at any R_2 obeying $R_2 \overset{\text{SC}}{>} R_1$. For those R_2 that are also smaller than R, i.e., that obey $R_2 < R$, there are subtractions in (10.85). By an inductive application of theorem 3 to region R_2, we find a suppression by the $1/V_{R_2, R_1}$ factor. There remain the cases $R_2 = R$, and $R_2 \overset{\text{SC}}{>} R$, which are allowed in (10.82).

For the second set, (10.86), our treatment uses the ideas given in Sec. 10.5.6. There we found for the one-loop Sudakov form factor that the collinear term $C_A\Gamma$ was suppressed in the opposite collinear region R_B. In this term, the factor T_A acts by first projecting the loop-momentum configuration down to the intersection R_S of the two regions. Then it extrapolates in the normal coordinates for A, preserving the value of the intrinsic coordinates. A momentum close to R_B gives an intrinsic coordinate close to the endpoint R_S of the R_A PSS. We then get a suppression because of the suppression of $C_A\Gamma$ at regions smaller than R_A. This idea applies generally, by changing R_A to R', R_B to R_1, and R_S to $R' \cap R_1$. The approximator $T_{R'}$ coerces a momentum configuration near R_1 to be effectively near $T_{R' \cap R_1}$.

For the third set, R' and R_1 do not intersect at all. Again the $T_{R'}$ operation coerces the momentum configuration to be changed from R_1-like to R'-like. The lack of intersection of R' and R_1 implies that the coerced configuration is a generic one for R' and that the radial variable is of order Q. More propagators are off-shell without a change in the integration measure, so we get a suppression.

This completes the proof of theorem 1_R.

Theorem 2_R

The application of the approximator T_R does not change the suppressions and degradations in (10.82). So theorem 2_R follows.

Theorem 3_R

The l.h.s. of (10.83) differs from that of (10.82) by a factor $1 - T_R$. From the basic approximation property, (10.81), this gives a factor $\Lambda_p((\lambda_R + m)/Q)$ on the r.h.s. The suppression factors for $\bar{C}_R\Gamma$ at smaller regions on the r.h.s. of (10.82) cancel the corresponding degradation terms in (10.81), while the $1/(1 + V_{R, R_1})$ factors cancel the effect of the V_{R_2, R_1} factors in (10.82) for the case that $R_2 = R$.

This gives (10.83).

Theorem 4

Theorem 4, (10.84) is the actual theorem we need to use in proving factorization, since it states that to power-law accuracy, Γ is given by the sum of $C_R\Gamma$ over regions. It is just theorem 3 applied to the largest possible region R_H, where all momenta are hard. For this region all coordinates are intrinsic, so we must set the radial coordinate to zero: $\lambda_H = 0$. There are no larger regions, so we need no $V_{R_2, R}$ terms. Thus theorem 4 is just an application of (10.83) for $R = R_H$.

10.8 Sudakov form factor factorization: first version

The general leading region for the Sudakov form factor was depicted in Fig. 10.3(b). For each region R of each graph Γ, we defined a corresponding contribution $C_R\Gamma$, and the sum over Γ and R gives a correct leading-power approximation to the form factor:

$$F = \sum_{\Gamma, R} C_R\Gamma + \text{power-suppressed}. \tag{10.88}$$

The sum can be specified by independent sums over the region subgraphs H, A, B, and S in Fig. 10.3 (subject to the constraint that there is a match of the numbers of gluon lines connecting the different subgraphs). We must convert this sum into the factorized form of hard, collinear and soft factors, as in (10.11), with definite definitions for the factors as matrix elements of certain operators containing Wilson lines.

The basis of our method is that the region approximators T_R allow Ward identities to be applied to the connections of gluons from S to the collinear subgraphs A and B, and to the gluons from A and B to the hard subgraph H. In each case there is a factor of the gluon momentum contracted with one of the subgraphs, which we will call the destination subgraph (A, B or H respectively). It is this contraction that allows Ward identities to be used, generalizing the results of Sec. 7.7.

Elementary Ward identities in an abelian gauge theory are for ordinary Green functions or matrix elements. Relative to these cases, we have two primary complications. The first is that our Green functions have subtractions for smaller regions. The second is that the graphs for A, B, and H are restricted by certain irreducibility requirements: Each collinear subgraph A and B is one-particle-irreducible (1PI) in the soft lines, while the hard subgraph H is 1PI separately in the A lines and the B lines.

10.8.1 Statement of definitions of factors

The Ward identities entail definitions for the soft and collinear factors that we state in this section.

The soft factor is

$$S(y_1 - y_2) = \frac{\langle 0|\, W(\infty, 0, n_2)^\dagger\, W(\infty, 0, n_1)\, |0\rangle}{\text{W.L. self-energies for } n_2 \text{ and } n_1}\, Z_S. \tag{10.89}$$

Here the Wilson-line operators are defined in (10.33), with directions n_1 and n_2, while Z_S is a UV renormalization factor defined by, say, the $\overline{\text{MS}}$ scheme. The denominator will be defined in (10.101); it removes graphs that contribute to the numerator but that are not produced from the Ward-identity argument. Applying Lorentz invariance shows that the dependence of S and Z_S on the Wilson-line rapidities y_1 and y_2 is only on the difference $y_1 - y_2$. However, it is sometimes convenient to write separate y_1 and y_2 arguments: $S(y_1, y_2)$ instead of $S(y_1 - y_2)$.

As for the collinear factors, I first define an unsubtracted collinear factor for the A side:

$$A^{\text{unsub}}(y_{p_A} - y_{u_2}) = \frac{\langle p_A | \, \bar{\psi}_0(0) \, W(\infty, 0, u_2)^\dagger \, \mathcal{P}_B \, |0\rangle}{(\text{W.L. self-energies for } u_2) \, \bar{u}_A \mathcal{P}_B} Z_A^{\text{unsub}}$$

$$= \frac{\langle p_A | \, \bar{\psi}(0) \, W(\infty, 0, u_2)^\dagger \, \mathcal{P}_B \, |0\rangle}{(\text{W.L. self-energies for } u_2) \, \bar{u}_A \mathcal{P}_B} Z_A^{\text{unsub}} Z_2^{1/2}. \quad (10.90)$$

In the first line, the numerator has a matrix element of a *bare* quark field and a Wilson line in a space-like direction $u_2 = (-e^{2y_{u_2}}, 1, \mathbf{0}_{\text{T}})$. The vector u_2 is just like n_2 except for a different rapidity y_{u_2}, and we will later use a limit with $y_{u_2} \to -\infty$. There is also a UV renormalization factor. The second line is simply the first line written in terms of the renormalized quark field, as appropriate for calculations. As in the soft factor, there is a denominator to cancel Wilson-line self-energy graphs.

The numerator is actually a Dirac spinor, and contains the factor $\mathcal{P}_B = \gamma^+\gamma^-/2$ which is used to connect the collinear and hard factors. As I now show, the numerator is just a factor times $\bar{u}_A \mathcal{P}_B$. Therefore we include in the denominator in (10.90) a factor to divide out the spinor dependence, so that the quantity A^{unsub} is a numerical-valued scalar quantity. To derive the spinor structure, we observe that the only vector variables on which the collinear factor depends are in the $(+, -)$ plane. After the use of parity invariance, the most general Dirac structure for A^{unsub} is

$$\bar{u}_A(aI + b^+\gamma^-)\mathcal{P}_B. \quad (10.91)$$

Because of the $\mathcal{P}_B$ factor, all other combinations of Dirac matrices can either be reduced to this by anticommutation relations or give zero. By use of $\bar{u}_A(\not{p}_A - m) = 0$, it is easily checked that the most general form is actually proportional to $\bar{u}_A \mathcal{P}_B$.

An unsubtracted B factor is defined exactly similarly:

$$B^{\text{unsub}}(y_{u_1} - y_{p_B}) = \frac{\langle p_B | \, W(\infty, 0, u_1) \, \mathcal{P}_B \, \psi_0(0) \, |0\rangle}{(\text{W.L. self-energies for } u_1) \, \mathcal{P}_B v_B} Z_B^{\text{unsub}}$$

$$= \frac{\langle p_B | \, W(\infty, 0, u_1) \, \mathcal{P}_B \, \psi(0) \, |0\rangle}{(\text{W.L. self-energies for } u_1) \, \mathcal{P}_B v_B} Z_B^{\text{unsub}} Z_2^{1/2}, \quad (10.92)$$

with a Wilson line in the direction $u_1 = (1, -e^{-2y_{u_1}}, \mathbf{0}_{\text{T}})$.

Not only do soft and collinear factors like S, A^{unsub}, and B^{unsub} depend on the rapidities of their non-light-like Wilson line(s), but so do their renormalization factors Z_S, Z_A^{unsub}, and Z_B^{unsub}. For S and Z_S this is simply a dependence on $y_1 - y_2$, as in (10.47).

The renormalization factors Z_A^{unsub}, and Z_B^{unsub} are mass independent and so variables to parameterize their dependence on the Wilson-line rapidities must use the massless limit of p_A and p_B. Appropriate variables for Z_A^{unsub}, and Z_B^{unsub} are, respectively,

$$\zeta_{A,u_2} \overset{\text{def}}{=} 2(p_A^+)^2 e^{-2y_{u_2}} = m^2 e^{2(y_{p_A} - y_{u_2})}, \quad (10.93\text{a})$$

$$\zeta_{B,u_1} \overset{\text{def}}{=} 2(p_B^-)^2 e^{2y_{u_1}} = m^2 e^{2(y_{u_1} - y_{p_B})}. \quad (10.93\text{b})$$

Next we define subtracted collinear factors. Their names, A and B, are decorated with a superscript "basic" to indicate that the definitions are in a sense preliminary, since in

later sections we will construct an improved factorization with modified definitions of the factors. Each subtracted collinear factor is defined by dividing the unsubtracted collinear factor by a version of the soft factor, and then taking the light-like limits u_1 and u_2 in a certain way. Thus the subtracted A factors are

$$A^{\text{basic}} = \frac{\langle p_A | \, \bar{\psi}_0(0) \, W(\infty, 0, w_2)^\dagger \, \mathcal{P}_B \, |0\rangle \; \text{(W.L. self-energies for } n_1)}{\langle 0 | \, W(\infty, 0, w_2)^\dagger \, W(\infty, 0, n_1) \, |0\rangle \; \bar{u}_A \mathcal{P}_B} Z_A^{\text{basic}}$$

$$= \frac{\langle p_A | \, \bar{\psi}(0) \, W(\infty, 0, w_2)^\dagger \, \mathcal{P}_B \, |0\rangle \; \text{(W.L. self-energies for } n_1)}{\langle 0 | \, W(\infty, 0, w_2)^\dagger \, W(\infty, 0, n_1) \, |0\rangle \; \bar{u}_A \mathcal{P}_B} Z_A^{\text{basic}} Z_2^{1/2},$$

$$(10.94a)$$

$$B^{\text{basic}} = \frac{\langle p_B | \, W(\infty, 0, w_1) \, \mathcal{P}_B \, \psi_0(0) \, |0\rangle \; \text{(W.L. self-energies for } n_2)}{\langle 0 | \, W(\infty, 0, n_2)^\dagger \, W(\infty, 0, w_1) \, |0\rangle \; \mathcal{P}_B v_B} Z_B^{\text{basic}}$$

$$= \frac{\langle p_B | \, W(\infty, 0, w_1) \, \mathcal{P}_B \, \psi(0) \, |0\rangle \; \text{(W.L. self-energies for } n_2)}{\langle 0 | \, W(\infty, 0, n_2)^\dagger \, W(\infty, 0, w_1) \, |0\rangle \; \mathcal{P}_B v_B} Z_B^{\text{basic}} Z_2^{1/2}. \quad (10.94b)$$

The above definitions agree with our one-loop calculations in (10.42) and (10.43). The renormalization factors Z_A^{basic} and Z_B^{basic} depend on $\zeta_{A,n_1}/\mu^2$ and $\zeta_{B,n_2}/\mu^2$ respectively, as well as on g and ϵ. Here the ζ variables are defined by (10.93).

We will see that the denominators (10.94) are obtained as a result of the subtractions in $C_R \Gamma$ for smaller regions; they have the effect of compensating double counting between the collinear and soft factors. Closely related to this is that we will find that rapidity divergences associated with the Wilson lines in light-like directions cancel between the numerators and denominators. In effect,

$$A^{\text{basic}} = \underset{y_{u_2} \to -\infty}{\text{``lim''}} \frac{A^{\text{unsub}}(y_{p_A} - y_{u_2})}{S(y_1 - y_{u_2})}, \quad (10.95)$$

and similarly for B^{basic}. However, there is a non-uniformity in taking the infinite rapidity limits and removing the UV regulator, which impacts calculations. As indicated by the quotation marks, the limit in (10.95) is taken in a special way to be defined in Sec. 10.8.2.

Finally, the hard factor is essentially whatever is left over, in the limit that masses are neglected:

$$H = \left. \frac{F}{A^{\text{basic}} B^{\text{basic}} S} \right|_{m_g = m = 0, \, p_A, n_1, p_B, n_2 \text{ light-like}}. \quad (10.96)$$

Originally we choose n_1 and n_2 to be vectors with approximately the rapidities of p_A and p_B. So taking the massless limit for p_A and p_B implies that we replace n_1 and n_2 by their light-like limits, i.e., w_1 and w_2. Our definition of the collinear factors implies that H includes factors of spinors $\bar{u}_A \mathcal{P}_B$ and $\mathcal{P}_B v_B$ with a Dirac matrix between them.

10.8.2 Limit of infinite rapidity Wilson lines

The limit $y_{u_2} \to -\infty$ on the Wilson-line rapidity in (10.95) needs a little care in its definition concerning the hard region of large transverse momenta: there is non-uniformity

in combining the limits of infinite rapidities with the removal of a UV regulator. We use the following procedure to define A^{basic} and B^{basic}.

- For A^{unsub} and S, apply a UV regulator, e.g., dimensional regularization with $n < 4$.
- Take the limit $y_{u_2} \to -\infty$ on the r.h.s. of (10.95).
- Apply UV counterterms.
- Remove the UV regulator, e.g., take $n \to 4$.

This corresponds to our procedure for calculating $C_A \Gamma_1$ and $C_B \Gamma_1$ in (10.42) and (10.43).

If we reversed the limits, we would need to compensate by an extra hard factor, e.g.,

$$A^{\text{basic}} = \lim_{y_{u_2} \to -\infty} \left[\lim_{n \to 4} \frac{A^{\text{unsub}}(y_{p_A} - y_{u_2})}{S(y_1 - y_{u_2})} \tilde{Z}_A(\zeta_{A,n_1}/\mu^2, y_1 - y_{u_2}, g(\mu), \epsilon) \right]. \quad (10.97)$$

The factor $\tilde{Z}_A$ is to be adjusted so that we get the same results as in (10.94a). Now the non-uniformity of the limits $n \to 4$ and of infinite Wilson-line rapidities only concerns the limit of infinitely large transverse momentum; for $n < 4$, the limits can be exchanged. Thus the factor $\tilde{Z}_A$ is a pure UV factor, and can be regarded as a kind of generalized UV renormalization factor, chosen to make a renormalization prescription that agrees with the combination of $\overline{\text{MS}}$ renormalization and the opposite order of the limits.

Within the context of low-order perturbation theory, especially at one loop, the first description works; an example is in the calculation of the one-loop collinear term at (10.42).

An exactly similar procedure applies to the B factor.

10.8.3 Elements of diagrammatic Ward identities

Ward identities can be derived without perturbation theory, as properties of Green functions. From these we could try to derive identities for the factors, H, A, B, and S in Fig. 10.3, which are *modified* Green functions, with appropriate irreducibility properties and subtractions.[9] For our present work, it is considerably easier just to give a perturbative proof, valid to all orders, where we will take full account of the necessary subtractions and irreducibility properties. The general approach was seen in Sec. 7.7, where we derived a gauge-invariant parton model in a full non-abelian theory, i.e., QCD with a limited set of graphs.

Here we handle the full set of graphs, but restrict to an abelian theory in a covariant gauge. In deriving factorization, it will be important to understand which subgraphs are allowed and which are not, for A, for B, and particularly for H, in Fig. 10.3(b), given a specification of their external lines. This will modify the derivation of the Ward identities from the standard derivation, e.g., Sterman (1993, p. 334–340).

Consider one gluon from subgraph S to subgraph A, and its attachment to a quark line, as in the left-hand side of Fig. 10.12(a). The triangle at the vertex denotes the application of the soft approximation. *For the moment we ignore the subtraction terms.*

---

[9] Here Fig. 10.3(b) is treated as specifying the term $C_R \Gamma$, with the subgraphs H, A, B, S being those the specify the region R.
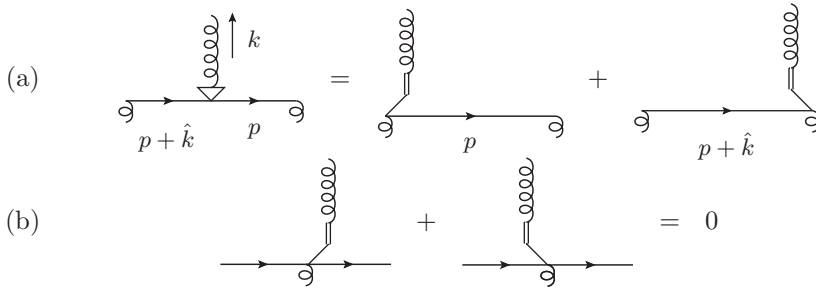
Fig. 10.12. Graphical elements of Ward identity: (a) application to line, (b) sum at vertex (in abelian gauge theory).

Let k be the gluon momentum, and let $\hat{k}$ be its approximant defined in (10.16). We apply the following identity:

$$\frac{n_1^\mu}{k \cdot n_1 + i0} \frac{i}{\not{p} - m + i0} (-ig\hat{\not{k}}) \frac{i}{\not{p} + \hat{\not{k}} - m + i0}$$

$$= \frac{i(-ign_1^\mu)}{k \cdot n_1 + i0} \left[\frac{i}{\not{p} - m + i0} - \frac{i}{\not{p} + \hat{\not{k}} - m + i0} \right]. \tag{10.98}$$

Thus one or other quark propagator is canceled, as pictured on the right-hand side of Fig. 10.12(a). The gluon is now attached to a special vertex that is at one or other end of the quark line. At this special vertex,[10] the double line denotes a factor of a Wilson-line propagator with an accompanying vertex, and the diagonal single line codes an overall sign. The sign essentially concerns the charge of the quark field.

We now sum over all places where the gluon can attach to the quark line. Now, when an S gluon attaches to an A quark, an equally allowed graph is where the S gluon attaches to the opposite side of a neighboring gluon vertex, as in Fig. 10.13. Note that the other gluon, of momentum l, may either be part of the A subgraph or the S subgraph; the argument works equally in both cases. This gives pairs of canceling terms, at each other gluon vertex on the quark, as illustrated in Fig. 10.12(b). If the quark line goes around in a loop inside the collinear graph, we get zero. But if the quark line goes out of the collinear graph, we are left with only the special vertices at the outside end(s) of the quark line. At the on-shell p_A end we in fact get zero, exactly as in the standard textbook case.[11] There remains one term, at the end of the quark line where it enters the hard scattering. The result is just as in the lowest-order case, (10.29), and is equivalent to a gluon attaching to a Wilson line.

In certain model calculations, we might use a scalar quark. In that case, we must take account of the vertex with two gluons. The necessary vertex identity is Fig. 10.14, which replaces Fig. 10.12(b) for spin-$\frac{1}{2}$ quarks. It is readily verified from the form of the two-quark–two-gluon vertex.

---

[10] In the context of diagrammatic proofs of Ward identities (e.g., Sterman, 1993, p. 351) the vertex represents the BRST transformation of the field at the end of the quark propagator, but in our work it is multiplied by an eikonal denominator.

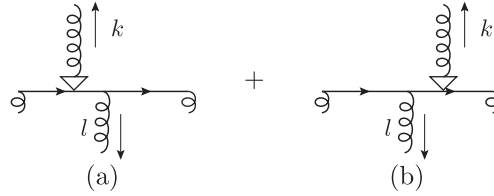[11] However, the details are not always made explicit in the textbooks!

Fig. 10.13. Example of graphical structure which leads to the canceling terms in Fig. 10.12(b).
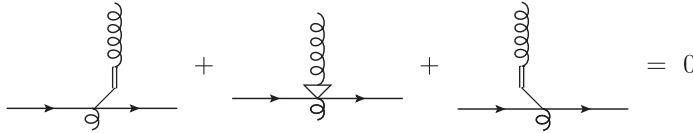

Fig. 10.14. Vertex sum as in Fig. 10.12(b), but for scalar quark.

10.8.4 Extraction of soft lines from collinear subgraphs

Now consider all the gluons entering collinear subgraph A from the soft subgraph S, continuing to omit the subtractions. We apply the Ward-identity argument of Sec. 10.8.3 to each gluon in turn, summing over allowed graphs for the A subgraph, given a particular set of external lines for the subgraph. Then we apply the same argument to the gluons from S to the other collinear subgraph B, and represent the result in Fig. 10.15(a) and (b). Each external gluon of the S subgraph now attaches to a Wilson-line factor of the form

$$\frac{i(-ign_1^\mu)}{k_j \cdot n_1 + i0} \quad \text{on } A \text{ side}, \qquad \frac{i(ign_2^\mu)}{k_j \cdot n_2 + i0} \quad \text{on } B \text{ side}, \qquad (10.99)$$

where k_j is the gluon momentum, defined to flow *into* the S subgraph.

We convert the result to exactly the Wilson-line form by using the following identity for the product of elementary Wilson-line propagators:

$$\prod_{j=1}^N \frac{i}{k_j \cdot n + i0} = \sum_{\text{permutations}} \frac{i}{k_1 \cdot n + i0} \times \frac{i}{k_1 \cdot n + k_2 \cdot n + i0}$$

$$\times \cdots \times \frac{i}{k_1 \cdot n + k_2 \cdot n + \ldots k_N \cdot n + i0}. \qquad (10.100)$$

This identity is readily proved by induction on N, and is applied separately to the parts of the diagram with $n = n_1$ and $n = n_2$. The right-hand side is exactly the product of lines resulting from the Feynman rules for a Wilson line (Sec. 7.6). Wilson-line vertex factors are exactly the $-ign_1$ and ign_2 factors in (10.99).

Next we observe that, with the region approximator T_R defined in Sec. 10.4.2, the approximated hard subgraph H is independent of the soft momenta. Thus we can contract the free ends of the Wilson lines together to give Fig. 10.15(c). The right-hand factor
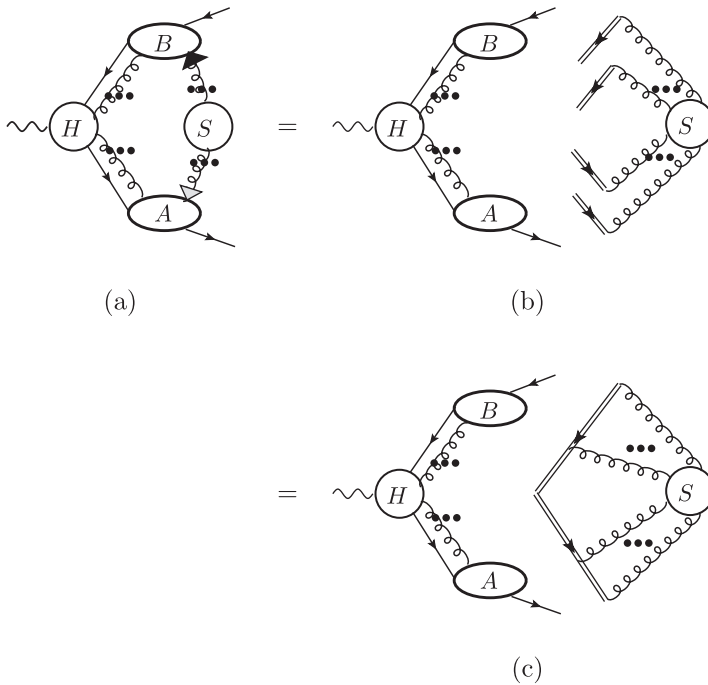
Fig. 10.15. Application of Ward identities to extract S gluons from the collinear subgraph with the soft approximation in (a). After use of Ward identities we get graph (b), and after use of (10.100), we get graph (c).
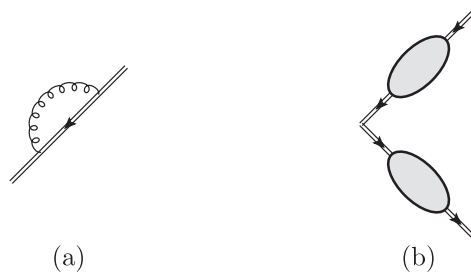

Fig. 10.16. (a) Example of Wilson-line self-energy graph. (b) Denominator of (10.89).

(summed over graphs for S) is just what we already stated as the definition (10.89) of the soft factor; there is one complication in the proof that I now explain.

Each connected component of an S subgraph joins the A and B sides. So no graph arises in Fig. 10.15(b) where a component of S just connects n_1 lines to themselves, or n_2 lines to themselves. However, such graphs do arise from the matrix element of the Wilson line, the numerator of (10.89), giving for example Fig. 10.16(a). If we were to sum over all such graphs, they would form extra factors in Fig. 10.15(b), which we call Wilson-line

self-energy factors. Converting these factors to the Wilson-line form gives the general form of Fig. 10.16(b), which has the operator form

$$\text{W.L. self-energy factor} = \langle 0|W(\infty, 0, n_2)^\dagger|0\rangle \, \langle 0|W(\infty, 0, n_1)|0\rangle \,. \qquad (10.101)$$

Since these graphs are not produced by our Ward-identity argument, they must be removed from the definition of the soft factor. Thus (10.101) is the denominator in the definition (10.89) of the soft factor.

A careful examination of calculations of the self-energy factor shows that it has a divergence as the length of the Wilson line goes to infinity. No such divergence arises from graphs that connect the n_1 to the n_2 lines. So for a correct definition of the soft factor, we first replace the occurrences of "∞" in (10.89) and (10.101) by some large finite length L. Then the soft factor (10.89) is defined with a limit $L \to \infty$.

Finally, there are UV divergences in many of the relevant graphs. Just as in the textbook treatment of conventional Ward identities (e.g., Collins, 1984, Ch. 9) we define these to be canceled by UV counterterms. Just as in that case, the counterterms preserve the derivation of the Ward identities, provided that an appropriate renormalization scheme is used, like $\overline{\text{MS}}$.

10.8.5 Subtractions and the derivation of the soft factor

We have extracted soft gluons from their attachments to the collinear factors. But our derivation so far has applied to $T_R\Gamma$, i.e., to the approximator for region R of graph Γ, followed by a sum over graphs. We now examine the effect of the subtractions that convert $T_R\Gamma$ to the region term $C_R\Gamma$, defined in (10.4). These prevent double counting with the terms for smaller regions $R' < R$. Note that for a general region and graph, the subtraction terms $-C_{R'}\Gamma$ themselves contain subtractions, recursively applied. We now show how the fundamental elements, Figs. 10.12 and 10.14, in the derivation of the Ward identities continue to apply in the presence of subtractions.

We represent the relation between a pair of relevant regions in Fig. 10.17. There, diagram (a) depicts the division of a graph into the hard, collinear, and soft subgraphs associated with a region R; it is a more abstract representation of Fig. 10.3(b). In a smaller region $R' < R$, either the soft subgraph is bigger than in R, or the hard subgraph is smaller, or both, as in Fig. 10.17(b).

A generic term in $C_R\Gamma$ corresponds to a set of nested regions R_j that obey $R_1 < R_2 < \cdots < R_n < R$, and the corresponding contribution to $C_R\Gamma$ is

$$(-1)^n T_R \prod_{j=1}^{n} T_{R_j}\Gamma. \qquad (10.102)$$

The T_{R_j} operations are applied from inside out, smallest region to largest. Then $C_R\Gamma$ is the sum over possibilities for (10.102), including the case $n = 0$. This follows from the definition (10.4) of $C_R\Gamma$, exactly as in the theory of renormalization (Collins, 1984). The differences with renormalization are only in the specification of the regions and in the definitions of the region approximators.
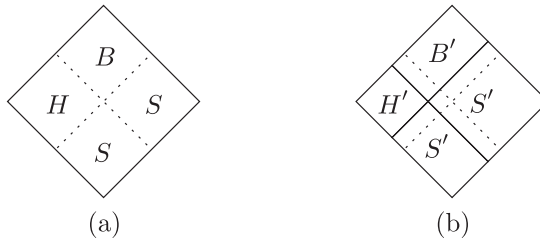
Fig. 10.17. (a) Partition of graph for Sudakov form factor by subgraphs for a region R. (b) Partition for a smaller region $R' < R$. The dotted lines indicate the boundaries of the subgraphs for the first region.

Now each region R_j corresponds to a pinch-singular surface (PSS) in the massless limit. Its approximator T_{R_j} is obtained from the leading power of the integrand expanded in powers of the radial variable λ_{R_j} for the region, with masses treated as an appropriate power of λ_{R_j}. This expansion is then slightly modified by the following replacements for soft loop momenta in the collinear subgraphs:

$$k_{AS} \cdot w_1 \mapsto k_{AS} \cdot n_1, \qquad k_{BS} \cdot w_2 \mapsto k_{BS} \cdot n_2, \tag{10.103}$$

as in (10.17) and (10.18). We now show that the Ward identities we use for extracting the soft factor continue to apply in the presence of the subtractions.

Let a gluon of momentum k from the S subgraph of R attach to an A quark. The line identity, (10.98) and Fig. 10.12(a), has the structure

$$\frac{1}{A_1} (A_1 - A_2) \frac{1}{A_2} = \frac{1}{A_2} - \frac{1}{A_1}, \tag{10.104}$$

up to an overall factor of a phase and a coupling. Here $1/A_1$ and $1/A_2$ are the quark propagators, and $A_1 - A_2$ is the vertex factor, $\hat{k}^- \gamma^+$.

Now, to get from $T_R \Gamma$ to $C_R \Gamma$ we sum (10.102) over all possibilities for nested sets of smaller regions. Each term in (10.102) has region approximator(s) applied to the graph, which contains the l.h.s. of (10.104) as a factor. Each region approximator replaces each factor in the graph by (the first term) in its expansion in powers of λ_{R_j}, supplemented by the replacements like (10.103). All of these operations can be applied equally well when the l.h.s. of (10.104) is replaced by one or other of the terms on the r.h.s. Furthermore, the same collection of operations can be applied to each of the terms in the vertex identity Fig. 10.12(b) or Fig. 10.14.

This indicates that the Ward identities that apply to $\sum_{R,\Gamma} T_R \Gamma$ are also valid in the presence of subtractions, so that the Ward-identity result should also apply to $\sum_{R,\Gamma} C_R \Gamma$. However, there is a potential problem that to use the vertex identity, we are combining terms obtained from different graphs, and these could have different regions. To see the difficulty, observe that the canceling terms at a vertex arise from different graphs, e.g., from Fig. 10.13. To make the vertex identity work in the presence of subtractions, we must use a correspondence between the regions for the different graphs. We need to determine the situations where the correspondence fails to exist, and to deal with the consequences.

Another related complication is that the region approximator T_{R_j} takes the leading power in λ_{R_j} of the factors in the graph; we must investigate what happens if an approximator gives a different power of λ_{R_j} when applied to A_1 and A_2 on the r.h.s. of (10.104).

Consider the application of T_{R_j} to (10.104). It takes the leading power in λ_{R_j} of each factor on the l.h.s. For the quantities A_1 and A_2, let the leading-most terms be $\hat{A}_1$ and $\hat{A}_2$. In the most general context, there are three possible cases for the power laws:

- The power of λ_{R_j} is the same for both quantities, and for $A_2 - A_1$. The line identity applies equally to the leading-power expansion

$$\frac{1}{\hat{A}_1} (\hat{A}_1 - \hat{A}_2) \frac{1}{\hat{A}_2} = \frac{1}{\hat{A}_2} - \frac{1}{\hat{A}_1}. \tag{10.105}$$

  The left-hand side gives the effect of T_{R_j} on the left-hand side of (10.104), and the two terms on the right are the effect of applying T_{R_j} to the terms on the right-hand side of (10.104). Effectively, T_{R_j} is a linear operation that commutes with the manipulations giving the Ward identity. If T_{R_j} had been defined to make different operations on the vertex factor and the propagators, this result need not be true. The quantity on the left-hand side and the two terms on the right-hand side have the same power-counting and therefore do not change the necessary set of subregions.

  The above situation is always the case for a soft line connected to a collinear line, with the one trivial exception that one line, e.g., A_2, is an external line. Then we omit the $1/A_2$ factor, and replace A_2 by zero.

- Another possibility is that the power of λ_{R_j} for one line, A_2 say, is larger than for the other line A_1. Thus $A_2/A_1 \to 0$ in the limit of $\lambda_{R_j} \to 0$. Then the leading power of the vertex factor $A_1 - A_2$ is just $\hat{A}_1$, and we must replace (10.105) by

$$\frac{1}{\hat{A}_1} \hat{A}_1 \frac{1}{\hat{A}_2} = \frac{1}{\hat{A}_2}. \tag{10.106}$$

  At the PSS R_j, the $\hat{A}_2$ line can be viewed as on-shell, and we get exactly one term on the right-hand side, just as when such a line is exactly on-shell. The term $1/\hat{A}_1$ is smaller by a power of λ_j than $1/\hat{A}_2$, and so is correctly neglected.

- A final possibility is that A_2 and A_1 are comparable, but $A_1 - A_2$ is much smaller. In that case, no subtraction associated with R_j is actually needed for the original graph. But for the individual terms on the right-hand side we do need subtractions. Even though R_j is not actually a leading region for the original graph, we add it to the catalog of leading regions.

The above treatment applies literally for scalar quarks, for then the quantities A_1 and A_2 are scalars, and the definition of their power is unambiguous. For fermions, each is a matrix, whose inverse is taken in the propagators. A slightly more complicated version of the argument leads to the same outcome.

Finally we apply the vertex identity. This relates graphs with the same set of denominators, and hence with the same subtractions. So the vertex identities continue to apply after all the subtractions for subregions have been applied.

When applying the vertex identity, we will have canceling terms obtained from applying the line identity to neighboring lines. In the above derivations we have only examined the vertex and lines in question. It is important that everything else in the graphs remains the same. For example, in defining the soft (and collinear) factors, we inserted Wilson-line denominators with non-light-like directions to cut off rapidity divergences. The success of the vertex identities depends on these non-light-like lines being the same everywhere they are encountered, e.g., always the same n_1 for a soft gluon connecting to a collinear-to-A quark.

The final result is that Ward identities apply in the presence of subtractions just as they did in the elementary case we examined where we ignored subtractions. However, we must take care to apply subtractions to the resulting factors.

So far we have extracted the soft factor. Since there are no smaller momentum classes than soft, this factor needs no subtraction. Thus we have completed the proof that the soft part of the form factor factorizes, and that the soft factor can be defined by (10.89). That is, after summing over graphs and regions, we get Fig. 10.15(c).

But subtractions are needed in the remaining parts of the graphs, and our next task is to convert them into hard and collinear factors (which will have subtractions).

10.8.6 Extraction of collinear factors from hard scattering, without effect of subtractions

We now extract the collinear gluon attachments from the hard scattering and convert them to attachments to Wilson-line operators, as in (10.94a) and (10.94b). As before, we start by examining the part of $C_R\Gamma$ without subtractions, and extract the collinear gluons one-by-one. The argument will be somewhat modified from that for soft gluons attaching to a collinear subgraph, because the allowed subgraphs for H have important restrictions by being 1PI in each set of collinear lines.

Of the two graphical elements for the Ward identity, a line identity like Fig. 10.12(a) continues to apply, with only the caveat that one of the lines p and $p + \hat{k}$, inside the H subgraph, may be set on-shell by the approximator applied to a quark line at the collinear edge of H. But for the vertex identity, Fig. 10.12(b), we can miss one of the graphs it implicates.

An example is shown in Fig. 10.18, where we sum over the possible attachments of a B gluon of momentum k to a one-loop hard subgraph. In graph (a), there is an on-shell quark to the right of the vertex with the gluon, so that one term in the line identity gives zero, as usual for an on-shell quark.[12] There is then the usual chain of cancellations, with graphs (b) and (c). But we do not have the graph where gluon k attaches one place to the right of where it is in (c), i.e., we are missing graph (d). This is because in graph (d), gluon k attaches to another B line at its lower end, so that vertex is not part of the hard subgraph;

---

[12] Note that in the general case, with a non-trivial collinear-to-B subgraph, the quark in question is on-shell not because it is an external quark, but because it is the outermost quark line of the hard scattering. Our definition of the approximator for a region replaces the (possibly off-shell) external quarks of the hard scattering by exactly on-shell quarks.
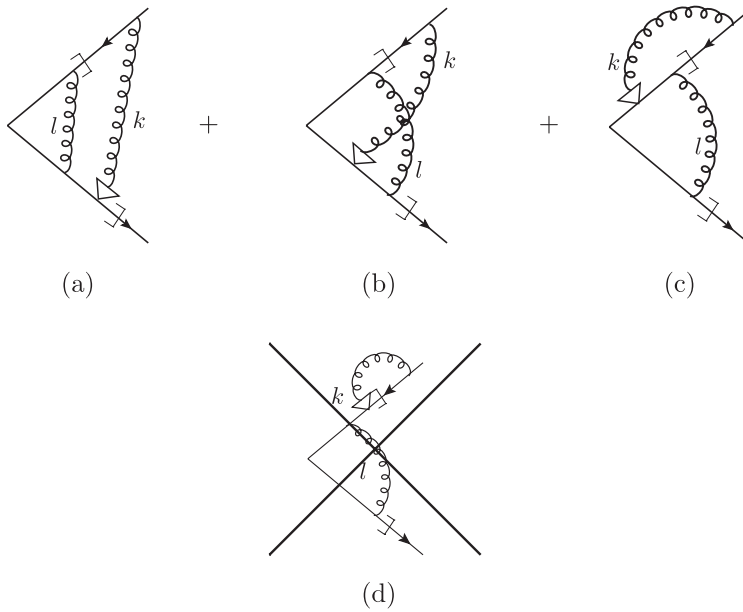
Fig. 10.18. Example of sum over attachments of gluon from collinear subgraph to hard subgraph. The gluon l is in subgraph H, and the gluon k is in subgraph B. The hooks on the quark lines indicate lines that are approximated as on-shell in the hard subgraph H. The big arrow at the bottom of line k has the same meaning as in Fig. 10.6(a), except that it uses the vector w_1 instead of n_1. Graphs (a)–(c) are summed, while graph (d) is excluded by the condition that the hard subgraph is 1PI in collinear-to-B lines.

we see here an example of the general result that a hard subgraph is 1PI in lines that are collinear to a particular direction.

The result is shown in Fig. 10.19, and it shows that the sum over attachments of gluon k to a hard subgraph has extracted the gluon from the hard scattering and attached it instead to a Wilson line. The Wilson line has exactly the form that results from the definition, (10.94b), of the collinear-to-B factor. The remaining factor is a one-loop graph for the hard subgraph without any extra gluons.

In the general case of a B gluon connecting to any H subgraph, what possibilities are there? They are when one but not the other of the two graphs in Fig. 10.13 is not allowed, given that gluon k is in the B subgraph, and that, at least on one side, the quark line is in the H subgraph. It is easily checked that there are two cases, each where one of the two subgraphs would have a collinear quark line.

One corresponds to Fig. 10.19(a), where the quark on one side of the vertex for k is in the B subgraph. This gives the expected Wilson-line vertex.

The other case is where the other gluon l and the quark line on one side are in the A subgraph, as in Fig. 10.20. We get an extra term in the sum over attachments of the k gluon, Fig. 10.20(c). This graph is in fact zero. The reason, which applies generally, is that at the attachment of gluon l the approximator picks out exactly the minus component of the
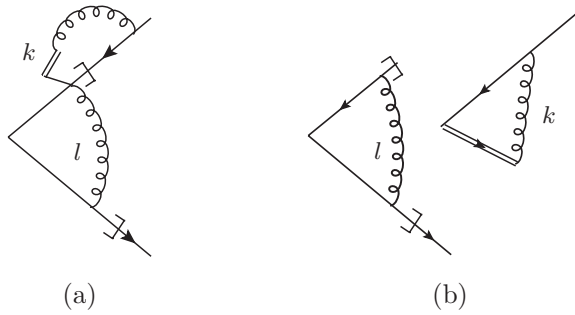
Fig. 10.19. Result of sum in Fig. 10.18: (a) in the notation of Fig. 10.12, (b) as an attachment to a Wilson line.
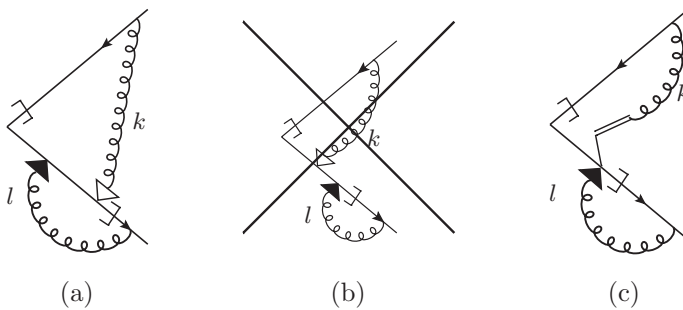

Fig. 10.20. Simplest example of the other case that the vertex cancellation in the Ward identity has a missing term. Approximators are applied for the case that k is collinear to B, and l is collinear to A.

vertex; see (10.23), where the H subgraph is contracted with $P_{HA}(k_{HA})$, which is exactly in the w_1 direction. But the vertex is now exactly at the edge of the hard subgraph where there is a quark that is exactly in the plus direction. It has a projection onto on-shell massless wave functions for the quark, by the matrix $\mathcal{P}_B$. Therefore multiplying by the vertex factor γ^- gives zero; this is essentially from the Dirac equation for a massless quark in the plus direction:

$$0 = \bar{u}_{A\,\text{massless}} \gamma^- p_A^+. \tag{10.107}$$

Although we have formulated this argument for one graph, and for Dirac quarks, the argument is actually general. It concerns an approximation where both the quark and the gluon l have been made exactly massless and collinear in the plus direction in one part of the hard subgraph. The minus component of the vertex goes to zero under an infinite boost from a rest frame.

We now repeat the above arguments for all gluons entering the H subgraph from the collinear subgraphs, first from the collinear-to-B subgraph and then from the collinear-to-A subgraph. After a sum over all graphs, we get two collinear factors times a hard factor. As with the soft factor, each collinear factor has a product of one-gluon Wilson-line factors,
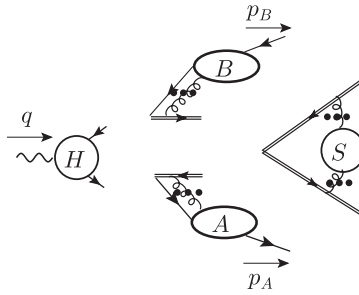
Fig. 10.21. Factorized structure for Sudakov form factor. The double lines are Wilson lines with the following rapidities: $-\infty$ for A, $+\infty$ for B, y_1 and y_2 for S. Subtractions in H, A, and B are not indicated explicitly.

and we use (10.100) to convert them to exactly a Wilson-line matrix element. Again, just as with the soft factor, Wilson-line self-energies are missing. So we must divide by a Wilson-line self-energy factor. The Wilson lines are exactly those with light-like directions that are in the numerators of the previously stated definitions of the collinear factors, (10.94).

10.8.7 Collinear factors, with subtractions

Subtractions arise in a more complicated way than for the soft factor, and specific examples in multiloop graphs can become quite elaborate.

The most general method of dealing with subtractions is to appeal to the argument given in Sec. 10.8.5, which applies quite generally. This is that subtractions apply whenever a graph would have singularities in the massless limit, and that they are obtained from the analytic structure of the denominators, together with power-counting. We showed that the Ward identities apply in the presence of subtractions.

Therefore all we have to do to convert the unsubtracted result is to apply subtractions. Without the subtractions, the arguments so far give the factorized structure shown in Fig. 10.21. We have separate hard, collinear and soft factors multiplied together. The correct formula is obtained simply by applying subtractions to the factors.

For the soft factor, as already explained, no subtractions are needed, because there are no momentum regions smaller than a soft configuration. (Beyond this we also need the Wilson-loop denominator in (10.89), to remove the Wilson-line self-energies, which do not arise from the Ward-identity argument.)

For each collinear factor we have soft subtractions and for the hard factor we have soft and collinear subtractions.

The easiest way to obtain an operator form for a subtracted collinear factor is to apply the factorization argument to the unsubtracted collinear factor, e.g., to the limit $y_{u_2} \to -\infty$ of (10.90), which has a non-light-like Wilson line, of rapidity y_{u_2}. The leading regions have the form shown in Fig. 10.22(a). These each have a collinear-to-A subgraph and a soft graph that connects the Wilson line to the collinear subgraph, by arbitrarily many
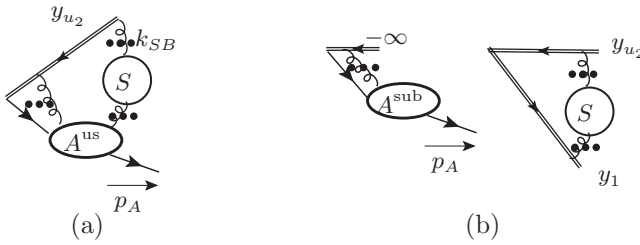
Fig. 10.22. (a) Regions for unsubtracted collinear matrix element (10.90). Here A^{us} is an abbreviation for A^{unsub}. (b) After applying Ward identities to the gluons attaching the soft subgraph to the collinear subgraph, we get this factorized form. Here A^{sub} denotes the subtracted collinear factor. Next to each Wilson line is a label indicating its rapidity.

gluons. We define the soft region with respect to u_2 rather than the overall center-of-mass. In accordance with the order of limits specified in Sec. 10.8.2, we take the limit $y_{u_2} \to -\infty$ with fixed space-time dimension $4 - 2\epsilon < 4$, so that loop corrections to the hard subgraph are power-suppressed, and we need no hard subgraph, just the connections from the collinear subgraph to the Wilson line.

Since the collinear-B part is already in a Wilson-line form, it is enough to combine the soft factor and the collinear-B factor in a new soft factor, denoted S in Fig. 10.22. The usual Ward-identity argument is applied to gluons entering the collinear-A subgraph from S. The same argument that we applied to the whole form factor now applies here, and results in a soft factor times a subtracted collinear factor:

$$A^{\text{unsub}}(y_{p_A} - y_{u_2}) = A^{\text{sub}} \times S(y_1 - y_{u_2}), \tag{10.108}$$

up to terms that are power-suppressed in the limit $y_{u_2} \to -\infty$. The soft factor is the same as in factorization for the form factor itself, *except that* the direction of the Wilson line on the B side is u_2 instead of n_2. This is depicted in Fig. 10.22(b).

Dividing by the soft factor on both sides of the above equation gives the subtracted A factor as the unsubtracted matrix element (10.90) divided by the relevant soft factor. Taking the limit $y_{u_2} \to \infty$, i.e., $u_2 \to w_2$, gives our definition of the subtracted soft factor A^{basic} in (10.94a). The subtractions are the same as in the collinear factor used for the form factor, so it has the same definition. Thus A^{basic} is to be identified with the graphical factor A both in Fig. 10.21, and in the factorization formula (10.11).

An exactly similar argument applies to the collinear-to-B factor, of course.

10.8.8 Hard factor

At this point, we have actually proved a form of factorization, (10.11), given in diagrams in Fig. 10.21, and we have given explicit definitions of the soft and collinear factors.

Now we obtain an explicit formula (10.96) for the hard factor H. The graphs for H are the same as for the form factor itself, i.e., for the reaction $\gamma^* \to q\bar{q}$, but they have subtractions for soft and collinear regions. The graphs are to be 1PI in the external quark

and antiquark, since external propagator corrections are always part of a collinear subgraph. The formula (10.96) is obtained simply by observing that the power-suppressed corrections in (10.11) go to zero as masses are taken to zero. Taking the massless limit means not only setting the quark and gluon masses to zero in graphs, but also taking the light-like limits for the vectors n_1 and n_2 in the Wilson lines associated with the quark and antiquark. The one-loop expansion of (10.96) reproduces the result (10.45) which we already obtained from the subtraction formalism.

Later, we will find a slightly simpler formula (10.120), after we examine the evolution equations of the soft factor S with respect to the rapidities of its Wilson lines.

In addition to the kinematic variable Q, the hard factor depends on the renormalization scale μ. As usual, the μ dependence is governed by an RGE. So we can use the RGE to set μ of order Q, and then the hard factor would be perturbatively calculable (in a QCD problem). For the evolution, anomalous dimension are generally perturbatively calculable.

10.9 Factorization in terms of unsubtracted factors

To compensate double counting between soft and collinear regions, we implemented subtractions in the collinear factors. We then saw that after summing over graphs and regions, the subtractions were implemented by dividing out a certain factor.

We can write the factorized form factor in terms of the unsubtracted matrix elements:

$$
F \sim \lim_{\substack{y_{u_1} \to +\infty \\ y_{u_2} \to -\infty}} H \; \frac{A^{\text{unsub}}(y_{p_A} - y_{u_2}) \; B^{\text{unsub}}(y_{u_1} - y_{p_B}) \; S(y_1 - y_2)}{S(y_{u_1} - y_2) \; S(y_1 - y_{u_2})}. \tag{10.109}
$$

Here, we have indicated the dependence of the factors on the directions of the Wilson lines. Of course, the dependence on the Wilson-line rapidities must disappear after taking the product $HABS$, at least to leading power in Q, since the Wilson lines do not appear in the original form factor. If the rapidity limits in (10.109) are taken *after* the UV regulator is removed, then the definition of the hard factor must be modified, as follows from Sec. 10.8.2.

In the definitions of A^{unsub}, B^{unsub}, and S, Wilson-line self-energies are canceled by dividing each quantity by the appropriate version of (10.101). When we combine all the factors in (10.109) the self-energies exactly cancel, since there are equal numbers of each direction of Wilson line in the numerator and denominator of (10.109).

After deriving evolution equations, it will be convenient to reorganize this formula to give it more convenient properties; see Sec. 10.11.

10.10 Evolution

We need evolution equations for the dependence of the soft and collinear factors on the rapidities of their Wilson lines. Evolution equations provide much of the predictive power of factorization.
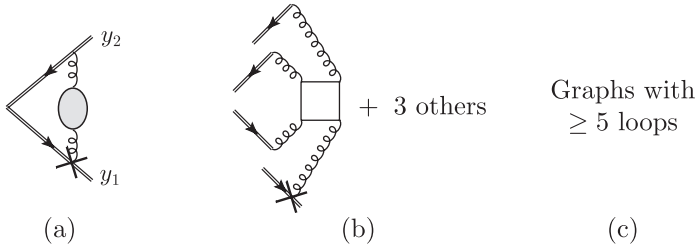
Fig. 10.23. Graphs for the connected part of the derivative of the soft factor, up to four loops. The blob on the gluon line in (a) denotes all corrections to the gluon propagator. The crossed vertex is the same as in Fig. 10.10, and is defined from (10.49). The left-hand ends of the Wilson lines are intended to be joined together, to implement the l.h.s. of (10.100).

Without the evolution equations, we would have no better predictive power than from direct perturbative calculations of the form factor, and accuracy would be particularly compromised by the two logarithms per loop. With the evolution equations including the RGEs, we can obtain all the factors in terms of quantities that are free of large logarithms.

The evolution equations given below were first obtained by Collins (1980), but by different and less general methods, and with different, but closely related, gauge-dependent definitions of the factors.

10.10.1 Evolution of basic soft factor

We start with the dependence on y_1 or y_2 of $S(y_1 - y_2)$. Deriving its evolution equation is a fairly simple generalization of our one-loop calculation in Sec. 10.5.10.

Since we are in an abelian theory, we use the identity (10.100) to write the value of a Wilson line as the product of elementary one-vertex Wilson lines. Then S is the exponential of its irreducible connected part:

$$S(y_1 - y_2) = \exp(S_{\text{conn}}). \qquad (10.110)$$

Differentiating with respect to y_1 gives

$$\frac{\partial S(y_1 - y_2)}{\partial y_1} = S \frac{\partial S_{\text{conn}}}{\partial y_1}. \qquad (10.111)$$

As illustrated in Fig. 10.23, graphs for $\partial S_{\text{conn}}/\partial y_1$ have one vertex for a differentiated Wilson line, just as in the lowest-order case, Fig. 10.10, together with at least one Wilson-line vertex on the other side, and any number of extra Wilson-line vertices, but no Wilson-line self-energies. Notice that the corrections at two- and three-loop order only arise from corrections to the gluon propagator.

We now perform a region analysis for $\partial S_{\text{conn}}/\partial y_1$. Because of the restriction to connected graphs and because of the differentiated vertex, this analysis is very simple. As usual, graphs

for $\partial S_{\text{conn}}/\partial y_1$ can have H, A, B, and S subgraphs.[13] These subgraphs must be connected to each other, and this must occur through one or more quark loops, since the connections to the Wilson line are to single line segments, after we used (10.100).[14] Therefore, if a region for $\partial S_{\text{conn}}/\partial y_1$ has more than one of the subgraphs H, A, B, and S, we get zero, after applying a Ward identity to the sum over graphs. Exactly as in the one-loop case, the differentiation with respect to y_1 at the crossed vertex forces the gluon line at the differentiated vertex to have rapidity close to y_1; thus it is either collinear-to-A (i.e., to n_1) or hard. It follows that the only two leading regions are where the whole of $\partial S_{\text{conn}}/\partial y_1$ is collinear-to-A or where it is all hard.

Thus the situation we saw for the one-loop case in Sec. 10.5.10 immediately generalizes to all orders:

- The limit $y_2 \to -\infty$ can be taken, so that we can write the evolution equation in terms of a rapidity-independent kernel

$$K\left(m_g, m, \mu, g(\mu)\right) \overset{\text{def}}{=} 2 \lim_{y_2 \to -\infty} \frac{\partial S_{\text{conn}}}{\partial y_1}, \qquad (10.112)$$

plus power-suppressed corrections. Thus in Fig. 10.23, the upper Wilson line can be taken light-like in the minus direction without encountering any divergence.

The above definition of K is asymmetric between the two Wilson lines of S, and we will later make a symmetric definition in (10.122), which leads to the same numerical results for calculations in a covariant gauge.

- The kernel K has an additive anomalous dimension γ_K, as in (10.56).

Hence the previously stated results (10.53) and (10.56) apply generally.

It follows that at large $y_1 - y_2$, the $y_1 - y_2$ and μ dependence of the soft factor has the form

$$S = S_0(m_g, m, \mu_0, g(\mu_0))$$
$$\times \exp\left\{-\frac{y_1 - y_2}{2}\left[\int_{\mu_0}^{\mu} \frac{d\mu'}{\mu'} \gamma_K(g(\mu')) - K(m_g, m, \mu_0, g(\mu_0))\right]\right\}, \qquad (10.113)$$

where μ_0 is a fixed reference value of the renormalization scale, and S_0 is independent of $y_1 - y_2$. Because of power-suppressed corrections, S_0 does *not* equal the value of S when $y_1 = y_2$ and $\mu = \mu_0$.

Naturally, we could equally well have performed the differentiation with respect to y_2 instead of y_1. In that case there would be a change of sign, and the Feynman rules would have the crossed vertex in Fig. 10.23 on the opposite Wilson line. We will redefine K more symmetrically later, in Sec. 10.11.3; the redefinition also remedies a lack of gauge independence of K when one uses a non-covariant gauge.

---

[13] It should be possible to simplify this by a classification of lines by rapidity: collinear-to-B, and n_1-rest-frame.

[14] An example would be Fig. 10.23(b), when the quark loop and the lines to the lower Wilson lines are collinear-to-A, but one or both of the upper gluons are soft.
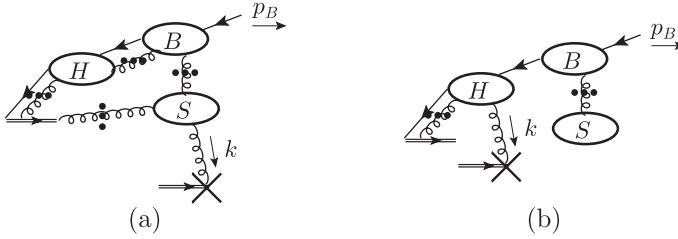
Fig. 10.24. Leading regions for $\partial B(y_1 - y_{p_B})/\partial y_1$, (10.114). *In (b), the soft subgraph has at least one gluon attachment to the main Wilson line*, but we do not show this, to avoid complicating the graph.

10.10.2 Evolution of collinear factor

We now obtain an equation for the derivative with respect to y_1 of the *unsubtracted* collinear factor $B^{\text{unsub}}(y_1, y_{p_B})$. The effect of differentiating the Wilson line is

$$\frac{\partial B^{\text{unsub}}(y_1 - y_{p_B})}{\partial y_1} = \quad \text{(10.114)}$$

As in Fig. 10.23, the left-hand end of the differentiated Wilson-line element is attached to the main quark-Wilson-line vertex, and we used (10.100) to allow us to treat each vertex of the Wilson line independently.

We now apply the same arguments as we used for factorization. But we simplify the argument by using a frame where n_1 has zero rapidity, so that the momentum categories are soft, hard, and collinear-to-B. A soft momentum has rapidity comparable to y_1, and there is now no separate collinear-to-A category. As usual, the momentum k at the differentiated vertex is restricted to have a rapidity close to y_1, so that it is either soft or hard. There correspond two types of leading region, shown in Fig. 10.24(a) and (b) respectively.

For the case that k is soft, graph (a), we examine the component of the soft subgraph to which is attaches, and apply Ward identities for all the gluons that couple it to the collinear subgraph. This gives a factor of exactly the kernel $\frac{1}{2}K$ for the evolution of the soft factor, and it multiplies the original collinear factor.

When k attaches to the hard subgraph, we use Ward identities to extract the collinear gluon attachments. The result is a factor times the original collinear factor. To this must be applied subtractions for the soft-gluon part. Since there are now no collinear or soft contributions to the hard factor, we can apply the massless limit to it. This gives the following evolution equation (Collins, 1980):

$$\frac{\partial B^{\text{unsub}}(y_{u_1} - y_{p_B})}{\partial y_{u_1}} = \frac{1}{2}\left[K(m, m_g, \mu) + G(\zeta_{B,u_1}, \mu)\right]B^{\text{unsub}}$$

$$+ \text{ non-leading power of } \zeta_{B,u_1}, \quad \text{(10.115)}$$

where ζ_{B,u_1} is defined in (10.93b).

Since G only involves hard momenta, it can be defined in terms of B^{unsub} by a massless limit as

$$G = 2 \lim_{\substack{m \to 0 \\ m_g \to 0}} \left[\frac{\partial \ln B^{\text{unsub}}(\zeta_{p_B, u_1})}{\partial y_{u_1}} - K \right]. \tag{10.116}$$

Here the massless limit is taken with ζ_{p_B, u_1} fixed, and thus with p_B^- fixed. (Note that y_{p_B} would not be a good variable to use, since the rapidity of a massless momentum is infinite.)

If we dimensionally regulate, G decreases like a power of $\zeta_{B, u_1}/\mu^2$. But the power-suppression goes away when $n \to 4$. This gives another view of how, in defining A^{basic} and B^{basic}, we took the $y_{u_1} \to \infty$ and $y_{u_2} \to -\infty$ limits. The limits are of $A^{\text{unsub}}(y_{p_A} - y_{u_2})/S(y_1 - y_{u_2})$ and $B^{\text{unsub}}(y_{u_1} - y_{p_B})/S(y_{u_1} - y_2)$. In accordance with Sec. 10.8.2, these limits are taken with $n < 4$. With $n < 4$ the evolution equations only involve the K terms in the infinite rapidity limit. Since the u_2 (or u_1) Wilson line appears in both numerator and denominator, the evolution equation shows that the K terms cancel, so that the infinite rapidity limits exist. This is consistent with and confirms what we earlier derived by another method.

The companion equation for A has a reversed sign:

$$\frac{\partial A^{\text{unsub}}(y_{p_A} - y_{u_2})}{\partial y_{u_2}} = -\frac{1}{2} \left[K(m, m_g, \mu) + G(\zeta_{A, u_2}, \mu) \right] A^{\text{unsub}}$$

$$+ \text{non-leading power of } Q \text{ and } \zeta_{A, u_2}, \tag{10.117}$$

where ζ_{A, u_2} was defined in (10.93a).

These equations bring under control the dependence of the collinear factors on the Wilson-line rapidities. We then use the RG to tame the logarithms of μ: to set μ to be a fixed scale in K and in the collinear factors, but to be of order Q in G and H. We will discuss this in more detail after we perform a final reorganization of the factorization formula.

10.11 Sudakov: redefinition of factors

The above formalism has some defects, particularly in its generalization to measurable cross sections in QCD:

1. The soft factor has no independent experimental consequences. It always appears multiplied by two collinear factors.

    In QCD applications of factorization, the soft factor is non-perturbative. Although the values of non-perturbative quantities are in principle predicted by QCD, our ability to actually calculate them is currently close to zero. So generally we have to measure them from experiment, and rely on universality to make predictions for the same reactions at different energies and for different reactions. But there is no experimental probe of the soft factor by itself.

2. Feynman rules for the soft factor involve non-light-like Wilson lines. Perturbative calculations of such quantities are more difficult than when at least one Wilson line is light-like. (But, of course, with light-like Wilson lines, there must be subtractions to cancel rapidity divergences.)

3. Associated with the non-light-like Wilson lines in S are power-suppressed corrections to the evolution equation (10.53).

4. The definitions of the factors involve removal of Wilson-line self-energies (10.101). However, these cancel in the complete factorization formula, which suggests a non-optimality in the formulation.

5. The removal of Wilson-line self-energies makes the factors gauge-dependent.

6. Related to this is that although the evolution kernel K defined in (10.112) is gauge independent when restricted to covariant gauges, it changes when the gauge is transformed to an axial or Coulomb gauge. See problem 10.9.

These defects are to be regarded not as errors in the formalism, but as practical problems that make the formalism more complicated to use.

We will now perform a redefinition of the soft, collinear, and hard factors to remove these defects as much as possible. A useful starting point is (10.109), where factorization is given in terms of unsubtracted collinear factors and three occurrences of the basic soft factor S with different rapidity arguments. We can use (10.113), which shows that S has exponential rapidity dependence, to reorganize the factors of S.

Then we will absorb the S factor(s) into redefined collinear factors, to give a new factorization formula with no soft factor:

$$F = HAB + \text{power-suppressed.} \tag{10.118}$$

This overcomes the lack of experimental probes of the soft factor.

The definitions of the new collinear factors are at first sight surprisingly complicated. I will first state the definitions (which supersede those proposed by Collins and Hautmann, 2000). Then I will show how they correspond to the previous factorization formula in the form (10.109). After that I will give the rationale for the new definitions; they are unique given certain reasonable requirements.

10.11.1 Collinear factors

The redefined collinear factors A and B involve an arbitrary rapidity parameter y_n. We assign y_n the physical significance of separating left- and right-moving quanta; the A factor contains the effects of right-movers and B the effects of left-movers. The new collinear factors depend on the difference in rapidity between their particle (p_A or p_B) and y_n.

We will find that the dependence of each collinear factor on y_n is governed by an exactly homogeneous evolution equation involving the kernel K. Thus we can express each collinear factor in terms of its value when its particle has the same rapidity as y_n. This gives an optimal form of factorization.

The redefined collinear factors are

$$A(m, m_g, g, \mu, y_{p_A} - y_n)$$

$$\stackrel{\text{def}}{=} \lim_{\epsilon \to 0} \lim_{\substack{y_1 \to +\infty \\ y_2 \to -\infty}} Z_A \, A^{\text{unsub, bare}}(y_{p_A} - y_2) \sqrt{\frac{S^{\text{bare}}(y_1 - y_n)}{S^{\text{bare}}(y_1 - y_2) \, S^{\text{bare}}(y_n - y_2)}}$$

$$= A^{\text{unsub}}(y_{p_A}, -\infty) \sqrt{\frac{S(+\infty, y_n)}{S(+\infty, -\infty) \, S(y_n, -\infty)}}, \tag{10.119a}$$

$$B(m, m_g, g, \mu, y_n - y_{p_B}) = B^{\text{unsub}}(+\infty, y_{p_B}) \sqrt{\frac{S(y_n, -\infty)}{S(+\infty, -\infty) \, S(+\infty, y_n)}}. \tag{10.119b}$$

As in Sec. 10.8.2, we first take the limits of infinite rapidity, and then we remove the UV regulator $\epsilon \to 0$, with the aid of renormalization factors Z_A and Z_B. This order of limits entails adjusting the renormalization coefficients relative to our previous definitions. Thus it is convenient to write the new definitions in terms of bare soft and collinear factors, i.e., quantities defined without the renormalization factors Z_S, Z_A^{unsub}, and Z_B^{unsub} used in (10.89), (10.90), and (10.92). It is convenient to use a notation with infinite rapidities for the Wilson lines, as in the third and fourth lines of (10.119). It implies the limits given on the second line.

Each of the factors on the r.h.s. of (10.119) was originally defined to have Wilson-line self-energies divided out. It can be shown that the self-energy factors cancel in the combinations used in (10.119). (The total power of self-energy factors for each direction of Wilson line is zero. The only complication is that the Wilson lines for direction n are for opposite charges, but charge-conjugation invariance can be used to show that this is irrelevant.)

I now show that the product of A and B defined in (10.119) equals the product of the soft and collinear factors in our first form of factorization, when it is expressed in terms of unsubtracted collinear factors in (10.109).

First we examine the limits $y_{u_1} \to \infty$ and $y_{u_2} \to -\infty$ in (10.109), by using the evolution equations (10.53), (10.115) and (10.117). The K terms cancel for the y_{u_1} and y_{u_2} dependence in (10.109). This leaves just the G terms from (10.115) and (10.117). These concern a hard momentum region, and are effectively absorbed in UV renormalization factors. From (10.53), we see that the y_1 and y_2 dependence also cancels in (10.109). Thus the unsubtracted collinear factors are the same in (10.109) and in the product of (10.119a) and (10.119b).

After that, we apply the solution (10.113) for S, to show that the combination of S factors in (10.109) agrees with the combination of S factors in the product of (10.119a) and (10.119b).

Hence the two forms of factorization agree.

Notice that Wilson-line self-energies cancel for each of the different types of Wilson line in (10.119), so we do not need to insert any Wilson-loop factor to cancel Wilson-line self-energies, unlike our previous definitions. In fact, the definitions above are unique given the following requirements:
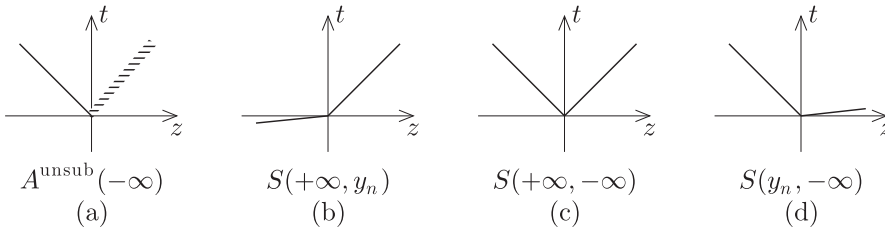
Fig. 10.25. Directions of Wilson lines in the factors in (10.119a): the solid lines are the Wilson lines (which should extend to infinity), which are either light-like or in the direction n, which is here drawn with a slightly positive rapidity y_n. The shaded part of (a) is intended to suggest the final-state quark itself, which moves in a time-like direction.

1. A collinear factor is a product of an unsubtracted collinear factor and powers of S-type objects.
2. Non-light-like Wilson lines only appear in S factors with one light-like and one non-light-like line.
3. Rapidity divergences cancel.[15]
4. Only one light-like direction y_n is used.
5. The definitions obey charge-conjugation symmetry; thus the definition of B is obtained from the definition of A, simply by changing $A^{\text{unsub, bare}}$ to $B^{\text{unsub, bare}}$ and by exchanging the roles of y_1 and y_2.
6. The factorization formula is $H A B$, without any soft factor.

The actual directions of the Wilson lines are shown in Fig. 10.25. In all the S objects, the two Wilson lines are at space-like separations. All the Wilson lines are either space-like or are obtained from a limit of space-like lines. Thus we do not have to be concerned with the ordering of the gauge-field operators on the Wilson lines. At least in covariant gauge, the fields commute at space-like separation. Thus the path ordering on the lines creates no conflict with the time ordering needed to define Green functions that use time-ordered fields. There is also maximum compatibility with Euclidean lattice gauge theory, which is important for attempts to compute non-perturbative collinear factors in QCD.

One perhaps unexpected feature is that the Wilson lines of rapidity y_n in the numerator and denominator of each collinear factor have opposite directions. For example, in (10.119a), y_n in the numerator factor $S(y_1 - y_n)$ corresponds to a Wilson line related to the antiquark. Therefore it has the charge of the antiquark and goes in the direction of a vector $n_B = (-e^{y_n}, e^{-y_n}, \mathbf{0}_{\text{T}})$ whose minus component is positive. But y_n in the denominator factor $S(y_n - y_2)$ corresponds to a Wilson line with the charge of the quark and in the direction of a vector $n_A = (e^{y_n}, -e^{-y_n}, \mathbf{0}_{\text{T}})$ whose plus component is positive. Thus the cancellation of Wilson-line self-energies for the y_n lines in (10.119a) is not as transparent as it would be if the lines were in exactly the same direction. This should be investigated.

In Sec. 10.8.2 was mentioned a non-uniformity of the limits of infinite rapidity and of $n \to 4$. For the newly defined collinear factors, we can see this from Fig. 10.26, which

---

[15] Except for regions of $k_{\text{T}} \to \infty$, which can be canceled by UV renormalization.
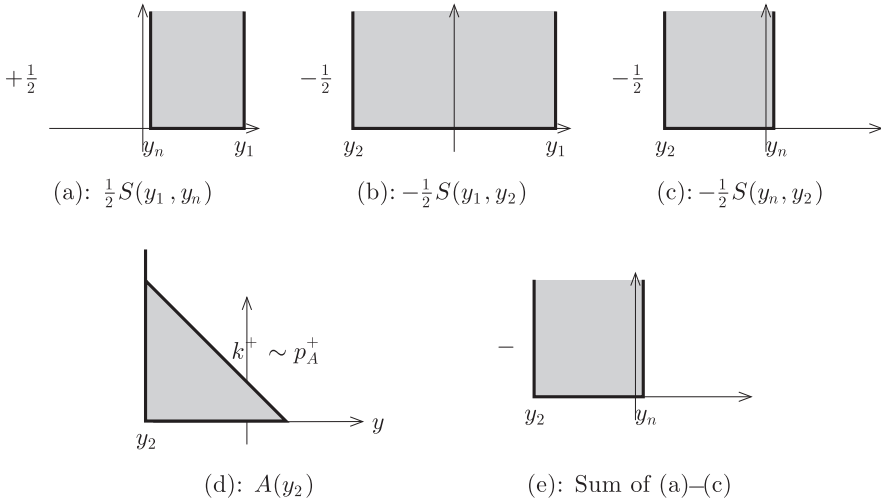
Fig. 10.26. Like Fig. 10.7, but showing the main regions for the one-loop contributions to (10.119a), with y_n chosen slightly positive. The diagrams are written before the limits $y_1 \to \infty$ and $y_2 \to -\infty$ are taken. The scale is reduced from Fig. 10.7.

shows the regions in gluon k_T and rapidity that contribute at one-loop order to the factors in (10.119a). In the region of low transverse momentum, the S terms combine to give a negative contribution running between y_2 and y_n that cancels the corresponding contribution from the one-loop term in the A term. This cancels the rapidity divergence as $y_2 \to -\infty$. But as the transverse momentum increases, the upper limit on gluon rapidity decreases in the A term, but not in the sum of the S terms. This weakens the cancellation, leaving an uncanceled contribution from a triangular region above the diagonal line in Fig. 10.26(d). With a UV regulator applied (e.g., $n < 4$) the integral is convergent at large k_T, so the limit $y_2 \to -\infty$ exists.

When the UV regulator is removed, the contribution of the triangle is a doubly logarithmic infinity, to be canceled by a UV counterterm. As in Sec. 10.8.2 the limits are applied in the order $y_2 \to -\infty$ and then $n \to 4$. Because of the doubly logarithmic divergence, the UV divergence has the two poles of $\epsilon = 2 - n/2$ per loop instead of the conventional single pole, and it is energy dependent. See (10.139).

10.11.2 *Factorization and re-examination of hard factor*

The new collinear factors (10.119a) and (10.119b) are obtained from the original collinear and soft factors by reorganizing the S factors. Changes are only by power-suppressed corrections. Thus the hard factor H is unchanged. But we can convert the old formula for H, (10.96), to use the new version of factorization:

$$H(Q, \mu, g(\mu)) = \lim_{\text{massless}} \frac{F}{AB} = \lim_{\text{massless}} \frac{F \, S(+\infty, -\infty)}{A^{\text{unsub}}(-\infty) B^{\text{unsub}}(+\infty)}. \qquad (10.120)$$

As before, the notation of infinite rapidity for the Wilson lines includes the definition that the infinite rapidity limit is applied before the removing the UV regulator by $\epsilon \to 0$.

10.11.3 Evolution kernel K

The final versions of the collinear factors A and B in (10.119) depend on the rapidity parameter y_n, only via the factors $S(y_1 - y_n)$ and $S(y_n - y_2)$, in the limit $y_1 \to \infty$, $y_2 \to -\infty$. So to get an equation for the dependence on y_n, we need the kernel K defined earlier.

This earlier definition was appropriate for differentiating $S(y_1 - y_2)$ with respect to y_1, and thus the diagrammatic definition was *not* symmetric between the positive and negative rapidity directions. However, since S depends on the difference of the two rapidities an equal result is obtained by differentiating with respect to the other rapidity argument, except for a sign. For use with the new collinear factors, we now make a more symmetric definition of K, and we put it into an operator form. We first define the vector $n = (e^{y_n}, -e^{-y_n}, \mathbf{0}_T)$, and define a differentiated vector

$$\delta n \overset{\text{def}}{=} \frac{\mathrm{d} n}{\mathrm{d} y_n} = (e^{y_n}, e^{-y_n}, \mathbf{0}_T). \tag{10.121}$$

Then we redefine

$$
\begin{aligned}
K\left(m_g, m, \mu, g(\mu)\right) & \overset{\text{def}}{=} \frac{\partial}{\partial y_n} \ln \frac{S(y_n, -\infty)}{S(+\infty, y_n)} \\
& = \frac{\langle 0 | T \; W(\infty, 0, w_2)^\dagger \; W(\infty, 0, n) \, (-i g_0) \int_0^\infty \mathrm{d}\lambda \, \Delta_1(n\lambda) | 0 \rangle}{\langle 0 | T W(\infty, 0, w_2)^\dagger W(\infty, 0, n) | 0 \rangle} \\
& \quad + \frac{\langle 0 | T \; W(\infty, 0, -n)^\dagger \; W(\infty, 0, w_1) \, (i g_0) \int_0^\infty \mathrm{d}\lambda \, \Delta_2(-n\lambda) | 0 \rangle}{\langle 0 | T W(\infty, 0, -n)^\dagger W(\infty, 0, w_1) | 0 \rangle}
\end{aligned}
$$

$$\text{with renormalization,} \tag{10.122}$$

where w_1 and w_2 are the light-like vectors defined in (10.15a), and

$$\Delta_1(x) = \delta n^\mu A_\mu^{(0)}(x) + \lambda \delta n^\nu n^\mu \frac{\partial A_\mu^{(0)}(x)}{\partial x^\nu} \qquad \text{with } x = \lambda n, \tag{10.123a}$$

$$\Delta_2(x) = \delta n^\mu A_\mu^{(0)}(x) - \lambda \delta n^\nu n^\mu \frac{\partial A_\mu^{(0)}(x)}{\partial x^\nu} \qquad \text{with } x = -\lambda n. \tag{10.123b}$$

The Feynman rules for the special vertices are given in Fig. 10.27.

See problem 10.9 for the gauge independence of K with the new definition.

10.11.4 Factorization, evolution equations: Final form

In this section, we collect all the results in their final form: the factorization formula, and the evolution equations for the dependence on the Wilson-line rapidity and on the renormalization scale. The evolution equations are the key to practical applications. We will refer back to the definitions of all the factors.
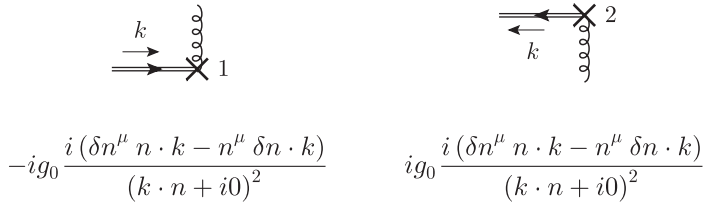
Fig. 10.27. Feynman rules for special vertices for K. See Fig. 10.23 for examples using the vertex labeled 1. The first rule agrees with that in (10.49).

The factorization equation is

$$F = H(Q, \mu, g(\mu)) \, A(y_{p_A} - y_n, m_g, m, \mu, g(\mu))$$
$$\times \, B(y_n - y_{p_B}, m_g, m, \mu, g(\mu)) + \text{power-suppressed}, \tag{10.124}$$

where A and B are defined in (10.119) and H in (10.120).

Initially, the rapidity y_n might be taken to be zero in the overall center-of-mass frame, so that the collinear factors A and B can be characterized as giving the contribution of quanta of, respectively, positive and negative rapidities. Then both the rapidity difference arguments $y_{p_A} - y_n$ and $y_n - y_{p_B}$ are $\ln(Q/m)$. Evolution equations, that we now summarize, enable us to adjust the values of y_n differently for each collinear factor, and thereby express them in terms of values with fixed rapidity-difference arguments. Similarly, we will use RG equations to make suitable (and different) choices for the scale μ in each factor.

From the results in Sec. 10.11.3, it follows that the evolution equations with respect to y_n for the collinear factors are

$$\frac{\partial A}{\partial y_n} = -\frac{1}{2} K(m_g, m, \mu, g(\mu)) \, A, \tag{10.125a}$$

$$\frac{\partial B}{\partial y_n} = \frac{1}{2} K(m_g, m, \mu, g(\mu)) \, B, \tag{10.125b}$$

where K is defined by (10.122). It follows that the product AB that appears in the factorization formula is independent of y_n.

The RG equations have the form

$$\frac{\mathrm{d} K}{\mathrm{d} \ln \mu} = -\gamma_K(g(\mu)), \tag{10.126a}$$

$$\frac{\mathrm{d} A}{\mathrm{d} \ln \mu} = \gamma_A(\zeta_A/\mu^2, g(\mu)) \, A, \tag{10.126b}$$

$$\frac{\mathrm{d} B}{\mathrm{d} \ln \mu} = \gamma_B(\zeta_B/\mu^2, g(\mu)) \, B. \tag{10.126c}$$

The anomalous dimensions can be obtained from the renormalization counterterms for K, A and B. Now, the renormalization factors for the two collinear factors are energy dependent, for reasons explained earlier with the aid of Fig. 10.26. This causes energy dependence in the anomalous dimensions. Since the anomalous dimensions are determined by UV phenomena, they involve only the large components of quark momenta, i.e., p_A^+ and

p_B^-. So we write the energy dependence in terms of

$$\zeta_A \stackrel{\text{def}}{=} 2(p_A^+)^2 e^{-2y_n} = m^2 e^{2(y_{p_A} - y_n)}, \tag{10.127a}$$

$$\zeta_B \stackrel{\text{def}}{=} 2(p_B^-)^2 e^{2y_n} = m^2 e^{2(y_n - y_{p_B})}, \tag{10.127b}$$

which are versions of (10.93a) and (10.93b), but now defined relative to the single rapidity y_n. Note that these differ by power-suppressed corrections from the corresponding definitions in Collins and Soper (1981) and Soper (1979), which are $\zeta_{A,\text{CS}} = |4 p_A \cdot n^2 / n^2|$, and $\zeta_{B,\text{CS}} = |4 p_B \cdot n^2 / n^2|$. Note also that $\zeta_A \zeta_B = (2 p_A^+ p_B^-)^2 = Q^4 \left(\frac{1}{2} + \frac{1}{2}\sqrt{1 - 4m^2/Q^2} \right)^4 \simeq Q^4$.

Since the collinear factors differ only by an exchange of plus and minus coordinates and by a charge-conjugation transformation, the anomalous dimensions γ_A and γ_B of A and B are the same.

The final ingredient we need is an equation for the energy dependence of γ_A. This is obtained by applying $d/d \ln \mu$ to (10.125a) and then exchanging the order of differentiation:

$$\frac{d}{d \ln \mu} \frac{\partial A}{\partial y_n} = \frac{1}{2} \gamma_K A - \frac{1}{2} K \gamma_A A, \tag{10.128a}$$

$$\frac{\partial}{\partial y_n} \frac{dA}{d \ln \mu} = \frac{\partial \gamma_A}{\partial y_n} A - \frac{1}{2} K \gamma_A A. \tag{10.128b}$$

Hence

$$\frac{\partial \gamma_A (\zeta_A / \mu^2, g(\mu))}{\partial y_n} = -\frac{\partial \gamma_A}{\partial \ln \zeta_A^{1/2}} = \frac{1}{2} \gamma_K (g(\mu)), \tag{10.129}$$

thereby completely determining the energy dependence of γ_A (and γ_B):

$$\gamma_A (\zeta/\mu^2, g(\mu)) = \gamma_B (\zeta/\mu^2, g(\mu)) = \gamma_A(1, g(\mu)) - \frac{1}{4} \gamma_K(g(\mu)) \ln \frac{\zeta}{\mu^2}. \tag{10.130}$$

The above equations, together with the definitions of A, B, H, and K, are a complete formulation of factorization.

10.11.5 Solution

We now use the evolution equations to set the arguments of H, A and B to avoid large logarithms.

- In H, we set μ proportional to Q: $\mu = C_2 Q$.
- In A, B, and K we set μ to a fixed value μ_0, of order the particle masses.
- In A, we set $y_n = y_{p_A}$.
- In B, we set $y_n = y_{p_B}$.
- In γ_A and γ_B, we set the ζ/μ^2 argument to $1/C_2^2$, as with H.

For the coefficient of proportionality C_2 between μ and Q, the notation C_2 is that of Collins and Soper (1981).

It can be readily deduced from the evolution equations that

$$
\begin{aligned}
F &= H(1/C_2, g(C_2 Q)) \, A\big(y_{p_A} - y_n, m_g, m, C_2 Q, g(C_2 Q)\big) \\
&\quad \times B\big(y_n - y_{p_B}, m_g, m, C_2 Q, g(C_2 Q)\big) \\
&= H(1/C_2, g(C_2 Q)) \, A\big(0, m_g, m, \mu_0, g(\mu_0)\big) \, B\big(0, m_g, m, \mu_0, g(\mu_0)\big) \\
&\quad \times \exp\left\{ -\int_{\mu_0}^{C_2 Q} \frac{\mathrm{d}\mu}{\mu} \left[\ln \frac{C_2 Q}{\mu} \, \gamma_K(g(\mu)) - 2\gamma_A\big(1/C_2^2, g(\mu)\big) \right] \right\} \\
&\quad \times \exp\left[\frac{1}{2}(y_{p_A} - y_{p_B}) \, K\big(m_g, m, \mu_0, g(\mu_0)\big) \right],
\end{aligned}
\tag{10.131}
$$

where power-suppressed corrections are ignored.

10.11.6 Properties and use of solution

Results of the same structure appear in many important problems in QCD (Chs. 13 and 14). So we now examine the solution (10.131) with a view to QCD applications.[16] In QCD, the effective coupling is large at small momenta, and is small at large momenta. Thus perturbative calculations are not valid for collinear factors for light particles in QCD.

By setting the renormalization scale proportional to Q in the hard scattering H, we removed large logarithms in the perturbative expansion of H. This enables effective perturbative predictions to be made for H.[17] But then the collinear factors have Q dependence; see the *first* line of (10.131).

We remedied this by using the evolution equations to give *different values of μ and y_n in the different factors*, in the lower three lines of (10.131). There, each of the collinear factors has a Q-independent value of the renormalization mass and of the rapidity difference argument. In a weak-coupling situation, this enables a perturbative calculation to be made without logarithms. In QCD, it allows us to use universality to make predictions: the same collinear factors appear at all values of Q and in all processes with the same kind of factorization. Thus determination of a collinear factor can be made from experimental data in one process at one energy, and the value used for the otherwise unknown quantity both in the same process at other energies, and in different processes.

The exponential in (10.131) shows that our solution radically differs from a straightforward use of perturbation theory, in a way that is much stronger than in cases containing only ordinary RG logarithms. The anomalous dimensions γ_K and γ_A are to be used in the weak-coupling regime, so that low-order perturbation calculations are effective. The generally biggest term in the exponent is the γ_K term; it has a logarithm relative to γ_A.

There remains the term involving K in the exponent. It gives a substantially energy-dependent factor:

$$
\exp\left[\frac{1}{2}(y_{p_A} - y_{p_B}) \, K\big(m_g, m, \mu_0, g(\mu_0)\big) \right] = \left(\frac{Q^2}{m^2} \right)^{\frac{1}{2} K\big(m_g, m, \mu_0, g(\mu_0)\big)} .
\tag{10.132}
$$

---

[16] But (10.131) is also useful in a QED-like theory with a coupling that is weak at all relevant scales.

[17] The coefficient C_2 can be adjusted to further optimize perturbative coefficients.

In QCD this would give a power-law dependence on Q with a non-perturbative exponent. The exponent $K(\mu_0)$ can be determined from the derivative of the amplitude with respect to energy, at one value of energy. Then the same exponent is used at all energies and in other processes. Determination of generalizations of K to other process appear as a critical element of good phenomenology (e.g., Landry *et al.*, 2003) for the Drell-Yan and other processes. It gives a substantial and characteristic energy dependence to the shape of Drell-Yan cross sections differential in transverse momentum.

If the IR coupling were weak, as in QED, the exponent K would be perturbatively calculable.

10.11.7 Asymptotic large Q behavior

The biggest term in the exponent in (10.131) is the one with γ_K. It implies that at large enough Q, the factorized formula for the form factor goes to zero faster than any power of Q; this happens both for our form factor in an abelian theory (at least if we stay in a weak-coupling regime), and for analogous quantities in an asymptotically free theory.

However, the derivation ignored power-suppressed corrections, which therefore have the potential to be asymptotically larger than the final factorized answer: the leading-power contributions have undergone a strong cancellation. Thus beyond some energy, the precise numerical result of the factorization formula is phenomenologically irrelevant.

To assess the significance of such a factorization in QCD, we observe that in e^+e^- annihilation to hadrons, the Sudakov form-factor graphs give the component of the cross section that has a pure quark-antiquark final state. But in the *total* cross section we found a cancellation of all IR-sensitive regions, with the total cross section going to a constant at large Q; see Ch. 4. This cancels the strong decrease of the Sudakov form factor in the quark-antiquark component. At high energy the cross section for $e^+e^- \rightarrow$ hadrons is dominantly highly inelastic.

In Chs. 13 and 14, we will investigate reactions where the amount of cancellation of IR-sensitive effects depends on the value of a measurable transverse-momentum variable. In these situations, a generalization of the factorization derived in this chapter will be very useful.

10.11.8 Relation of factorization to LLA

From (10.131), we see systematically how all logarithms arise. We derive the leading-logarithm approximation (LLA) as follows: (a) expand γ_K to lowest order in coupling; (b) ignore the running of the coupling; (c) neglect the other terms in the exponent; (d) set the outside H, A and B factors to their lowest-order values (i.e., unity). This reproduces (10.38), when μ_0 is of the order of particle masses.

There are important gains from the factorization formalism relative to the LLA, particularly in generalizations in QCD. In the first place the factorization formalism shows how corrections arise, and how they may be made systematically. The corrections are in the
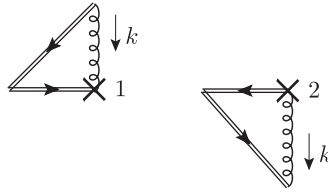
Fig. 10.28. One-loop graphs for K. The vertical heights of the graphs are adjusted to symbolize the rapidities of the light-like lines. The rules for the vertices with a cross are given in Fig. 10.27.

exponent, and also in non-logarithmic corrections to the H, A and B factors preceding the exponential.

In contrast, the logic of the LLA alone gives no information on non-leading logarithms. For example, the LLA itself does not prevent there from being an *additive* correction, e.g.,

$$g^2 \times \text{constant}, \tag{10.133}$$

which does not vanish as $Q \to \infty$. This would completely change the qualitative behavior. Such a phenomenon actually occurs for the Drell-Yan and related cross sections at zero transverse momentum. There the LLA gives a cross section that vanishes at zero transverse momentum, but the true result from a correct factorization theorem is non-zero (Collins and Soper, 1982a).

An important result is that the factorization method indicates how non-perturbative effects should affect the Q dependence in analogous QCD problems, by the factor (10.132). Of course our formal derivation stayed within perturbation theory. But the structures we use have a much more general appearance.

10.12 Calculations for Sudakov problem

In this section we show how the Feynman rules for H, A, B and K work out at one-loop order.

10.12.1 Evolution kernel K

First we calculate the evolution kernel K. From the rules given in Fig. 10.27, we have the one-loop graphs shown in Fig. 10.28. They give

$$\begin{aligned}
K &= \frac{i g^2 \mu^{2\epsilon}}{(2\pi)^{4-2\epsilon}} \int d^{4-2\epsilon} k \, \frac{1}{(k^2 - m_g^2 + i0)(-n \cdot k + i0)^2} \\
&\quad \times \left[\frac{n^+ \delta n \cdot k - \delta n^+ n \cdot k}{k^+ + i0} + \frac{n^- \delta n \cdot k - \delta n^- n \cdot k}{-k^- + i0} \right] + \text{UV c.t.} + O(g^4) \\
&= \frac{i g^2 \mu^{2\epsilon}}{(2\pi)^{4-2\epsilon}} \int d^{4-2\epsilon} k \, \frac{-2n^2}{(k^2 - m_g^2 + i0)(-n \cdot k + i0)^2} + \text{UV c.t.} + O(g^4)
\end{aligned}$$

$$= -\frac{g^2 \, \Gamma(\epsilon)}{4\pi^2} \left(\frac{4\pi\mu^2}{m_g^2}\right)^\epsilon + \frac{g^2 \, S_\epsilon}{4\pi^2\epsilon} + O(g^4)$$

$$= -\frac{g^2}{4\pi^2} \ln \frac{\mu^2}{m_g^2} + O(g^4). \tag{10.134}$$

(In obtaining this, note the reversal of the direction of k compared with Fig. 10.27, and remember the reversed sign of the ordinary vertex on a Wilson line that corresponds to an antiquark.) The calculation of the integral can be done by contour integration on k^- followed by an elementary integral for k^+. Then the k_{T} integral gives a beta function. The result agrees with our previous calculation at (10.54), but now we used our updated Feynman rules. Note that the evolution equation has no power corrections, in contrast with (10.53).

As an exercise the reader can show that the sole two-loop graph gives the $O(g^4)$ term in γ_K:

$$\gamma_K = \frac{g^2}{2\pi^2} - \frac{10}{9} \left(\frac{g^2}{4\pi^2}\right)^2 + O(g^6). \tag{10.135}$$

10.12.2 Collinear factor A

We now calculate the collinear factor A at one-loop order. This will illustrate the peculiar energy dependence of the counterterm. The graphs, obtained from the definition (10.119a), are shown in Fig. 10.29. To this is to be added a term associated with the external propagator correction.

The graphs in Fig. 10.29(a) give

$$A_{1a} = \frac{ig^2\mu^{2\epsilon}}{(2\pi)^{4-2\epsilon}} \frac{1}{\bar{u}_A \mathcal{P}_B} \int \mathrm{d}^{4-2\epsilon} k \, \frac{1}{(k^2 - m_g^2 + i0)} \bar{u}_A$$

$$\times \left\{ \frac{\gamma^+(\not{p}_A - \not{k} + m)}{[(p_A - k)^2 - m^2 + i0]\,(k^+ + i0)} + \frac{\frac{1}{2}e^{-y_n}}{(-k^- + i0)\,(k^+ e^{-y_n} - k^- e^{y_n} + i0)} \right.$$

$$\left. - \frac{\frac{1}{2}e^{y_n}}{(-k^- e^{y_n} + k^+ e^{-y_n} + i0)\,(k^+ + i0)} - \frac{\frac{1}{2}}{(-k^- + i0)\,(k^+ + i0)} \right\} \mathcal{P}_B, \tag{10.136}$$

to which is to be added a UV counterterm. The $e^{\pm y_n}$ factors in the exponents arise from the vertices for the Wilson lines of rapidity y_n. As usual, we use the residue theorem to perform the k^- integral. This gives

$$A_{1a} = \frac{-g^2(2\pi\mu)^{2\epsilon}}{8\pi^3} \int \mathrm{d}^{2-2\epsilon} k_{\mathrm{T}}$$

$$\times \left\{ \left[\int_0^1 \frac{\mathrm{d}x}{x} \left[\frac{1-x}{k_{\mathrm{T}}^2 + m_g^2(1-x) + m^2 x^2} + \frac{1}{-k_{\mathrm{T}}^2 - m_g^2 + 2(x p_A^+ e^{-y_n})^2 + i0} \right] \right. \right.$$

$$\left. \left. + \int_1^\infty \frac{\mathrm{d}x}{x} \frac{1}{-k_{\mathrm{T}}^2 - m_g^2 + 2(x p_A^+ e^{-y_n})^2 + i0} \right\} + \mathrm{UV \ c.t.}, \tag{10.137}$$
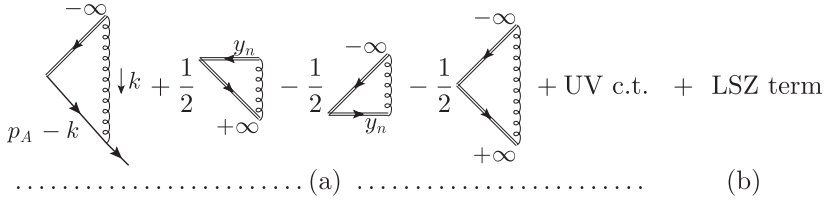
Fig. 10.29. Graphs for A at one-loop, including subtractions and the counterterm for canceling the UV divergence. Next to each double line representing a Wilson line is a label for its rapidity, $-\infty$, $+\infty$ or y_n. The factors of $\frac{1}{2}$ multiplying the Wilson-line terms arise from the one-loop expansion of the factors in the square root in (10.119a). The upper Wilson lines have the charge of an *anti*quark. The LSZ term is a self-energy graph for the on-shell quark.

where the potential divergence at $x = 0$ has canceled. Much of the x integral, including all the Wilson-line terms, can be performed by very elementary methods to give

$$A_{1a} = \frac{-g^2 (2\pi\mu)^{2\epsilon}}{8\pi^3} \int \frac{\mathrm{d}^{2-2\epsilon}\boldsymbol{k}_{\mathrm{T}}}{k_{\mathrm{T}}^2 + m_g^2} \left\{ -\int_0^1 \mathrm{d}x \, \frac{k_{\mathrm{T}}^2 + m^2 x}{k_{\mathrm{T}}^2 + m_g^2(1-x) + m^2 x^2} \right.$$

$$\left. + \frac{1}{2} \ln \frac{2(p_A^+ e^{-y_n})^2}{k_{\mathrm{T}}^2 + m_g^2} - i\frac{\pi}{2} \right\} + \text{UV c.t.} \quad (10.138)$$

The remaining x integral is well behaved.

A simple computation of the UV counterterm in the $\overline{\mathrm{MS}}$ scheme uses the techniques of Sec. 3.4. The UV divergence is governed by the leading large k_{T} behavior of the integrand, which is therefore independent of the masses:

UV c.t. $= -\overline{\mathrm{MS}}$ pole part of integral in (10.138)

$$= -\overline{\mathrm{MS}} \text{ pole part of } \frac{-g^2 (2\pi\mu)^{2\epsilon}}{8\pi^3} \int_{k_{\mathrm{T}}>\mu} \frac{\mathrm{d}^{2-2\epsilon}\boldsymbol{k}_{\mathrm{T}}}{k_{\mathrm{T}}^2} \left[-1 + \frac{1}{2} \ln \frac{2(p_A^+ e^{-y_n})^2}{k_{\mathrm{T}}^2} - i\frac{\pi}{2} \right]$$

$$= \frac{g^2 S_\epsilon}{8\pi^2} \left[\frac{-1}{2\epsilon^2} + \frac{1}{\epsilon} \left(-1 + \frac{1}{2} \ln \frac{2(p_A^+ e^{-y_n})^2}{\mu^2} - i\frac{\pi}{2} \right) \right]. \quad (10.139)$$

As in Sec. 3.4, the use of the lower limit μ on the k_{T} integral gives exactly the $\overline{\mathrm{MS}}$ pole part with its accompanying factor of S_ϵ with no further finite part. This relies on exactly our specific definition of S_ϵ in (3.18).

The k_{T} integral in (10.138) is readily performed. To get the complete one-loop contribution to the collinear factor, the LSZ reduction formula tells us to add half the one-loop residue of the quark propagator:

$$\frac{1}{2}\Sigma_1 = \frac{g^2}{8\pi^2} \left\{ \frac{1}{4} + \int_0^1 \mathrm{d}x \, \frac{1}{2}(1-x) \ln \frac{m_g^2(1-x) + m^2 x^2}{\mu^2} + \int_0^1 \mathrm{d}x \, \frac{m^2 x(1-x^2)}{m_g^2(1-x) + m^2 x^2} \right\}.$$

$$(10.140)$$

Then the full one-loop contribution to A at $n = 4$ is

$$
A_1 = \frac{-g^2}{8\pi^2} \left\{ -\int_0^1 \frac{dx}{x} \ln\left(1 - x + x^2 m^2/m_g^2\right) \right.
$$

$$
+ \int_0^1 dx \, \frac{1}{2}(1 + x) \ln \frac{m_g^2(1 - x) + m^2 x^2}{\mu^2} - \int_0^1 dx \, \frac{m^2 x(1 - x^2)}{m_g^2(1 - x) + m^2 x^2}
$$

$$
\left. -\frac{1}{4} + \frac{1}{4} \ln^2 \frac{2(p_A^+ e^{-y_n})^2}{m_g^2} - \frac{1}{4} \ln^2 \frac{2(p_A^+ e^{-y_n})^2}{\mu^2} + i\frac{\pi}{2} \ln \frac{m_g^2}{\mu^2} \right\}. \quad (10.141)
$$

We can now check the evolution and RG equations. First, we see from (10.94a), and its generalization to the new definition of A, that the counterterm in (10.139) gives the one-loop contribution to $Z_A Z_2^{1/2}$. With the aid of (3.23) for Z_2, we find that

$$
Z_A = 1 + \frac{g^2 S_\epsilon}{8\pi^2} \left[\frac{-1}{2\epsilon^2} + \frac{1}{\epsilon} \left(-\frac{3}{4} + \frac{1}{2} \ln \frac{2(p_A^+ e^{-y_n})^2}{\mu^2} - i\frac{\pi}{2} \right) \right] + O(g^4). \quad (10.142)
$$

From this we get the anomalous dimension:

$$
\gamma_A = \frac{d \ln A}{d \ln \mu} = \frac{d \ln Z_A}{d \ln \mu}
$$

$$
= \frac{\partial \ln Z_A}{\partial \ln \mu} + \frac{dg^2/16\pi^2}{d \ln \mu} \frac{\partial \ln Z_A}{\partial g^2/16\pi^2}
$$

$$
= \frac{g^2}{8\pi^2} \left[\frac{3}{2} - \ln \frac{2(p_A^+ e^{-y_n})^2}{\mu^2} + i\pi \right] + O(g^4) \qquad \text{(at } \epsilon = 0\text{)}, \quad (10.143)
$$

where the first line uses $A = Z_A A_0$ and the RG invariance of A_0, defined in terms of bare fields, while the third line uses (3.44) for $d(g^2/16\pi^2)/d \ln \mu$. The explicit μ dependence of the single-pole counterterm was needed to get finiteness of γ_A. It is readily checked that the dependence on y_n is as predicted from (10.129) with the calculated value of γ_K from (10.135).

10.12.3 Hard factor

From the definition, (10.120), we find that the one-loop hard-scattering coefficient arises from the graphs in Fig. 10.30. This gives

$$
H_1 = \frac{-ig^2 \mu^{2\epsilon}}{(2\pi)^{4-2\epsilon}} \int d^{4-2\epsilon} k \, \frac{\bar{u}_A \mathcal{P}_B \, I_H(k) \, \mathcal{P}_B v_B}{k^2 + i0}, \quad (10.144)
$$

where

$$
I_H(k) = \frac{\gamma^\kappa (p_A^+ \gamma^- - \slashed{k}) \gamma^\mu (-p_B^- \gamma^+ - \slashed{k}) \gamma_\kappa}{(-2p_A^+ k^- + k^2 + i0)(2p_B^- k^+ + k^2 + i0)} + \frac{-\gamma^\mu}{(-k^- + i0)(k^+ + i0)}
$$

$$
- \frac{\gamma^+ (p_A^+ \gamma^- - \slashed{k}) \gamma^\mu (-1)}{(-2p_A^+ k^- + k^2 + i0)(k^+ + i0)} - \frac{\gamma^\mu (-p_B^- \gamma^+ - \slashed{k}) \gamma^-}{(-k^- + i0)(2p_B^- k^+ + k^2 + i0)}. \quad (10.145)
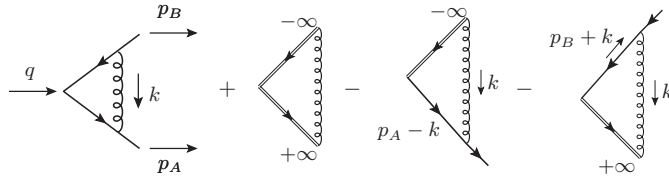$$

Fig. 10.30. Graphs for one-loop hard coefficient.

The factors of (-1) in two of the numerators are for the negative charges of the upper Wilson lines. To (10.144) is to be added a UV counterterm, as usual.

The integrals over k^- and k^+ can be performed analytically, to give

$$
H_1 = \frac{-g^2 (4\pi\mu^2)^\epsilon \bar{u}_A \mathcal{P}_B \gamma^\mu \mathcal{P}_B v_B}{8\pi^2 \Gamma(1-\epsilon)} \int_0^\infty \frac{dk_T^2}{(k_T^2)^{1+\epsilon}}
$$

$$
\times \left\{ \ln\frac{k_T^2}{Q_E^2} + \frac{1 + (3+2\epsilon)k_T^2/Q_E^2}{\sqrt{1+4k_T^2/Q_E^2}} \ln\frac{\sqrt{1+4k_T^2/Q_E^2}+1}{\sqrt{1+4k_T^2/Q_E^2}-1} \right\}, \tag{10.146}
$$

where $Q_E^2 = -Q^2 - i0$: the integral is defined by continuing from a positive value of Q_E^2 to $-Q^2$ approaching from the appropriate side of the real axis. Observe that the Wilson-line terms combine to remove the divergence at $k_T = 0$.

From the behavior of the integrand at large k_T, it can be computed that the necessary $\overline{\text{MS}}$ counterterm is

$$
H_{1,\,\text{c.t.}} = \frac{g^2 S_\epsilon \bar{u}_A \mathcal{P}_B \gamma^\mu \mathcal{P}_B v_B}{8\pi^2} \left[\frac{1}{\epsilon^2} + \frac{1}{\epsilon}\left(-\ln\frac{Q_E^2}{\mu^2} + \frac{3}{2} \right) \right]
$$

$$
= \frac{g^2 S_\epsilon \bar{u}_A \mathcal{P}_B \gamma^\mu \mathcal{P}_B v_B}{8\pi^2} \left[\frac{1}{\epsilon^2} + \frac{1}{\epsilon}\left(-\ln\frac{Q^2}{\mu^2} + i\pi + \frac{3}{2} \right) \right]. \tag{10.147}
$$

This is exactly equal and opposite to the sum of the one-loop contributions to Z_A and Z_B, so that for the one-loop contribution to HAB the total counterterm is zero. This corresponds to the non-renormalization theorem for matrix elements of a conserved current. Notice that the counterterm has a logarithm, just as for the collinear factors. Thus the one-loop anomalous dimension of H is also momentum dependent:

$$
\gamma_H(Q^2/\mu^2, g) \stackrel{\text{def}}{=} \frac{d\ln H}{d\ln\mu}
$$

$$
= \frac{g^2}{8\pi^2}\left(2\ln\frac{Q^2}{\mu^2} - 2i\pi - 3 \right) + O(g^4)
$$

$$
= -\gamma_A(\zeta_A/\mu^2, g(\mu)) - \gamma_B(\zeta_B/\mu^2, g(\mu)), \tag{10.148}
$$

with the last line being a general result following from the RG invariance of the whole form factor, and hence of its factorized form HAB. Observe that the dependence of γ_H on the ratio Q^2/μ^2 can be derived from the ζ dependence of γ_A and γ_B. Thus from (10.129) we

have

$$\frac{\partial \gamma_H\left(Q^2/\mu^2, g\right)}{\partial \ln(Q^2/\mu^2)} = \frac{1}{2}\gamma_K(g), \tag{10.149}$$

so that

$$\gamma_H\left(Q^2/\mu^2, g\right) = \gamma_H\left(1, g\right) + \frac{1}{2}\gamma_K(g)\ln\frac{Q^2}{\mu^2}. \tag{10.150}$$

10.13 Deduction of some non-leading logarithms

Our formalism gives a lot of information on the structure of non-leading logarithms even in the absence of explicit Feynman-graph calculations beyond lowest order. To see some of the results, we examine the perturbation series for the *logarithm of the form factor*. We keep the logarithmic dependence on Q, expressing the coefficients as polynomials in $t = \ln(-Q^2/\mu^2)$, with power corrections dropped:

$$\ln F = \frac{g^2}{4\pi^2}\left(C_{12}t^2 + C_{11}t + C_{10}\right)$$
$$+ \left(\frac{g^2}{4\pi^2}\right)^2 \left(C_{24}t^4 + C_{23}t^3 + C_{22}t^2 + C_{21}t + C_{20}\right) + O(1/Q^2), \tag{10.151}$$

where the coefficients may depend on m, M and μ, but not on Q.

The leading logarithm results imply that $C_{24} = 0$. But we can deduce considerable more from the factorization formula (10.124) and the evolution equations (10.125). We do this by deducing an equation for the Q dependence of $\ln F$:

$$\frac{\partial \ln F}{\partial \ln Q} = \frac{\partial \ln J_A}{\partial \ln Q} + \frac{\partial \ln J_B}{\partial \ln Q} + \frac{\partial \ln H}{\partial \ln Q} + \text{power correction}$$
$$= K(m_g, m, g, \mu) + G(Q/\mu; g) + \text{power correction}, \tag{10.152}$$

where G is a purely UV quantity that obeys $dG / d\ln\mu = -\gamma_K$. Now, from (10.151) we have

$$\frac{\partial \ln F}{\partial \ln Q} = \frac{g^2}{4\pi^2}\left(4C_{12}t + 2C_{11}\right) + \left(\frac{g^2}{4\pi^2}\right)^2 \left(6C_{23}t^2 + 4C_{22}t + 2C_{21}\right) + \ldots \tag{10.153}$$

In order that G in (10.152) be independent of the masses m and M, C_{12}, C_{23} and C_{22} must be independent of m and M (and hence of μ). Furthermore, once one puts in the one-loop values, the requirement that G satisfies its RG equation implies that

$$C_{23} = -\frac{1}{36}. \tag{10.154}$$

Hence the new information for the form factor F at two loops is two logarithms down from the leading logarithm, i.e. it is in C_{22} and the less leading coefficients, C_{21} and C_{20}. The double logarithm coefficient C_{22} is related to the two-loop term in γ_K, given in (10.135);

this was the result of a relatively easy calculation. Hence

$$C_{22} = \frac{5}{36}. \tag{10.155}$$

The remaining information, for which a full two-loop calculation of the form factor is needed, is in the terms with one and no logarithms of Q. These are three and four logarithms down from the leading $\ln^4 Q$ term.

10.14 Comparisons with other work

In this section, I give a brief comparison between the present treatment of the Sudakov and other work on the same and related problems. I restrict attention to work that aims at something like a complete factorization theorem, rather than just obtaining a LLA.

The first treatment in a similar fashion was in Collins (1980). There I used Coulomb gauge in a frame with a time-like rest vector n, where the numerator of the gluon propagator is

$$-g^{\mu\nu} + \frac{(n^\mu k^\nu + k^\mu n^\nu)n \cdot k}{n \cdot k^2 - k^2 n^2} - \frac{k^\mu k^\nu n^2}{n \cdot k^2 - k^2 n^2}. \tag{10.156}$$

The collinear factors are defined by formulae like (10.90) and (10.92) except that the Wilson lines are removed, so that the matrix elements are $\langle p_A | \bar{\psi}_0(0) | 0 \rangle$ and $\langle p_B | \psi_0(0) | 0 \rangle$. Thus the rapidity of the vector n plays the same role as y_n in our final definitions (10.119). Factorization and evolution equations of a similar kind were derived, differing from those in Sec. 10.11 essentially by a change of scheme. But the old evolution equations had power-suppressed corrections, rather than being exactly homogeneous. There was also a separate soft factor, which we have now eliminated.

A treatment in covariant gauge with Wilson lines was given in Collins (1989). The collinear factors were now defined as what are here called the "unsubtracted" collinear factors (10.90) and (10.92), but with the Wilson lines now having a rapidity y_n corresponding to that in our final definitions (10.119). In this formalism, it is the soft factor that has the subtractions, which is harder to justify from a systematic approach. The evolution equations continue to have power-suppressed corrections, and the factorization formula has a separate soft factor. They also have not only the K we use, but also a G term, as in (10.117).

An earlier approach is found in Mueller (1979), but the methods are less general, particularly as regards their extension to inclusive processes in QCD.

When the methods of Collins (1980) were extended (Collins and Soper, 1981) to inclusive processes in QCD, it was found convenient to replace Coulomb gauge by a non-light-like axial gauge, where the numerator of the gluon propagator is

$$-g^{\mu\nu} + \frac{k^\mu n^\nu + n^\mu k^\nu}{k \cdot n} - \frac{k^\mu k^\mu n^2}{(k \cdot n)^2}. \tag{10.157}$$

This gives definitions (Collins and Soper, 1982b; Soper, 1979) of parton densities and fragmentation functions exactly like those in a *non-gauge* theory, i.e., without Wilson lines.

Essentially these are equivalent to gauge-invariant definitions with Wilson lines in direction n. Applied to the Sudakov form factor, these definitions amount to using our unsubtracted definitions (10.90) and (10.92) as the actual collinear factors in the factorization formula, but with the Wilson lines having rapidity y_n. The factorization formula still has a subtracted soft factor. Again the evolution equation for a collinear factors has power-suppressed corrections and a G term. The use of a non-light-like vector rather than a light-like vector in the collinear factors complicates calculations. The singularity in (10.157) at $k \cdot n = 0$ is defined as a principal value, which causes problems with the Glauber region; the definitions are not exactly equivalent to the definition with a Wilson line going to infinity in a definite direction. The difficulties have become particularly apparent when inclusive processes with transversely polarized beams are treated (Secs. 13.16 and 13.17). Furthermore, it was not realized that there is a need for the equivalent of what in Feynman gauge is the removal of Wilson-line self-energies. A version of this formalism was applied to semi-inclusive DIS in Meng, Olness, and Soper (1996), with a gauge-invariant version being given in Ji, Ma, and Yuan (2005).

Exercises

10.1 Show explicitly how the formulae in Sec. 8.9, like (8.70) and (8.74), give particular cases of the general formulae for the subtraction method in Sec. 10.1.

10.2 (**) *This problem refers both to material in this chapter and related material in Ch. 13.* Work out more details of the comparison with other work summarized in Sec. 10.14, and with any other papers you can find. Compare the various definitions of the collinear and soft factors. To what extent do they agree up to an allowed scheme change? Are there important differences or errors?

10.3 Assume that a solution of the form of (10.131) applies to some quantity in QCD, with the standard results for the numerical value the effective coupling as a function of μ. Deduce the form of the asymptotic large-Q behavior of the form factor. It would be appropriate to use the same one-loop value of γ_K we derived above, except for an insertion of a factor C_F. This would arise exactly as in the calculations of $e^+e^- \to$ hadrons in Sec. 4.1.

10.4 Estimate the fractional error in the LLA for the Sudakov form factor. When does the LLA give a usefully accurate approximation to the true form factor, in the following different types of theory?
    (a) In the QED-like situation where the coupling is weak over the whole range of scales involved, and the coupling is smallest in the infra-red.
    (b) In the QCD-like asymptotically free situation when the coupling is small only in the UV.
    (c) In an asymptotically free situation, like QCD, except that the masses are large, so that the largest relevant effective coupling is $g(M)$, where M is a scale characterizing the masses of the theory.

10.5 In momentum space the renormalization of the collinear factor A is by a P^+-dependent multiplicative factor. What does this correspond to in coordinate space?

10.6 In our standard definition of the soft approximations we used space-like auxiliary vectors n_1 and n_2, for maximum universality with QCD factorization theories.

    (a) Show that, for the Sudakov form factor, time-like vectors work.

    (b) Take these vectors to be (proportional) to the external particle momenta (i.e., $n_1 = p_A$ and $n_2 = p_B$). Examine the IR divergence when the gluon mass goes to zero. Show that the divergence is completely contained in the soft factor.

    (c) In contrast, examine the case that the auxiliary vectors are space-like or are not proportional to the external momenta. Use the version of the definition of H where masses are preserved, but collinear and soft subtractions are made. Show that there is a power-suppressed divergence as $m_g \to 0$. (It should be proportional to something like $(m^2/Q^2)\ln m_g^2$. The divergence is associated with the gluon mass, but the power-suppression with the quark mass.)

10.7 Verify the two-loop term in (10.135) by explicit calculation.

10.8 When masses are retained in a hard scattering, the external lines are approximated by massive on-shell lines. Show that appropriate choices of the projectors for Dirac fields are as follows.

- For a Dirac particle of momentum $\hat{k}$ *leaving* H to A: $\dfrac{\gamma^+(\hat{k}+m)}{2\hat{k}^+}$. Here the collinear function and the actual wave function $\bar{u}_A$ are on the left.

- For a Dirac antiparticle of momentum $\hat{k}$ *entering* H from A: $\dfrac{(\hat{k}-m)\gamma^+}{2\hat{k}^+}$. Here the collinear function and the actual wave function v_A are on the right.

- For a Dirac particle of momentum $\hat{k}$ *leaving* H to B: $\dfrac{\gamma^-(\hat{k}+m)}{2\hat{k}^-}$. Here the collinear function and the actual wave function $\bar{u}_B$ are on the left.

- For a Dirac antiparticle of momentum $\hat{k}$ *entering* H from B: $\dfrac{(\hat{k}-m)\gamma^-}{2\hat{k}^-}$. Here the collinear function and the actual wave function v_B are on the right.

A general projector has to project onto an on-shell wave function from a general spinor, and should be non-singular in the limit $m \to 0$.

10.9 A change of gauge condition in an abelian theory can be implemented by changing the numerator of the gluon propagator by

$$-g^{\mu\nu} \mapsto -g_{\mu\nu} + f_\mu k_\nu + k_\mu f_\nu, \qquad (10.158)$$

for some vector function f of momentum. In a covariant gauge, f^μ is proportional to k^μ times a function of the scalar k^2. There are also more general gauges; such non-covariant gauges are exemplified by the Coulomb and axial gauges.

    It can be proved that physical matrix elements of gauge-invariant operators are unchanged under such a change of gauge condition, i.e., that they are gauge

independent.[18] Our definitions of collinear and soft factors etc (S, A^{unsub}, B^{unsub}, A^{basic}, B^{basic}, A, B, and K) involve operators that are not exactly gauge invariant, since the operators in them have open Wilson lines.

In this problem, investigate to what extent these quantities are gauge independent at the one-loop level.

As an example, you should find that K with its first definition (10.112) is gauge dependent, but with the second definition (10.122) it is gauge independent. But with a restriction to covariant gauges, even the first definition is gauge independent, and the two definitions agree.

10.10 (**) Consider those quantities that in the previous problem you found to be gauge independent at one-loop order. Try to prove gauge independence to all orders of perturbation theory.

---

[18] Note carefully that gauge invariance and gauge independence are distinct concepts.